In presenting this dissertation as a partial fulfillment of the requirements for an advanced degree from Emory University, I agree that the Library of the University shall make it available for inspection and circulation in accordance with its regulations governing materials of this type. I agree that permission to copy from, or to publish, this dissertation may be granted by the professor under whose direction it was written when such copying or publication is solely for scholarly purposes and does not involve potential financial gain. In the absence of the professor, the dean of the Graduate School may grant permission. It is understood that any copying from, or publication of, this dissertation which involves potential financial gain will not be allowed without written permission.

_____

Tamara Jackson Henderson

Photoaffinity Labeling of the Human Dopamine Transporter Using Cocaine Analogs

By

Tamara Jackson Henderson
Doctor of Philosophy

Department of Chemistry

_____
Joseph B. Justice, PhD.
Adviser

_____
Dale E. Edmondson, Ph.D.
Committee Member

_____
Michael J. Kuhar, Ph.D.
Committee Member

Accepted:

_____
Lisa A. Tedesco, Ph.D.
Dean of the Graduate School

_____
Date

Photoaffinity Labeling of the Human Dopamine Transporter Using Cocaine Analogs

By

Tamara Jackson Henderson
B.S., Hampton University, 2002

Adviser: Joseph B. Justice, PhD

An abstract of a dissertation submitted to the Faculty of the Graduate School of Emory University in partial fulfillment of the requirements of the degree of Doctor of Philosophy

Department of Chemistry

2008

Abstract

The photoaffinity ligand [^{125}I]MFZ 2-24 has been used for labeling the human dopamine transporter (hDAT) to characterize the cocaine binding site. [^{125}I]MFZ 2-24 has been shown to label a region within transmembrane domains (TM) 1-2 (Parnas et al., 2003). To further determine the site of photoincorporation, membranes from HEK 293 cells expressing hDAT were photolabeled and digested with trypsin. Following the digest, the labeled peptides were attached to the transmembrane domains. Residues R60 and R125 seem to be accessible to trypsin during the digest of the membrane preparation. Hydrolysis of these residues would cause the peptides formed during the digest to become displaced from the membranes and be found in the solution, which was shown to contain limited to no radioactivity. These results suggest that within TM 1-2 residues 1-60 and 126-139 are not labeled by [^{125}I]MFZ 2-24. This implies that the region between E61-R125 likely contains the radiolabeled residue. To further identify the labeled domain, [^{125}I]MFZ 2-24 labeled hDAT was digested with enzymatic and chemical agents. The radiolabeled peptides were run on a high percentage gel and separated with HPLC, where fractions were collected. Radioactive fractions were subjected to subsequent enzymatic digestions and reanalyzed via HPLC. Shifts in the retention time of the labeled fragments suggested that the cleavage site of the corresponding enzyme was present in the initial peptide. The HPLC retention time of the peptide produced from a CNBr digest of hDAT suggests that the sequence PLFYM in TM2 contains the site of [^{125}I]MFZ 2-24 incorporation. This is consistent with previous CNBr digests of hDAT, in which the peptide PLFYM in TM2 was thought to be labeled by [^{125}I]MFZ 2-24 (Wirtz, 2004). Following HPLC separation of the peptides generated from a thermolysin digest of

hDAT, the radiolabeled peptide was analyzed by Edman degradation. The second degradation cycle selectively released the most radioactivity, indicating that the second residue from the amino terminal end of the peptide is photolabeled. Considering the results from the CNBr digest of hDAT, HPLC analyses of a complete thermolysin digest and the Edman degradation results suggest that Y115 is possibly labeled by [^{125}I]MFZ 2-24.

Photoaffinity Labeling of the Human Dopamine Transporter Using Cocaine Analogs

By

Tamara Jackson Henderson
B.S., Hampton University, 2002

Adviser: Joseph B. Justice, PhD

A dissertation submitted to the Faculty of the Graduate School of Emory University in partial fulfillment of the requirements of the degree of Doctor of Philosophy

Department of Chemistry

2008

Acknowledgements

I would like to thank Dr. Joseph Justice for his advisement. He has allowed me to develop the skills and intellect necessary to become a successful scientist. I am now able to critically analyze and interpret data, draw conclusions about results, design meaningful experiments, and use my knowledge to create new ideas. My committee members Dr. Michael Kuhar and Dr. Dale Edmondson have also helped in developing me into a more critical thinker.

I acknowledge and thank everyone in the Justice lab for their help as well. I really appreciate the extensive training I received from Dr. Anh Pham and Dr. Sara Wirtz. I am also grateful for the moral support and helping hand I received from Uliana Danilenko and Muhsinah Morris. Everyone made my adjustment to the Justice lab a very comfortable and memorable experience.

It is with the support of God, my husband, my family, and friends that I was able to persevere through the hard times I encountered while at Emory University.

Table of Contents

List of Figures

List of Tables

Chapter One

Introduction

Introduction to the Thesis

The cocaine binding site on the human dopamine transporter (hDAT) remains unknown. In one approach to identify it, photoaffinity labeling has been combined with immunoprecipitation and mutagenesis to identify the regions of hDAT near the cocaine binding site (Vaughan et al., 2001; Parnas et al., 2008). In the present work, the photoaffinity label [^{125}I]MFZ 2-24 was examined to investigate its site of incorporation. When reacting with hDAT, the pharmacophore is proposed to bind reversibly to the cocaine binding site. Upon irradiation with UV light, the aryl azide group becomes a highly reactive nitrene, which reacts with nearby amino acids. The site of [^{125}I]MFZ 2-24 photoincorporation is investigated by conducting chemical and enzymatic digest of radiolabeled hDAT. Cyanogen bromide (CNBr) and thermolysin are used in the present study, either separately or sequentially. The digests are separated using SDS-PAGE and HPLC. The labeled peptide in the radioactive HPLC fraction is immobilized on an aryl amine disk and Edman degradation performed. The location of the labeled residue in the peptide is indicated by the cycle from which significantly greater radioactivity is obtained.

Dopamine Transporter: A Membrane Protein and Transporter

Membrane Proteins

Membrane proteins are responsible for vital physiological activities and constitute a third of the proteins in the complete genome. The dopamine transporter (DAT) is a transmembrane-spanning protein located on the presynaptic nerve terminal of dopamine neurons (Torres, 2006). Transmembrane, or integral, proteins are amphiphilic proteins that span from the internal to the external surface of the biological membrane or lipid bilayer in which it is embedded. They are classified as amphiphilic because many transmembrane proteins have multiple membrane-spanning alpha helix segments that anchor them to the membrane (Yu et al., 2000), the section of these proteins that is within the lipid bilayer consists primarily of hydrophobic amino acids and the portion of the polypeptide that projects from the bilayer tends to have a higher percentage of hydrophilic amino acids. Despite the importance and abundance of transmembrane proteins, few have been structurally determined. This is due to the lack of purified functional protein and the experimental difficulties encountered using various techniques (Torres et al., 2003c). Inadequate amounts of purified functional protein may result from low expression levels as well as the complexity of determining the perfect solubilization conditions in which the protein can be removed from the membrane without being denatured. Although several advances have been made in improving the solubilization and expression of transmembrane proteins, such as synthesizing various detergents with novel structures and overexpressing the protein in recombinant systems, the structural determination of transmembrane proteins is slowly developing.

Methods Used for Studying Membrane Proteins

X-ray crystallography is a widely used experimental approach employed to determine the structure of proteins. Upon obtaining high-quality crystals, standard x-ray crystallographic analysis can give insight into many structural aspects, including the substrate and inhibitor binding site, the transport mechanism, the arrangement of transmembrane domains (TMDs), and the orientation of extracelluar and intracellular loops. However, difficulties in the expression, isolation, and purification of transmembrane proteins impede the growth of quality crystals. Abramson et al. (2003) were able to determine the crystal structure of Lactose Permease (LacY) by isolating and expressing the protein in *Escherichia coli*. LacY is a transmembrane protein that co-transports its substrate (lactose) and H^+ down a transmembrane concentration gradient (Locher et al., 2003). The crystal structure revealed that LacY is organized into two domains composed of 6 transmembrane helices in the N-terminal and 6 transmembrane helices in the C-terminal. Both the N- and C-terminals form a hydrophilic crevice that contains residues responsible for ligand binding. In addition to the structure of LacY, the three-dimensional structure of a calcium-gated potassium channel was also resolved using x-ray crystallography (Jiang et al., 2002). Calcium-gated potassium channels are membrane-spanning proteins that allow ion conduction upon intracellular binding of calcium. The crystal structure of the calcium-gated potassium channel shows that two membrane-spanning domains form the conduction pathway. The C-terminal, which contains the calcium binding site, regulates the opening and closing of the channel. Recently, the crystal structure of the leucine transporter (LeuT) (Figure 1.1), a Na^+/Cl^--dependent neurotransmitter, was determined (Yamashita et al., 2005). This transporter

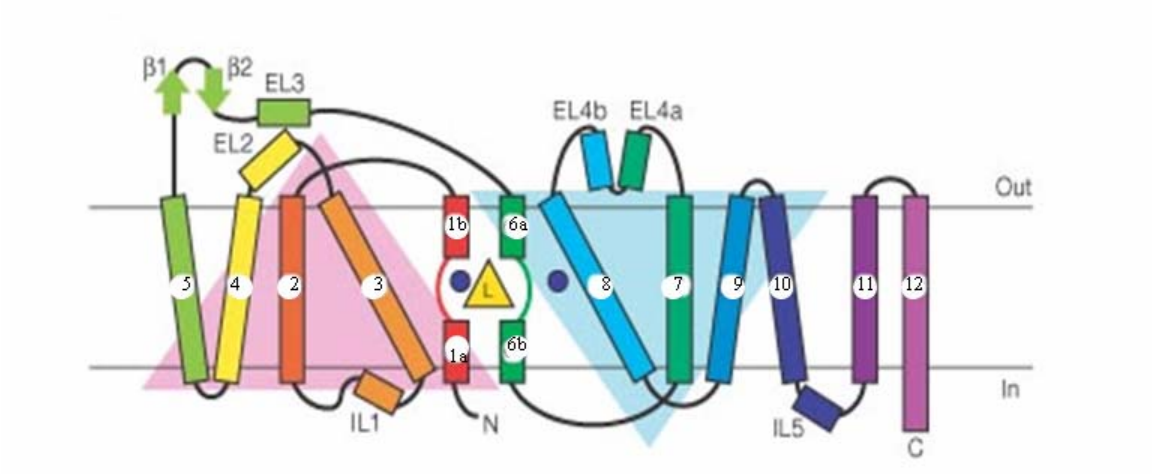

Figure 1.1 Secondary Structure of the Leucine Transporter (LeuT). The protomer has 12 transmembrane helical regions with several loops and helices on the intracellular and extracellular surfaces. The leucine and two sodium ions are shown as a triangle and circles, respectively (from Yamashita et al., 2005).

consists of 12 transmembrane domains where TM1-5 and TM6-10 are superimposable by a rotation of 176.5º. Leucine and the sodium ions are bound between the superimposable domains in a hydrophobic pocket. These studies show that although there are a number of factors that affect the crystallization of membrane proteins, conditions for crystal growth and expression level can be obtained.

Photoaffinity labeling is another technique that can be used for identifying binding domains and protein-protein interactions of membrane proteins. In photoaffinity labeling, the label or photoprobe is chemically introduced into a biologically active molecule. Upon irradiation, a covalent bond is formed between the light-sensitive ligand and the targeted protein. The ligand contains a tag that allows for detection of the labeled molecule (Dorman and Prestwich, 2000). Unfortunately, photoaffinity labeling also has its pitfalls. For example, proteins with low expression levels may not produce sufficient signals when analyzed with mass spectrometry or Edman degradation, thus hindering the identification of the binding domain. In spite of this limit, a study performed on the Human Angiotensin II type 1 receptor (AngII), which is a transmembrane protein, showed that ligand incorporation occurred between Phe^{293} and Asn^{294} within the seventh TMD (Perodin et al., 2002). The protein was labeled with a radioactive photoaffinity analog of AngII and cleaved with a CNBr solution, and the labeled amino acids were identified using manual Edman degradation. These results illustrate how photoaffinity labels can provide useful information with regards to the location and binding region of membrane proteins.

Mutagenesis is another well-established technique used to study structural and functional characteristics of membrane proteins (Uhl and Lin, 2003; Surratt et al., 2005). A substitution of F93 with alanine in the human erythropoietin receptor resulted in a dramatic decrease in substrate binding (Middleton et al., 1996). Substitutions with tyrosine or tryptophan at F93 produced less dramatic effects on substrate binding. Mutational studies performed on the human dopamine transporter showed that substitution of isoleucine 152 for valine resulted in reduced substrate transport and CFT binding (Lee et al., 2000). These results demonstrate how mutagenesis studies are useful for identifying residues that contribute to substrate and inhibitor binding, as well as transport.

Transporters

Membrane transport proteins, or transporters, are involved in the movement of ions, small molecules, or macromolecules, such as other proteins, across biological membranes. Transport proteins are transmembrane, or integral membrane, proteins, which makes them capable of transporting extracellular molecules into the cell. The movement of molecules by transporters may be carried out through facilitated diffusion or active transport (Voet & Voet, 1995c). Facilitated diffusion speeds the movement of a chemical through a membrane in the absence of energy input, while active transport requires energy input from the cell (Voet & Voet, 1995c). Potassium channels act as pores by utilizing facilitated diffusion to allow the transport of potassium through the cell (Jiang et al., 2002). On the other hand, neurotransmitter sodium symporters use sodium

and chloride gradients as energy sources to transport neurotransmitters into the cell (Ravna et al., 2003a; Yamashita et al., 2005).

One example of a transport protein is the DAT, which is a monoamine transporter responsible for the reuptake of dopamine from the synaptic cleft back into the presynaptic neuron. Along with the DAT, the serotonin transporter is also a monoamine transporter that removes excess serotonin from the synapse (Ravna et al., 2003a). The norepinephrine transporter is another monoamine transporter that terminates neurotransmission through uptake of norepinephrine (Blakely et al., 1994). All three of these monoamine transporters are also Na^+/Cl^--dependent transporters, or neurotransmitter sodium symporters (NSSs) (Chen and Reith, 2000; Ravna et al., 2003a;Yamashita et al., 2005). Sodium and chloride electrochemical gradients are used for movement of their substrates. Although LeuT is not a monoamine transporter, it is a NSS. Instead of terminating the synaptic transmission of biogenic amines, LeuT is responsible for the uptake of the amino acid leucine (Yamashita et al., 2005).

Transport proteins are thought to possess two gates that open and close sequentially (Figure 1.2), which allows access to the binding sites from either side of the membrane bilayer (Reith, 1997; Korkhov et al., 2006). The crystal structures of the LacY and Glycerol-3-Phosphate (GlpT) transporters revealed that both transporters undergo a conformational change, where the ligand binding site is alternatively accessible to only one side of the membrane for a period of time, not both simultaneously (Locher et al., 2003). Binding of the ligand causes the transporter to alternate between inward- and outward-facing orientations. This allows the ligands to be transported from the

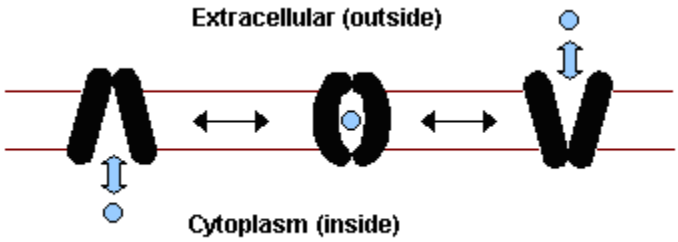

Figure 1.2 Transport Mechanism Used by Membrane Transport Proteins. Opening of the transporter occurs when one or more molecules bind to its particular binding site. The molecules are then transported into or out of the cell.

extracellular matrix into the cell. Similarly, a crystal structure of LeuT showed a bound substrate with both the intracellular and extracellular gates closed (Yamashita et al., 2005). This suggests that the transport mechanism of these transporters has three stages: open to extracellular, closed to both extracellular and intracellular, and open to intracellular (Henry et al., 2006a). Investigating the molecular mechanisms by which these and other transporters couple and transport their substrates will extend our knowledge to understanding the transport mechanism and structure of transport proteins.

Dopamine Transporter Function and Structure

Function of DAT

Dopamine (DA) uptake through the DAT is vital for the maintenance of normal DA homeostasis in the brain. The DAT is responsible for controlling extracellular DA concentrations by reuptaking synaptic DA molecules back into the presynaptic neurons (Uhl et al., 2002; Giros et al., 1996), which helps regulate the intensity and duration of dopaminergic transmission. The driving force for DA uptake is created from an ion concentration gradient that causes the co-transport of two Na^+ ions, one Cl^- ion, and the substrate (DA) (Torres et al., 2003b). The use of this ion concentration gradient classifies the DAT as a carrier and a member of the Na^+/Cl^--dependent family of neurotransmitter transporters.

Electrophysiological studies have revealed that DAT also exhibits channel-like properties (Kahlig et al., 2005; Carvelli et al., 2004). DAT has been shown to be capable

of mediating DA efflux (Khoshbouei et al., 2005). The activity of DAT was determined to be induced by DA and increased by neurons overexpressing DAT (Blakely and DeFelice, 2007). These studies demonstrate that in addition to a carrier, DAT also acts as a channel and directly modulates membrane potential and neuronal function.

Recently, a number of proteins that regulate the function of DAT have been identified (Torres, 2006). Using the yeast two-hybrid system (Y2H), Hic-5 and α-synuclein were identified as having protein-protein interactions with DAT (Carneiro et al., 2002; Lee et al., 2001; Wersinger and Sidhu, 2003). Hic-5 associates with the intracellular carboxyl terminus of DAT. Overexpression of Hic-5 has been shown to reduce DAT activity by decreasing the plasma membrane levels of the transporter, which suggests a role for this protein in the regulation of DAT. The non-Aß amyloid component of α-synuclein in both Ltk(-) and HEK293 cells binds directly to the carboxyl-terminal tail of hDAT. It has been suggested that this interaction alters the functional properties of DAT by accelerating cellular DA uptake and DA-induced cellular apoptosis. In contrast to these findings, Wersinger and Sidhu (2003) observed a decrease in DAT activity when α-synuclein was overexpressed. Their results show both an acceleratory and inhibitory effect of α-synuclein on DAT functionality, suggesting the importance of DAT-interacting proteins on the function of the transporter.

DAT is an essential membrane protein that controls locomotion, cognitive processes, neuroendocrine secretion, and reward systems (Giros et al., 1996; Lin et al., 2003). Consequently, dysfunctions of DAT contribute to the development of several neurological and psychiatric disorders (Torres, 2006). A major disorder with which DAT has been associated is attention-deficit hyperactivity disorder (ADHD). DAT inhibitors

(methylphenidate and amphetamine) are used in the therapeutic treatment of ADHD, which suggests DAT may be directly involved in the susceptibility of ADHD. Cook and colleagues (1995) evaluated the relationship between ADHD and polymorphisms in DAT using haplotype-based relative risk analysis. Results from this study suggest that DAT is associated with ADHD and that mutations to the DAT gene may increase susceptibility to ADHD. It has also been proposed that DAT contributes to the pathogenesis of Parkinson's disease (Miller et al., 1997; Kampen et al., 2000). DAT is thought to be responsible for the transport of neurotoxins that cause parkinsonism into DA neurons (Kampen et al., 2000). Parkinson's disease is characterized by a substantial loss of midbrain DA neurons. Studies have shown that there is a correlation between the density of DAT expression and the pattern of cell loss in Parkinson's disease (Miller et al., 1997). In addition to ADHD and Parkinson's disease, drug addiction has also been associated with DAT (Kuhar et al., 1991). Cocaine and other psychostimulant drugs are believed to work by blocking DAT, thereby increasing the concentration of DA in the synapse (Kuhar et al., 1991). Elevated levels of DA in the mesolimbic system appear to contribute significantly to the reinforcing and stimulating effects of cocaine (Ritz et al., 1987; Koob and Bloom, 1988; Kuhar et al., 1991). This effect of the psychostimulants establishes the important role DAT plays in drug addiction.

Structure of DAT

The human DAT (hDAT) is an 80kDa integral protein that contains 620 amino acids (Figure 1.3). Its size is relatively similar to that of other monoamine transporters (Qian et al., 1995) such as the norepinephrine (NET) and serotonin (SERT) transporter,

MSKSKCSVGLMSSVVAPAKEPNAVGPKEVELILVMEQNGVQLTSSTLTNPRQSPVEAQDRETW
GKKIDFLLSVIGFAVDLANVWRFPYLCYKNGGGAFLVPYLLFMVIAGMPLFYMELALGQFNREGA
AGVWKICPILKGVGFTVILISLYVGFFYNVIIAWALHYLFSSFTTELPWIHCNNSWNSPNCSDAHPG
DSSGDSSGLNDTFGTTPAAEYFERGVLHLHQSHGIDDLGPPRWQLTACLVLVIVLLYFSLWKGV
KTSGKVVWITATMPYVVLTALLLRGVTLPGAIDGIRAYLSVDFYRLCEASVWIDAATQVCFSLGVG
FGVLIAFSSYNKFTNNCYRDAIVTTSINCLTSFSSGFVVFSFLGYMAQKHSVPIGDVAKDGPGLIFII
YPEAIATLPLSSAWAVVFFIMLLTLGIDSAMGGMESVITGLIDEFQLLHRHRELFTLFIVLATFLLSLF
CVTNGGIYVFTLLDHFAAGTSILFGVLIEAIGVAWFYGVGQFSDDIQQMTGQRPSLYWRLCWKLV
SPCFLLFVVVVSIVTFRPPHYGAYIFPDWANALGWVIATSSMAMVPIYAAYKFCSLPGSFREKLAY
AIAPEKDRELVDRGEVRQFTLRHWLKV

Figure 1.3 Amino Acid Sequence of the Human Dopamine Transporter (hDAT)

(adapted from Giros and Caron, 1993).

which consist of 617 and 630 residues, respectively. Alignment of the amino acid sequences of these transporters reveals that some segments within these proteins share a higher degree of homology (Qian et al., 1995). Monoamine transporters are Na^+/Cl^- cotransporters, which may account for their homologous sequences. LeuT has a low level of similarity to DAT (20%), SERT (21%), and NET (24%), although it also belongs to the Na^+/Cl^--dependent family (Beuming et al., 2006). Despite this overall low sequence homology, a few regions are highly conserved throughout the family (Beuming et al., 2006). The conservation of transmembrane domains 1, 3, 6, and 8, which form the ligand binding site in LeuT, suggests that they are involved in substrate transport and are essential for function. Since the structures of DAT, NET, and SERT have not been determined, the crystal structure of LeuT (Yamashita et al., 2005) offers some insight into the architectural orientation of the other Na^+/Cl^--dependent transporters. LeuT consists of 12 transmembrane domains where TM1-5 and TM6-10 are superimposable by a rotation of 176.5º. TM1 and TM6 are in direct contact with the binding site of leucine (the substrate) and the sodium ions. If the molecular structure of LeuT and other Na^+/Cl^--dependent transporters correlate, TM1 and TM6 play a vital role in the substrate binding of DAT, SERT, and NET as well.

The topological arrangement of DAT consists of 12 membrane-spanning α-helices with intracellular amino and carboxyl-terminal domains (Figure 1.4). There are three putative N-linked glycosylation sites on the large extracellular loop between TM3 and TM4. DAT also contains a number of potential phosphorylation sites on the intracellular domains, which suggests that kinases may mediate regulation of the transport process. Numerous studies have examined the effects of phosphorylating conditions on DAT

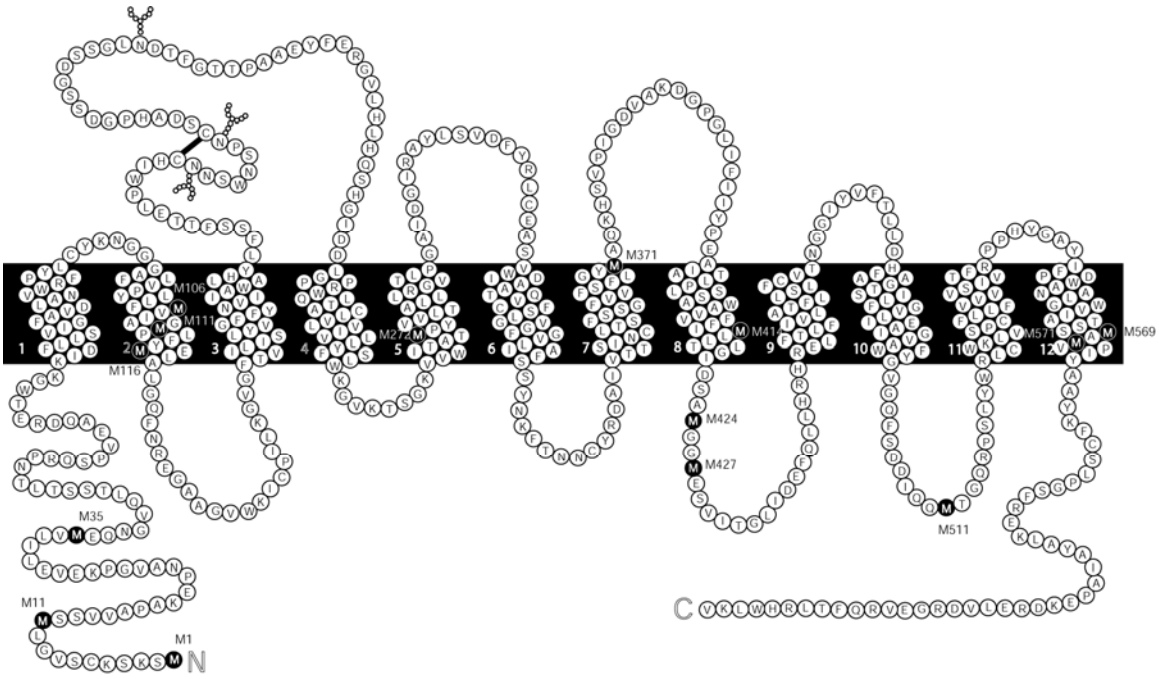

Figure 1.4 Sequence and Topology of the Human Dopamine Transporter (hDAT). Cysteines 180 and 189 in the second extracellular loop are disulfide bonded. Asparagine residues 181, 188, and 205 in the second extracellular loop are linked with glycosyl groups. Methionine residues are indicated as black circles with white letters (from Giros and Caron, 1993).

activity and trafficking (Carvelli et al., 2002; Morón et al., 2003). Activation of phosphatidylinositol (PI) 3-kinase increases DA uptake. On the other hand, inhibition of PI 3-kinase induces internalization of hDAT, thereby decreasing DA transport. Similarly, inhibition of mitogen-activated protein kinase (MAPK) also reduces DA transport (Morón et al., 2003). Overexpression of MAPK has been demonstrated to increase DA transport (Morón et al., 2003). These studies reveal that the phosphorylation of DAT correlates with its transporter activity and trafficking.

hDAT also contains a Zn^{2+} binding motif between extracellular loop 2, TM7, and TM8 (Norregaard et al., 1998). Zn^{2+} serves a structural role for stabilizing the transporter domains. Previous data have indicated that upon binding, Zn^{2+} can inhibit uptake of DA and enhance binding of cocaine analogs (Loland et al., 2003). Zn^{2+} has also been shown to reverse transport of hDAT (Scholze et al., 2002). Results from these studies illustrate the ability of Zn^{2+} to mediate conformational changes in hDAT that are critical for the transport process. In addition to having a Zn^{2+} binding motif, DAT also has a Leucine zipper-like motif within TM2 and TM9. Leucine mutations within TM2 yield a nonfunctional transporter that is smaller in size than wild-type hDAT and is unable to be expressed in the plasma membrane (Torres et al., 2003a). In contrast, site-directed mutagenesis studies on leucine residues in TM9 found similar kinetic and pharmacological properties to that of the wild-type transporter. It has been suggested that the leucine zipper motif in TM2 contributes to the oligomerization and trafficking of DAT, which are essential to the functionality of the transporter (Torres et al., 2003a).

The cellular orientation of DAT, along with its trafficking, contributes significantly to the function of the transporter. Recent studies have demonstrated that the

deletion of residues in the amino and carboxyl termini of hDAT inhibits DA uptake and trafficking of the transporter to the cell surface (Torres et al., 2003a). In the same study the oligomerization of DAT was determined to be directly involved in DA transport. Here, two nonfunctional mutant (Y335A and D79G) hDATs inhibited DA uptake in wild-type hDAT without interfering with the trafficking of wild-type hDAT to the plasma membrane. Torres and colleagues (2003a) also performed studies that showed oligomerization was required for trafficking of DAT. The co-expression of mutant hDAT and wild-type hDAT inhibited the expression of wild-type hDAT in the membrane. Results from these studies show that the proper assembly and trafficking of DAT to the plasma membrane are necessary for the function of the transporter.

Cocaine and its Effect on DAT

Introduction to Cocaine

Addiction to psychoactive drugs continues to be one of the most significant medical, social, and economic problems facing society. Traditionally, addiction to these drugs was treated as a psychological disorder; however, after scientists and doctors discovered the dangerous physiological effects of the drugs, their abuse was classified as a physiological disorder. Therefore, today drug addiction is defined as a brain disorder characterized by compulsive drug-seeking behavior and uncontrollable drug intake (Koob, 2000). It has been shown that the drugs interact with regions of the brain where

dopaminergic terminals are abundant, specifically the mesolimbic dopaminergic system (Kreek, 2001).

One of the most widely abused drugs is cocaine, a powerful central nervous system stimulant. In 2001, an estimated 27 million individuals in the Unites States had used cocaine at some time; of those, 2 million met the criteria of being dependent on or addicted to cocaine (Kreek, 2001). The key motivator for the usage of cocaine is its ability to create a feeling of excitement and euphoria. Providing the user with greater energy and optimism, cocaine reinforces self-esteem and motivation. Physiologically, cocaine dilates the pupils, constricts blood vessels, and increases blood pressure, body temperature, and respiratory rate (Dusek and Girando, 1988).

Effect of Cocaine on Monoamine Transporters

In recent years, science has progressed substantially toward identifying the site upon which cocaine acts, although the mechanism through which this action takes place has yet to be determined. Cocaine is a nonselective, competitive inhibitor of monoamine transporters (Ritz et al., 1987). Cocaine binds to the serotonin (5-HT) transporter (SERT) and thus inhibits presynaptic reuptake of 5-HT and elevates its concentration in the synaptic cleft. Cocaine also elevates the synaptic concentration of norepinephrine in the central nervous system by inhibiting presynaptic uptake of norepinephrine by the norepinephrine transporter (NET) (Blakely et al., 1994). The psychostimulant is believed to work on DAT by blocking DA uptake, therefore increasing the concentration of DA in the synapse, which then causes the overstimulation of DA receptors. Although cocaine affects all three monoamine transporters, the reinforcing and stimulating effects of

cocaine seem to depend primarily on its interaction with DAT (Ritz et al., 1987; Koob and Bloom, 1988; Kuhar et al., 1991).

Reinforcing Effect of Cocaine on DAT

Behavioral studies have shown that subjects will self-administer cocaine in order to experience the feeling of euphoria or the "high" that is accompanied with cocaine usage. In self-administration studies with rats, when cocaine was substituted with saline, the subjects ceased self-administering, which caused dopamine levels to rapidly decline (Weiss et al., 1992). Another experiment performed with DAT-knockout mice illustrated that cocaine had no effect on the locomotive activity of the mice when high doses of cocaine were administered (Giros et al., 1996). A study using human volunteers determined that at least 47% of DAT had to be blocked with cocaine for subjects to report a "high" feeling caused by the psychostimulant (Volkow et al., 1997). These results, along with others, helped to establish the important role DA and DAT have on the reinforcing effects of cocaine.

Binding of Cocaine and Other DAT Inhibitors

One of the many attempts to decrease the abuse of cocaine entails using DAT inhibitors (Figure 1.5), which may act as cocaine antagonists. The ideal inhibitor is designed to gradually eliminate the craving for the psychostimulant and facilitate entry into a rehabilitation program where abstinence is the ultimate goal (Rothman et al., 1989; Carroll et al., 1999). In 2005, Desai and coworkers reported the discovery of a DAT inhibitor, JHW007, that antagonizes the behavioral and inhibitory effects of cocaine. The

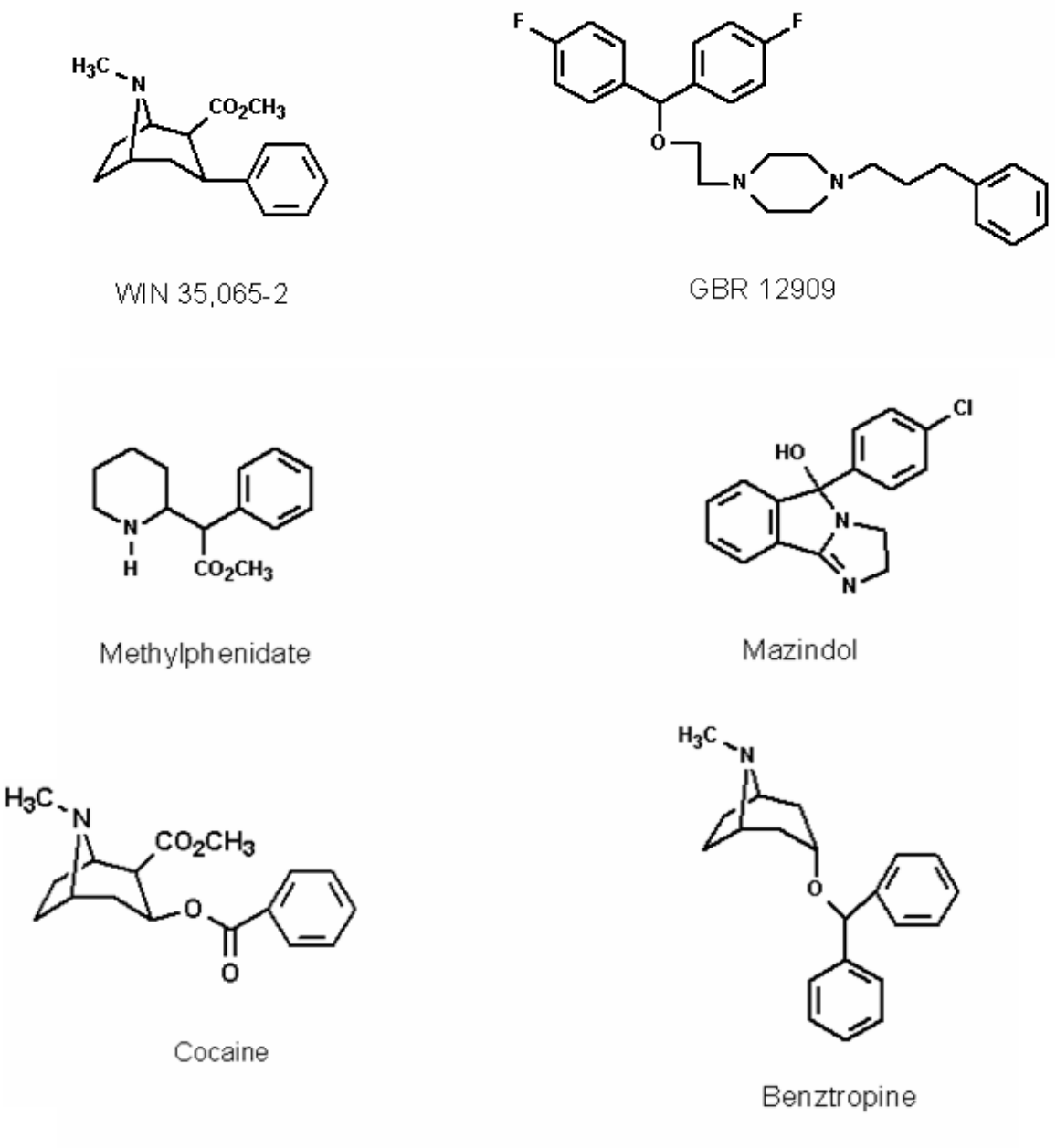

Figure 1.5 Inhibitors of DAT (from Carroll et al., 1999).

authors suggest that JHW007 has the potential to serve as a lead candidate for the therapeutic treatment of cocaine abuse. Studies also show that DAT inhibitors can aid in the identification of the binding domain of cocaine or other regions that may be in close proximity to that of the abused drug (Carroll et al., 1992; Meiergerd and Schenk, 1994). The selective effects of various DAT inhibitors such as GBR compounds, benztropine analogs, 3-aryl tropane compounds, mazindol, and methylphenidate have been characterized extensively for their ability to enhance dopaminergic activity due to inhibition of dopamine uptake (Anderson, 1989; Clarke et al., 1973; Coyle and Snyder, 1969; Hyttel, 1982; Janowsky et al., 1985).

(R)-Cocaine is a tropane alkaloid that is obtained from the leaves of the Erythroxylon coca plant. There are eight stereoisomeric forms of cocaine that currently exist. Carroll et al. (1991b) characterized all eight isomers. The naturally occurring (R)-cocaine had the highest affinity for the dopamine transporter, suggesting that the binding of cocaine to DAT is stereospecific. Other structure activity relationship experiments have shown that by removing the carboxylate group and attaching the phenyl ring of cocaine directly to the tropane ring, the binding affinity of cocaine to DAT is greatly increased (Carroll et al., 1991a). This modified compound, WIN 35,065-2, is a 3-aryl tropane. Tropanes are the largest class of compounds that have been thoroughly investigated due to their high affinity for DAT. Substitution of the para position on the phenyl ring of WIN 35,065-2 with electron-withdrawing (F, Cl, Br, I, NO_2), electron-donating (CH_3O), and neutral (CH_3) groups created analogs with a higher affinity for DAT than (R)-cocaine (Carroll et al., 1991a). In addition, relatively small (Cl, CH_3) as well as large (Br, I) para substituents produced compounds more potent than cocaine. The

binding affinity of WIN 35,065-2 has been reported to be 4.4 times greater than that of cocaine, implying that the aromatic ring of WIN 35,065-2 is more favorably guided into DAT's binding domain than the carboxyl aromatic ring of cocaine (Carroll et al., 1991a). The 3-aryl tropane class of compounds shares some of the basic properties of cocaine, which allows scientists potential avenues for developing medication for cocaine abuse.

GBR 12909 is a selective DA uptake inhibitor that is not a structural analog of cocaine. Because of this, it reduces cocaine's effect on the brain and may help treat cocaine addiction. Studies have shown that GBR 12909 is less efficient than cocaine at elevating DA-mediated behavior (Rothman, 1989). Nevertheless, GBR 12909 has a much higher binding affinity for DAT than cocaine and a slower dissociation from DAT (Newman and Kulkarni, 2002). In addition, several GBR analogs containing quinoline and naphthalene have structural elements that have been found to have a higher binding affinity for SERT than DAT (Matecka et al., 1997). This evidence, along with other information, has led researchers to the investigation of other receptors and transporters that cocaine affects. In the course of these studies, it has been determined that structural modifications to rimcazole, a sigma receptor antagonist that closely resembles GBR 12909, improve its binding affinity to DAT (Newman and Kulkarni, 2002). This discovery provides another interesting set of ligands for molecular modeling in order to further establish the structural elements important for high affinity and selectivity of GBR-related compounds to DAT.

Another drug, known as benztropine, is one of the most potent drugs used in the treatment of Parkinson's disease. Its ability to dramatically inhibit DA uptake over that of norepinephrine and serotonin demonstrates that benztropine has a high affinity to DAT as

opposed to the other monoamine transporters (Coyle and Snyder, 1969; Newman et. al., 1995; Agoston et al., 1997). Compared to 3-aryl tropanes, analogs of benztropine have reversed potency such that the β-isomers are less potent than the α–isomers (Kim et al., 2003). Preliminary behavioral evaluation of these analogs suggests that they lack the capability to cause cocaine-like effects on animal models, which makes them unsuitable for use as a therapeutic treatment for cocaine abuse (Kline et al., 1997). However, the tropane ring, as found in cocaine, and the diphenyl ether functionality, which is similar to that of GBR 12909, give rise to the possibility that benztropine may be an ideal template for the design of novel DA uptake inhibitors (Newman et al., 1994).

Mazindol, an imidazoisoindol derivative, is a tricyclic compound clinically used as an appetite suppressant. Binding studies have shown that mazindol is a potent inhibitor of both norepinephrine and DA uptake (Hyttel, 1982). By extending the five-membered imidazole ring to a six-membered ring, the binding affinity of mazindol to DAT increases by more than two fold. In contrast, expanding the five-membered ring to a seven-membered ring does not further enhance binding (Dutta et al., 2003). Due to the non-addictive effect of mazindol on humans (Chait et al., 1987) and its ability to inhibit DA uptake, further investigation of mazindol may lead to the development of medications for the treatment of cocaine abuse.

The psychostimulant methylphenidate, also a DAT inhibitor, has a higher affinity for DAT than for the other monoamine transporters (Pan et al., 1994). The binding of methylphenidate to DAT has been shown to be twice that of cocaine (Volkow et al., 1999). DL-Threo-methylphenidate (Ritalin), a derivative of methylphenidate, is used to sustain the attention of children with ADHD (Hubbard et al., 1989). The two chiral

centers of methylphenidate cause it to exist in four stereoisomeric forms. The D form of the threo-isomers is 14 times more potent than its L conjugate (Dutta et al., 2003). Animal behavioral studies suggest methylphenidate has reinforcing effects similar to that of cocaine (Bergman et al., 1989). However, in humans its reinforcing ability appears to be substantially lower (Volkow et al., 1999). These results suggest that methylphenidate has the attributes necessary to serve as a lead candidate for the treatment of cocaine dependence, although to date it is not used in the therapeutic treatment of cocaine abuse.

Understanding the Cocaine Binding Site in DAT

Numerous studies using DAT inhibitors have extended our understanding of the structural basis of the cocaine binding site on DAT. Site-directed mutagenesis is one of the many tools that have proven useful in obtaining information about the molecular structure of cocaine's binding pocket. Mutational analysis of Asp79 in TM1 of DAT has shown that aspartate at this position is important for cocaine binding (Kitayama et al., 1992). In this study, replacing aspartate with alanine, glycine, and glutamate reduced the affinity for the tritium-labeled cocaine analog, CFT. Other mutations of aspartate to asparagine at positions 68, 313, 345,and 436 also decreased the binding affinity of CFT, suggesting that aspartate at these locations has an influence on cocaine binding as well (Chen et al., 2001).

Other mutational studies using a substituted cysteine accessibility method (SCAM) have also been used to identify residues and transmembrane domains involved in cocaine binding. In SCAM, all reactive cysteines are removed from a target protein and single cysteine mutations are introduced back into the protein. Thiol-specific

reagents are then allowed to react with the cysteine to determine whether the region surrounding the cysteine is water accessible (Javitch, 1998). The water accessibility of the cysteine is measured by analyzing the effect the reaction between the thiol-specific reagents and cysteine has on substrate transport and/or inhibitor binding. Cysteines placed within transmembrane domains are inaccessible to some thiol-specific reagents (Bogdanov et al., 2005). Thus, if the cysteine does not react with the membrane impermeable thiol-specific reagent, that particular domain is considered impermeable to the reagent and therefore inaccessible to the binding of any ligand or substrate. Experiments performed using SCAM on hDAT alanine 399, which is located near transmembrane domain 8, determined that the sulfhydryl-reactive reagent MTSET reacts with the cysteine at position 399 (Norregaard et al., 2003). This derivatization was inhibited in the presence of the cocaine analog [^{3}H]CFT (Norregaard et al., 2003). These findings suggest that A399C or a segment of transmembrane domain 8 is exposed to an aqueous environment and may be in the cocaine binding site. There is also a possibility that cocaine causes a conformational change that decreases the accessibility of the functional groups at position 399. Another study performed with SCAM, where 21 residues in transmembrane domain 2 (TM2) were mutated to cysteines, demonstrated that TM2 was not water accessible due to its lack of reaction with MTS derivatives (Sen et al., 2005). TM2 was further analyzed in the same study by crosslinking several residues using mercuric chloride. Crosslinking of these residues was inhibited by the presence of the cocaine analog MFZ 2-12, suggesting that TM2 may indirectly contribute to the cocaine binding site (Sen et al., 2005).

As stated previously, x-ray crystallography is another well-known method used to determine the three-dimensional or tertiary structure of a protein that gives scientists insight into understanding not only the molecular conformations of a protein but also its inhibitor and substrate binding sites. This is done by purification and crystallization of the target protein followed by measurement and analysis of data, which then leads to model building and refinement (Voet and Voet, 1995a). Since the crystal structure of hDAT has yet to be determined, examining the structure of similar transporters could provide useful knowledge for determining the cocaine binding site of hDAT. As stated previously, Yamashita et al. (2005) resolved the crystal structure of LeuT and identified TM1 and TM6 as being in direct contact with the substrate (leucine) and sodium ion binding site. Further structural analysis of the LeuT determined that the inhibitor and substrate binding site are nonoverlapping (Zhou et al., 2007). This model identified residues in TM1, TM6, extracellular loop 4 (EL4), and TM10 as the main regions involved in the inhibitor binding site of LeuT. If the molecular structure of LeuT and DAT correlate, it is possible that TM1, TM6, EL4, and TM10 are involved in the cocaine binding site of DAT.

Photoaffinity labeling is another technique used to map out the cocaine binding site. This method employs DAT photoaffinity ligands (Figure 1.6) that have a similar pharmacophore to cocaine. Once irreversibly bound to the transporter, the ligands label specific sites on the protein, which leads to the possibility of identifying the interacting or binding site of cocaine at the molecular level. The overall peptide mapping pattern of DAT labeled with [^{125}I]DEEP, a GBR analog, identified a 4kDa region near transmembrane domains 1-2 (TM1-2) of the transporter (Figure 1.7) (Vaughan, 1995; Vaughan and Kuhar, 1996). Similarly, [^{125}I]GA 2-34, a tropane-based ligand, has also

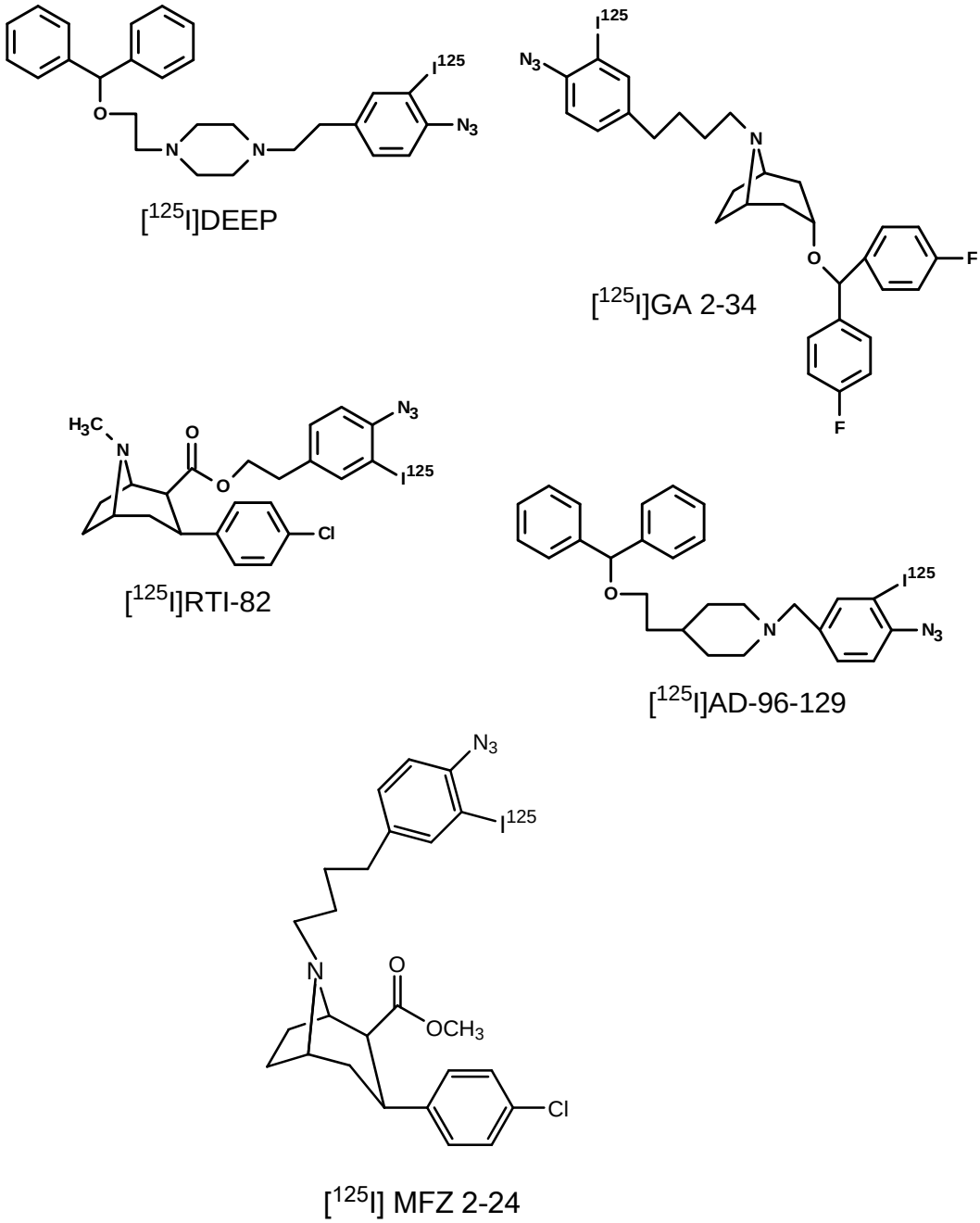

Figure 1.6 Radiolabeled Photoaffinity Ligands. DEEP and AD-96-129 are GBR analogs, RTI-82 is a cocaine analog, and MFZ 2-24 and GA 2-34 are tropane-based DA uptake inhibitors.

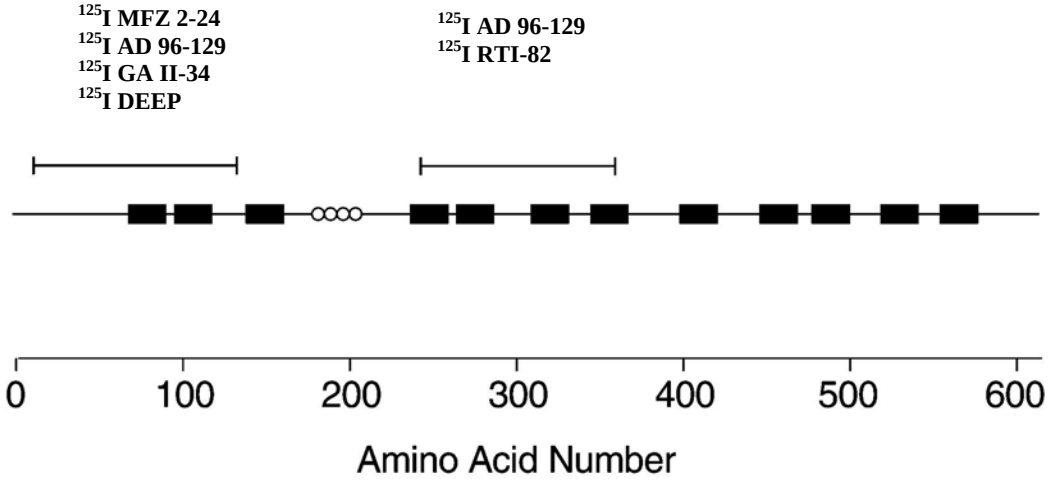

Figure 1.7 Summary of DAT Photoaffinity Ligand Binding Sites. This schematic of the rDAT primary structure shows the transmembrane domains represented by black rectangles. Consensus glycosylation sites are shown as open circles. The ligands are listed above the regions where they are photoincorporated (adapted from Vaughan et al., 2001).

been shown to label near TM1-2 and TM2 of DAT (Figure 1.7) (Vaughan et al., 1999). Experimental studies using [^{125}I]MFZ 2-24 suggest that it is incorporated within TM1 (residues 68-80) (Figure 1.7) (Parnas et al., 2008). On the other hand, [^{125}I]RTI-82, a cocaine analog, labeled a 10kDa fragment between TM4-TM6 (Vaughan et al., 1999). Further analysis by Vaughan et al. (2007) determined that TM6 (residues 292-344) is the [^{125}I]RTI-82 labeled fragment of hDAT (Figure 1.7). However, comparison of a novel photoaffinity ligand, [^{125}I]AD-96-129, with previously characterized labels suggests that it interacts with both regions to the same degree (Vaughan et al., 2001). The dual incorporation of [^{125}I]AD-96-129 establishes the possibility that TM1-2 and TM4-6 (Figure 1.7) may be in close proximity to one another and critical for the binding of multiple uptake inhibitors. From these findings it can also be proposed that these domains form a ligand binding pocket that accommodates the labels in a certain manner depending on their spatial orientation (Figure 1.8) (Vaughan et al., 2001). Further analysis of the region labeled by the photoaffinity labels may lead to the discovery of the specific amino acid residues that form the cocaine binding domain of hDAT. It has been hypothesized that the photoaffinity labels have different sites of incorporation (Vaughan et al., 2001). Through analysis of the labels by peptide mapping studies of DAT, it has been suggested that they are accommodated by a binding pocket that allows each label to bind in a distinct manner according to its molecular structure (Vaughan et al., 2001). Modification to this binding pocket may also provide evidence as to whether or not cocaine interacts with the same binding domain as multiple other DA uptake inhibitors.

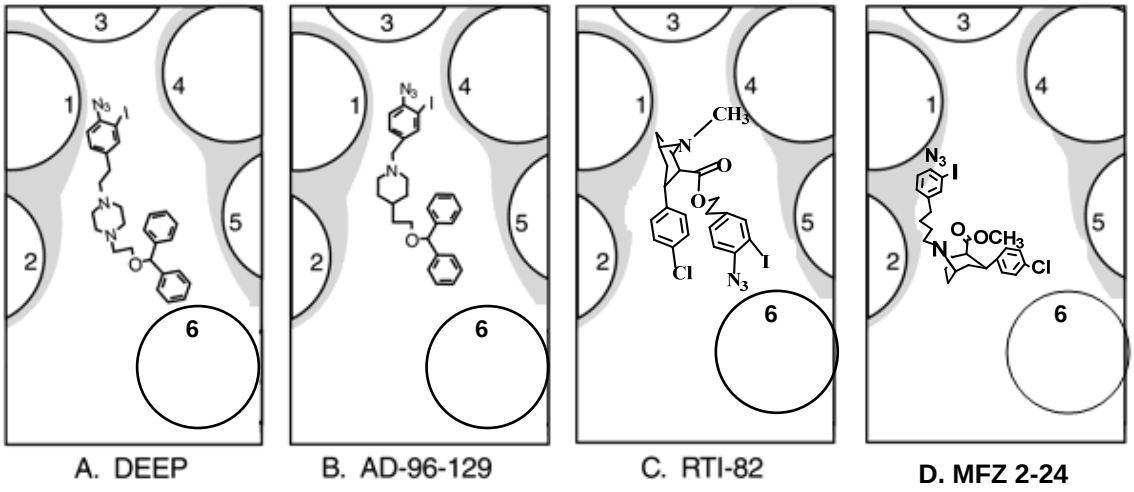

Figure 1.8 Photoaffinity Labels Binding to DAT. The cross-sectional view of the ligand binding pocket is shown. Transmembrane domains are indicated with numbered circles and arranged arbitrarily to accommodate the azido groups covalently labeling either TM1-2 (DEEP), TM1 (MFZ 2-24), TM6 (RTI-82), or TM1-2 and TM4-6 (AD 96-129) (adapted from Vaughan et al., 2001).

By utilizing the information obtained from mutational, x-ray crystallography, and photoaffinity labeling studies, a molecular model illustrating the possible orientation of the cocaine binding site of hDAT can be constructed. Recent modeling studies used the crystal structure of LeuT as a template for modeling the inhibitor binding site of DAT (Zhou et al., 2007). When the authors compared their structure of LeuT to that of LeuT with bound substrate (Yamashita et al., 2005), neither the leucine substrate nor the two sodium ions moved. From this finding, Zhou and coworkers (2007) concluded that the inhibitor binding site is distal from that of the substrate binding pocket. The desipramine (inhibitor) binding pocket is formed by interactions of the inhibitor with R30, Q34, F253, F319, F320, L400, and D401 of LeuT (R85, L89, F320, G386, P387, F472, and T473 in DAT, respectively) (Figure 1.9). R30 forms cation-π interactions with the third desipramine ring and the phenylalanine ring of F253.Q34 makes intermolecular contacts with the first ring of desipramine. Residues A319, F320, L400, and D401, in extracelluar loop 4 (EL4) and TM10, form salt bridges with the inhibitor that helps hold the molecule in place. This model suggests that TM1, TM6, EL4, and TM10 are the main regions involved in the inhibitor binding site of DAT. Using LeuT and other transporters as a model for DAT to map out the molecular structure of the cocaine binding site, will offer a better understanding of the interaction between cocaine and DAT.

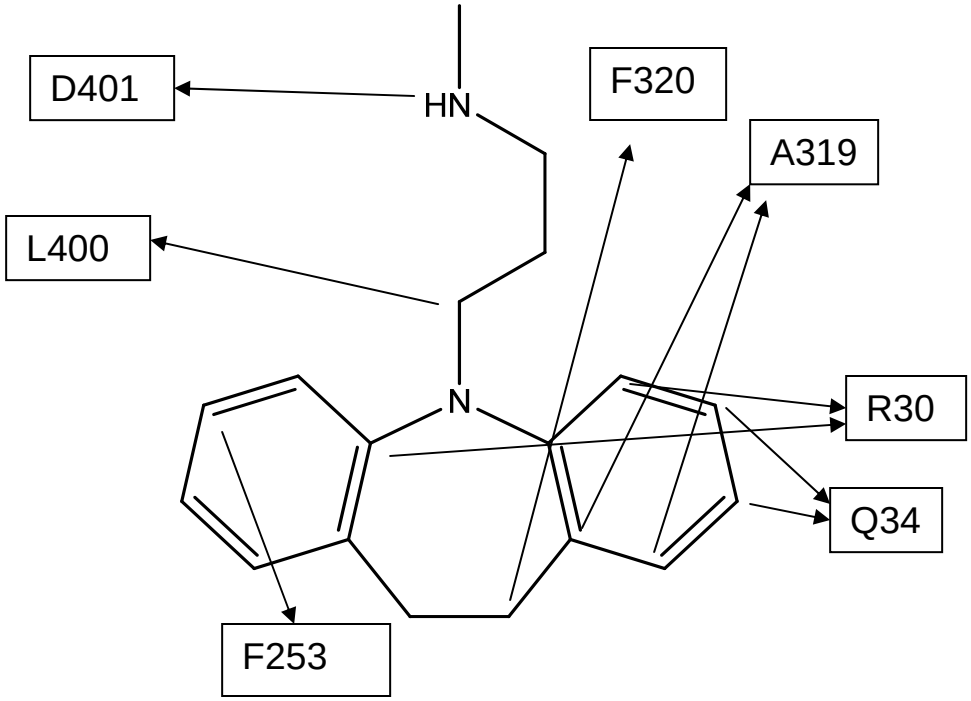

Figure 1.9 Molecular Contacts Between LeuT and a Bound Desipramine Molecule. The chemical structure of desipramine is shown together with LeuT residues that are in direct contact with the drug. Residues from LeuT are indicated in boxes (adapted from Zhou et al., 2007).

Photoaffinity Labeling

Introduction to Photoaffinity Labeling

Photoaffinity labeling is a widely used technique for identifying proteins, localizing binding domains, and determining targets of drugs (Fang et al., 1998; Dorman and Prestwich et al., 2000; Li et al., 2006; Robinette et al., 2006). When applied to DAT and other proteins that lack a crystal structure, photoaffinity labeling can offer some insight into the three-dimensional structure of their binding domains. Recently, a radioactive photoaffinity etomidate analog ([^{3}H] azietomidate) was used to identify the amino acids that contribute to the GABA type A receptor ($GABA_AR$) anesthetic binding site (Li et al., 2006). Edman degradation of the labeled fragments isolated from various proteolytic digests of $GABA_AR$ determined that M^{236} and M^{286} are in close proximity to the binding pocket for etomidate. By coupling a radioisotope (^{3}H) to the label, Li et al. (2006) were able to localize and identify the regions of the binding site. Fang et al. (1998) used the properties of photoaffinity labeling in combination with a photocleavable moiety to construct a bifunctional photoaffinity probe (Figure 1.10). The probe allowed separation of the labeled fragments from the nonlabeled fragments. The label was then detached from the cross-linked peptides by photocleavage and the respective peptide fragments were analyzed with tandem mass spectrometry. The advantage of having the photocleavable moiety attached to the label is that it offers identification of the peptide or amino acid residue(s) without any interference or complications from the radioisotope.

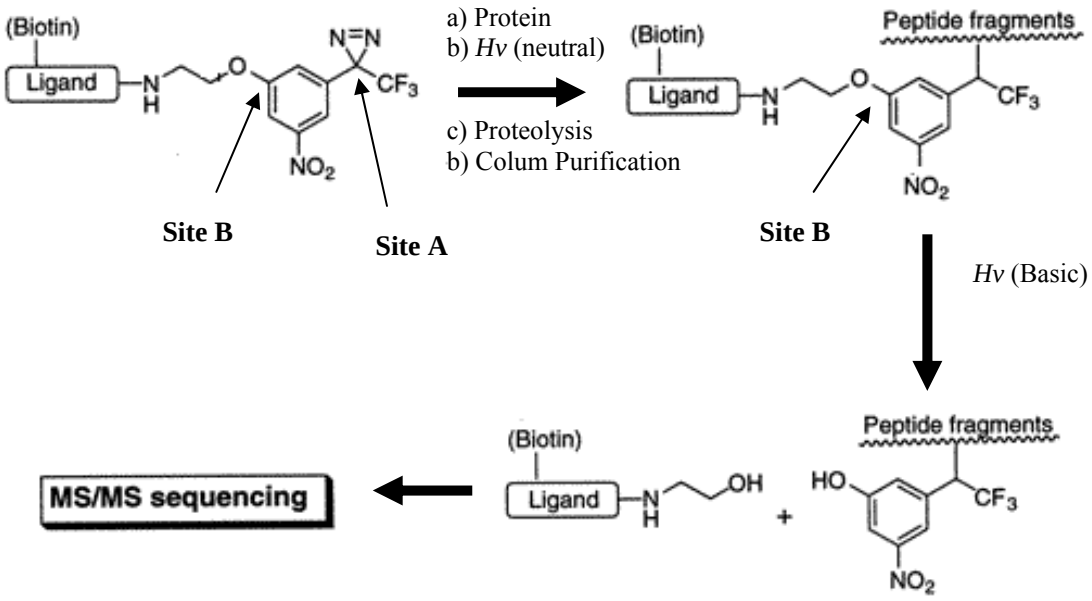

Figure 1.10 Conceptual Outline of Bifunctional Photoaffinity Probe. The bifunctional probe binds to its target protein through Site A. The protein is then cleaved chemically or enzymatically and the labeled fragments are separated from the nonlabeled fragments. Purification with this particular probe occurs using an avidin column and the biotin tag attached to the ligand. Once the labeled fragments are separated, the photocleavable moiety is detached from the fragments through Site B. The labeled fragments are then identified using mass spectrometry (from Fang et al., 1998).

Photoaffinity labels are designed to bind to a specific binding site (Figure 1.11). Once bound, the ligand is then irradiated to allow formation of a covalent bond between the target protein and the label. The labeled protein of interest then undergoes proteolytic and/or chemical fragmentation, which forms peptides. These labeled peptides are then localized using immunological methods, high performance liquid chromatography (HPLC), and/or gel electrophoresis. Identification of the residue(s) covalently linked to the ligand is determined by mass spectrometry or Edman degradation. The chemical structure of photoaffinity labels usually consists of radioisotope and photoreactive groups. The radioisotope group allows simple localization of the labeled peptides while the photoreactive group is responsible for forming or cleaving a bond. The photoreactive group in photoaffinity labeling forms a bond between the protein or surface of interest and the ligand (Dorman and Prestwich, 2000).

Types of Photophores Used in Photoaffinity Labeling

The common photoreactive groups used for photoaffinity labeling are benzophenones, diazirines, and aryl azides (Figure 1.12). Benzophenones are thought to be the most efficient photoprobe utilized in photoaffinity labeling studies. The chemical stability of benzophenones in protic solvents contributes to the high crosslinking yield that is absent when using diazirines and aryl azides (Dorman and Prestwich, 1994). In addition, benzophenone photophores remain reactive with C-H bonds in the presence of water. Benzophenones can also be manipulated in ambient light and activated at a

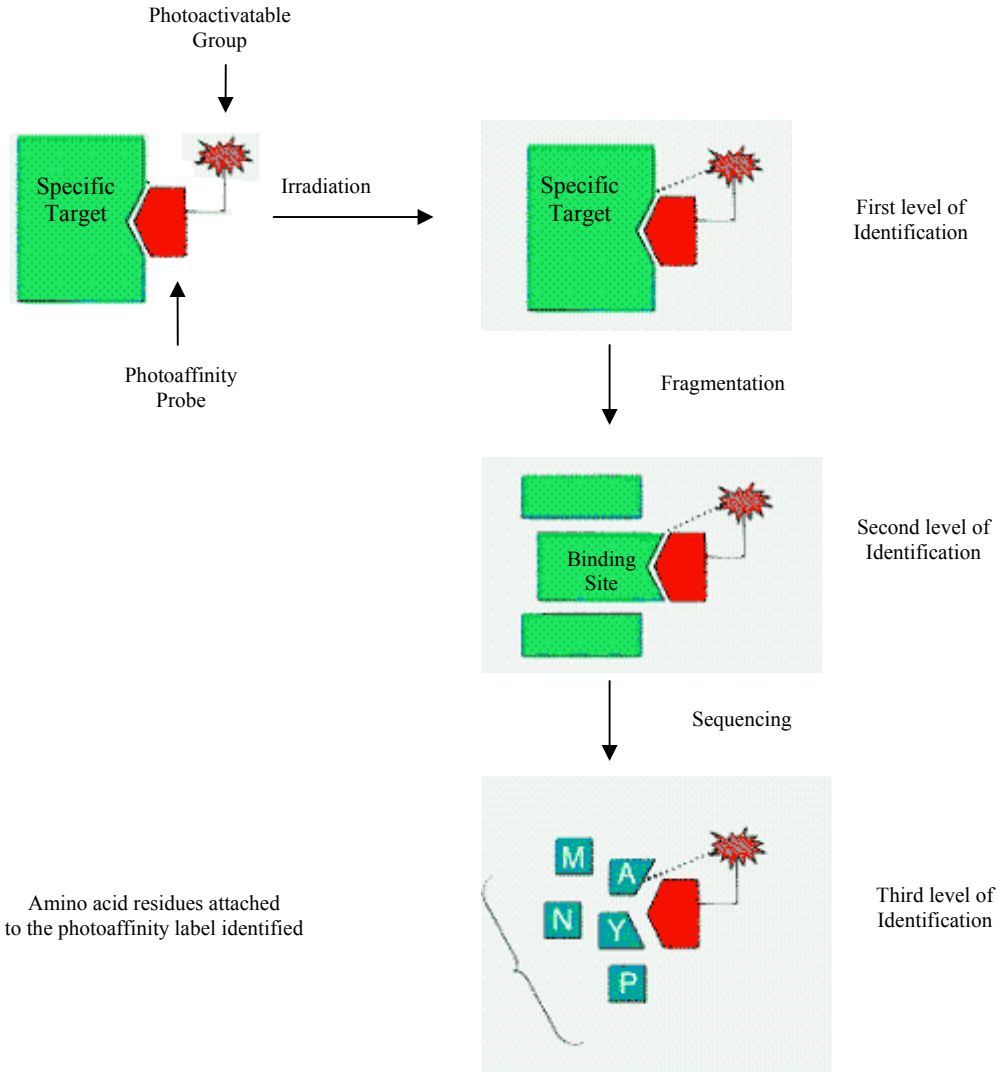

Figure 1.11 Photoaffinity Labeling Scheme. The photoaffinity label binds to its specific target protein. Prior to binding, the protein-label complex is irradiated, forming a covalent bond between the two entities. The dotted lines represent the covalent linkage formed by irradiation. The labeled protein is then fragmented (enzymatically or chemically) and separated from other unlabeled peptides. Residues attached to the photoaffinity label are then identified by sequencing (from Dorman and Prestwich, 2000).

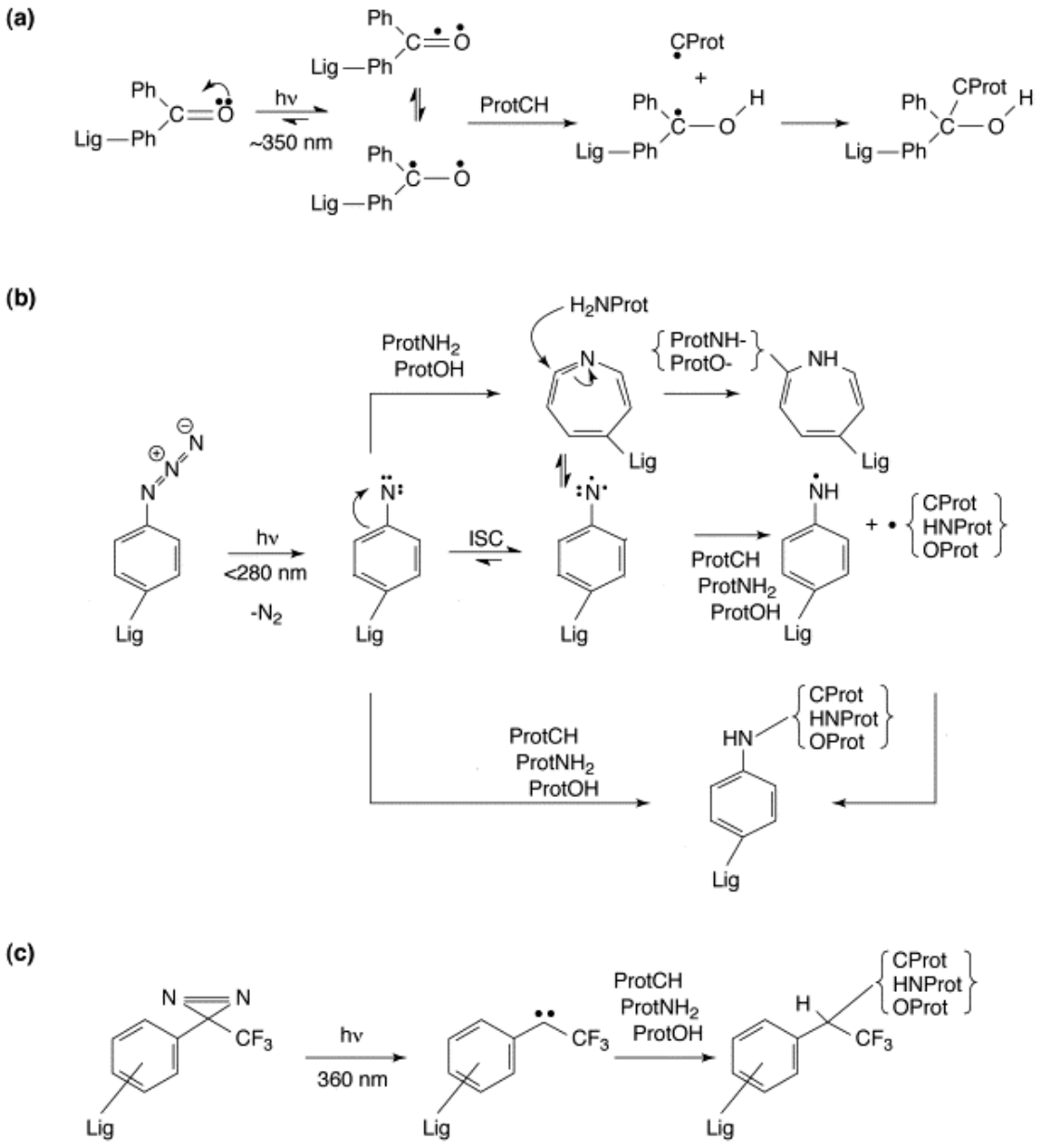

Figure 1.12 Photochemical Events of Three Major Photophores Used in Photoaffinity Labeling. The three major photophores used in photoaffinity labeling are benzophenone, aryl azide, and diazirine. This figure shows (a) benzophenone photochemistry, (b) aryl azide photochemistry, and (c) diazirine photochemistry. ISC; Intersystem crossing (from Dorman and Prestwich, 2000).

wavelength that does not damage the protein (Robinette et al., 2006). Benzophenone-based photoreactive reagents have been used for efficient protein crosslinking of several proteins, including ATP synthase (Vik and Ishmukhametov, 2005), troponin (Ward et al., 2003), glutamate dehydrogenase (Madhusoodanan and Colman, 2001), and calmodulin (Strasburg et al., 1988). Studies have also shown that the amino acid specificity of benzophenone can vary depending on the solvent used during photoirradiation (Deseke et al., 1998). In acetonitrile, benzophenone is more reactive with Gly and Met as opposed to Thr, Leu, Phe, Val, Ala, Ile, Ser, and Glu. On the other hand, when the reaction is performed in 80% pyridine, benzophenone reacted mostly with Pro and Met. The high reactivity of benzophenone with methionine despite the reaction media has been suggested to be due to the chemical stability of the labeled product. Although benzophenone is not the ideal photoprobe, due to its residue specificity, currently it is the most favored probe that produces an efficient single site covalent linkage.

Diazirines have also been recognized as a promising photoprobe for protein identification and characterization studies due to its favorable chemical properties and stability. Upon irradiation, diazirine produces a carbene, which is a strong electrophile that allows immediate reaction of the label with the target protein (Figure 1.12c) (Tomohiro et al., 2005). The unbound carbene species then reacts with any surrounding water molecules. Similarly to benzophenones, the specificity of diazirines varies depending on the solvent used during photoirradiation (Kotzyba-Hibert et al., 1995). In cyclohexane and alcohol, diazirines give C-H and O-H insertion products, respectively. The hydrophobic properties of this photoprobe allow more efficient labeling and

identification of transmembrane regions of integral membrane proteins than of hydrophilic proteins (White and Cohen, 1992). Studies performed with ^{3}H-diazirine demonstrated that the photoprobe can be used to map the contact regions of protein domains in macromolecular assemblies (Gomez et al., 2006). 3-Trifluoromethylphenyldiazirine is a widely used diazirine derivative for studying ligand binding domains. The cholinergic antagonist ^{125}I-TID (3-(trifluoromethyl)-3-*m*-([^{125}I]iodophenyl)diazirine) was shown to label residues L^{257}, L^{265}, V^{261}, and V^{269}, which surround the channel-forming region of the nicotinic acetylcholine receptor (White and Cohen et al., 1992; White et al., 1991). As described above, several insights into the molecular structure of protein binding sites and interactions have been obtained using diazirine as a photoprobe.

The use of aryl azides in photoaffinity labeling also provides structural data about ligand-protein interaction sites. When irradiated (Figure 1.13), the azide loses a nitrogen to form a singlet nitrene (Kotzyba-Hibert et al., 1995). Singlet nitrenes lack insertion reactions, which causes them to then form a triplet nitrene, bicyclic azirine, or didehydroazepine. Triplet nitrenes lead to a diradical, which then abstracts a hydrogen atom from any nearby molecule. This forms a covalent bond with a free radical on the molecule or protein. The ring expansion that forms bicyclic azirine and didehydroazepine reacts with proximal nucleophiles, which may lead to its insertion into the protein. The chemical reactivity of aryl azides relies on the presence of nucleophilic residues and various substituents on the aromatic

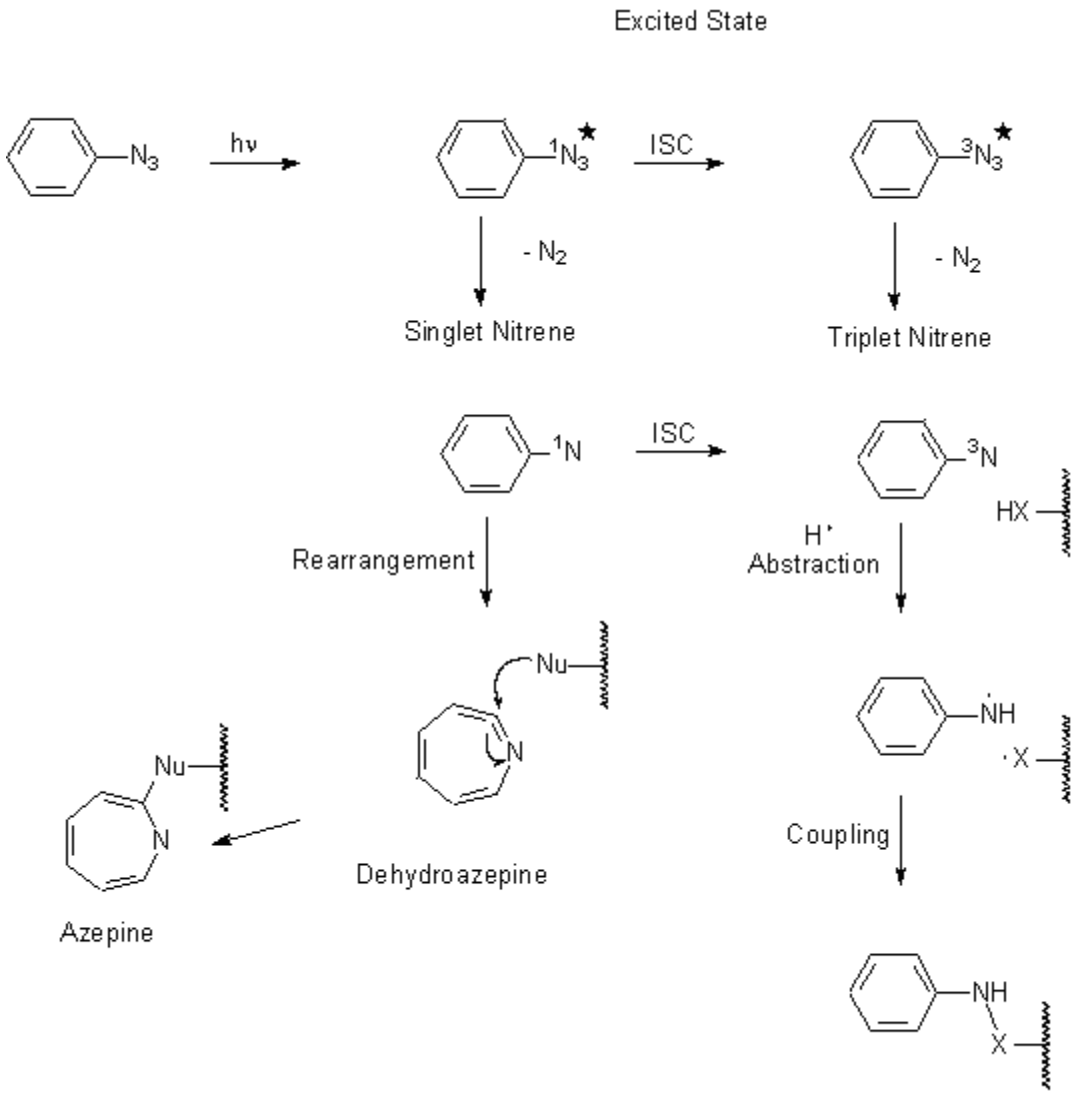

Figure 1.13 Possible Pathways for the Labeling Reaction of Aryl Azides to Biological Proteins. In one pathway, the singlet nitrene rearranges to form a dehydroazepine and reacts with a nucleophile on the target protein. In a second pathway, a triplet nitrene is formed by intersystem crossing (ISC). The triplet nitrene abstracts a hydrogen radical from the target protein and undergoes free radical coupling (adapted from Kotzyba-Hibert, 1995; Watt et al., 1989).

ring (Li et al., 1988; Kotzyba-Hibert et al., 1995). The C-H bond insertion of fluorinated aryl azides occurs at a higher efficiency than does the insertion of nonfluorinated aryl azides (Kotzyba- Hibert et al., 1995). A few caveats to using aryl azides as a photoprobe are its nonspecificity, the ability of the azide to alter the structure of its target residue, and the lack of stability that the nitrenes possess, which all hinder efficient identification of the binding sites (Kaneda et al., 2007; Mishchenko et al., 2000). Schwartz (1989) demonstrated that the specificity of aryl azides varies among amino acids and proteins. When labeled with HAHS amide (ethanolamine 5-azido-2-hydroxy benzoic acid), actin appeared to be about 20 times more reactive than collagen. The specificity HAHS amide has for actin over collagen is due to the reactive amino acids near the binding site on the target proteins. Follow-up studies were performed to determine the reactivity of different amino acids with phenyl nitrenes (Table 1.1). Cysteine was shown to be the most reactive amino acid and glycine the least reactive (Schwartz, 1989). Amino acids differ in reactivity to phenyl nitrenes by a factor of $>10^5$. This suggests that the reactivity of proteins depends on the type and number of reactive amino acids positioned near the label. Though the reactivity of aryl azides varies among amino acids, its use as a photophore for photoaffinity labeling has become a valuable tool for mapping and identifying the binding pocket of ligands.

Photoaffinity Labeling and DAT

Photoaffinity labeling has been used to investigate the cocaine binding site of the DAT. Specifically, labels using aryl azides as the photoprobe have led to the identification of regions involved in the binding domain of cocaine.

Amino Acid	Reactivity Coefficient (M/min)
Cysteine	5.56
Tryptophan	0.033
Cystine	0.001
Tyrosine	0.00067
Phenylalanine	0.00067
Histidine	0.00033
Lysine	0.00033
Arginine	>0.00033
Glycine	>0.000033

Table 1.1 Reactivity of Phenyl Nitrenes with Particular Amino Acids. The reactivity coefficient is defined as the concentration of the residues listed in the table that will react with phenyl nitrene per minute. Cysteine is the most reactive amino acid and glycine is the least reactive amino acid. It is apparent that amino acids differ in reactivity toward phenyl nitrenes by a factor of $>10^5$. This therefore suggests that proteins vary widely in their reactivity, depending on the number of exposed reactive amino acids (Schwartz, 1989).

Using epitope-specific immunoprecipitation of proteolytic fragments, [^{125}I]MFZ 2-24 (see Figure 1.6) is thought to be incorporated near TM1 (residues 68-80) of DAT (Parnas et al., 2008). Other photoaffinity labels such as [^{125}I]DEEP and [^{125}I]GA 2-34 have also been shown to label a region near TM1-2 of the transporter similarly to [^{125}I]MFZ 2-24 (Vaughan, 1995; Vaughan and Kuhar, 1996; Vaughan et al., 1999). Studies using mutagenesis, along with enzymatic and chemical digestion, determined that the photoactivatable cocaine analog, [^{125}I]RTI-82, labels TM6 (residues 291-344) (Vaughan et al., 2007). Investigation of another irreversible photoaffinity label, [^{125}I]AD-96-129, showed that a covalent bond is formed to residues near TM 1-2 and TM4-6 (Vaughan et al., 2001). Figure 1.8 illustrates the possible binding domain of DEEP, AD 96-129, RTI-82, and MFZ 2-24 in DAT. AD 96-129 is photoincorporated in the region labeled by DEEP, MFZ 2-24, and RTI-82.

This thesis focuses on identifying the amino acid residue covalently labeled by [^{125}I]MFZ 2-24. This novel irreversible cocaine analog contains a 2-beta-carboalkoxy-3-beta-(4'-chlorophenyl)tropane pharmacophore with a butyl linker between the tropane nitrogen and the 4'-azido, 3'-iodo-substituted pendant phenyl ring (Zou et al., 2001). MFZ 2-24, which contains the cocaine pharmacophore, is thought to bind in the cocaine binding pocket on the DAT. Upon irradiation, the azido group becomes a highly reactive nitrene that then reacts covalently with an amino acid in the vicinity of the cocaine binding site. Parnas and colleagues (2008) have localized the photoincorporated site of [^{125}I]MFZ 2-24 using enzymatic and chemical digest, immunoprecipitation, and mutagenesis. They propose that the radioligand labels a region within residues 68-80 of TM1. In their experiments, hDAT was electroeluted, dried down, and reconstituted with

an acidic CNBr solution. The drying down of hDAT, which is a hydrophobic protein, causes the protein to aggregate and become unmanageable and difficult to solubilize. Aggregation of hDAT can hinder hydrolysis of the protein by making cleavage sites inaccessible to chemical and/or enzymatic proteolysis. This method of solubilization, which leads to an incomplete digestion of DAT, suggests that the results obtained by Parnas et al. (2008) may not be valid.

The experiments presented in this dissertation utilize various techniques, such as chemical and enzymatic proteolysis, HPLC, and Edman degradation, to localize the photoaffinity labeling site of [^{125}I]MFZ 2-24. A CNBr digest of [^{125}I]MFZ 2-24 labeled hDAT suggests that a small peptide, PLFYM, originating in TM2 contains the site of photoincorporation. In another study, [^{125}I]MFZ 2-24 labeled hDAT was enzymatically digested with thermolysin and analyzed with edman degradation, which determined that the second amino acid from the N terminal end of the hDAT peptide was covalently labeled by [^{125}I]MFZ 2-24. Without a mass determination or sequence analysis of the labeled residue and/or peptide, one can only speculate its identity.

Using peptide mapping of the photoincorporation site of MFZ 2-24 and the other photoaffinity labels described in this introduction, it can be suggested that TM1-2 and TM4-6 may be near one another and essential for the binding of multiple uptake inhibitors. These findings also imply that TM1-2 and TM4-6 may form a ligand binding pocket that accommodates the labels in a certain manner depending on their chemical structure (Vaughan et al., 2001). The continued use of these and other photoaffinity labels will ultimately lead to the identification of the binding site for cocaine and other DAT inhibitors. As of now, the undetermined crystal structure of DAT leaves the door open for

photoaffinity labeling to contribute to understanding the inhibitor binding region and the overall tertiary structure of the membrane protein hDAT.

Chapter Two

Methods

Cell Culture and Photoaffinity Labeling

Cell Culture and Membrane Preparation

HEK 293 cells stably expressing 3xFLAG-6xHis-hDAT were grown on 150 mm plates and a 75 mm flask in a 37°C incubator with 5% CO_2. The medium used for growing HEK cells was DMEM/F12 50/50 Mix (Cellgro) (supplemented with 10% bovine calf serum, 100mg/mL penicillin-streptomycin, 200mM l-glutamine, and 0.001% G418).

Membranes were prepared from FLAG-His-DAT cells grown on 150mm tissue culture plates. Typically 12-36 plates were used in each experiment. Cells grown on plates were washed with 4ml KRH buffer (120mM NaCl, 4.7mM KCl, 2.2mM $CaCl_2$, 1.2mM $MgSO_4$, 1.2mM KH_2PO_4, 10mM glucose, pH 7.4), followed by lysis in 2mM HEPES, 1mM EDTA, for 10min, 4°C. Lysed cells were scraped from the plates and centrifuged (31,000 x g, 4°C, 20min). Membrane preparations were then stored in a -80°C freezer until further use.

Photoaffinity Labeling

Membranes were resuspended in incubation buffer (100mM NaCl, 50mM Tris-base) at pH 7.0. The procedure was repeated to thoroughly wash the membranes. Following the second wash, the pellet was resuspended in incubation buffer, and 5µl of the radioligand added. Ligands were incubated with membranes for 1hr on ice while shaking. For protection of hDAT binding site experiments, the membranes were first incubated with 1mM of WIN 35,428 for 1hr on ice while shaking followed by incubation of the radioligand for an additional hour. Irradiation (254nm) was carried out for 4

minutes using a UVG-11 mercury mineralight lamp (UVP). Labeled membranes were diluted 1:2 in incubation buffer and centrifuged (20,000 x g, 4°C, 20min). Pellets were resuspended in incubation buffer, to wash the membranes, and centrifuged again. If hDAT was to be purified with a nickel affinity column, pellets were brought up in nickel column solubilization buffer (1% Triton X-100, 6 M Urea, 10 mM Imidazole, 30 mM Na2PO4, 300 mM NaCl, pH 7.8) and incubated at 4°C overnight. When purification was not needed, cells were solubilized in FLAG solubilization buffer (1% Triton X-100, 1mM EDTA, 150mM NaCl, 50mM Tris-Cl, pH 7.4) and incubated overnight at 4°C. The sample was then centrifuged for 1 hr at 31,000 x g, 4°C. The supernatant, containing the solubilized radiolabeled membrane proteins, was removed and saved at 4°C for further use. Figure 2.1 summarizes the various methods used to localize the site of [^{125}I]MFZ 2-24 incorporation.

Purification and Isolation of Radiolabeled hDAT

Immobilized Metal Affinity Chromatography

Immobilized metal affinity chromatography (IMAC) columns were prepared by applying 0.4 mL of Ni-NTA agarose (Sigma) slurry to 15 mL columns (Qiagen) resulting in a 0.2 mL Ni-NTA column. The resin was equilibrated with 2 column volumes of equilibration buffer (50mM Na2PO4, 0.3M NaCl, pH 8.0). Solubilized radiolabeled membrane proteins were applied to the column and incubated with the resin for 15 minutes at room temperature to allow binding of hDAT. The resin was allowed to settle and the flow-through was collected. The column was washed with 5 column volumes of

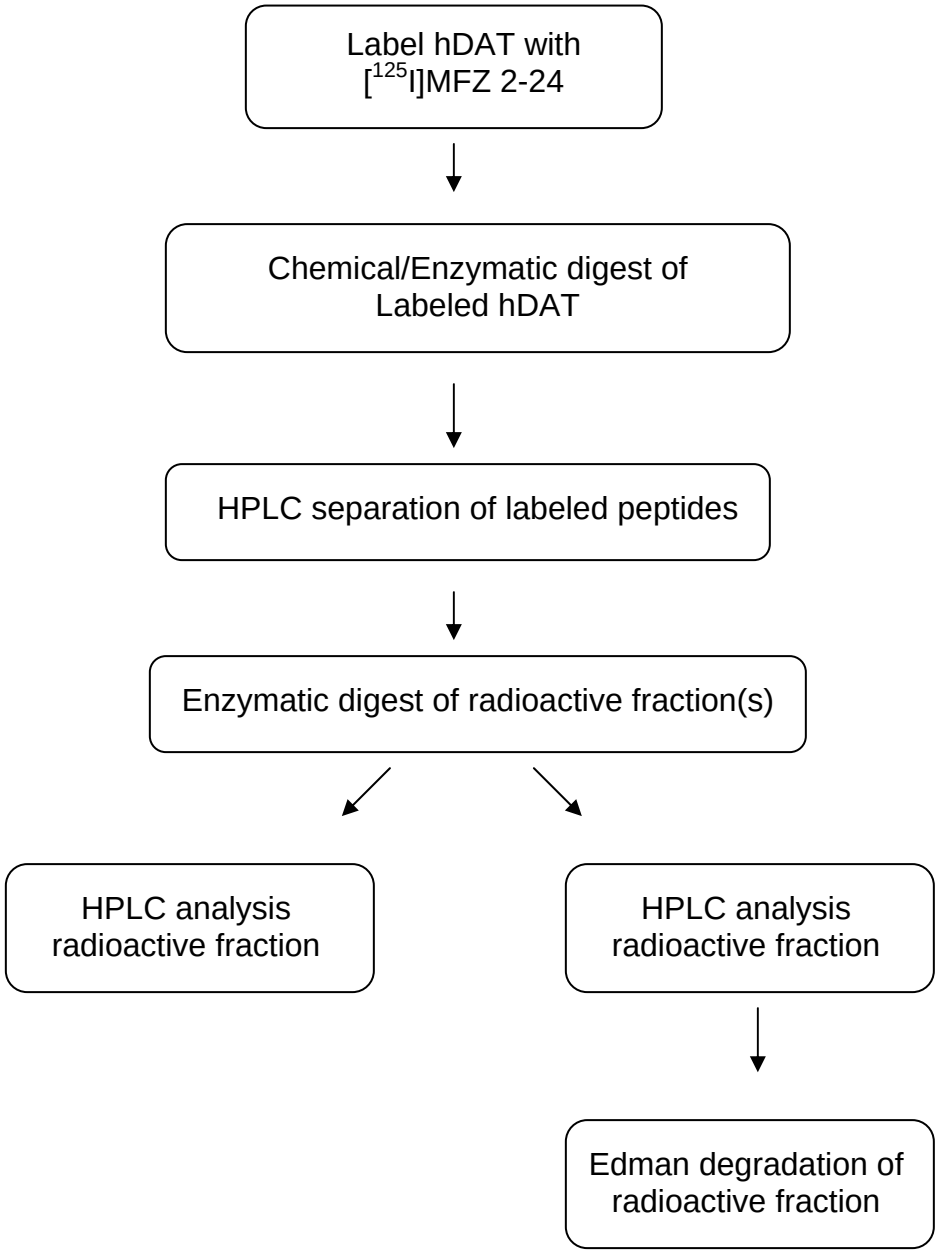

Figure 2.1 Scheme for Localizing the Amino Acid Residue of hDAT Labeled by [^{125}I]MFZ 2-24.

wash buffer (50mM Na2PO4, 0.3M NaCl, pH 8.0). The hexahistidine-tagged hDAT was eluted with 10 column volumes of elution buffer (1M Imidazole, 50mM Na_2PO_4, 0.3M NaCl, pH 8.0) and saved at 4°C for further use.

Gel Electrophoresis and Autoradiography

Radiolabeled hDAT and peptides were separated via SDS-PAGE. The dimensions of the 7.5% polyacrylamide gel for separating radiolabeled hDAT proteins were 16 x 14 x 0.1cm. The 18% mini gel used to separate the radiolabeled hDAT peptides was obtained from Biorad. Sample buffer (30% glycerol, 70% 50mM Tris-Cl, 0.35M SDS, 0.60M DTT, pH 6.8, with bromophenol blue) was added to the samples (1:2 ratio). Electrophoresis was run at 50-90 mA for 1-4 hrs. Gels were then dried under vacuum and heat (65-80°C). Film (Kodak BioMax MS) was placed under and over the dried gel and placed in an exposure cassette. Film was exposed for 1-5 days at -80°C. Development of the film was performed in a dark room by hand with Kodak developer and fixer. The developed film was used to guide subsequent cutting of gel bands.

Western Blotting

Immediately following gel electrophoresis, precast gels were soaked in transfer buffer consisting of 39 mM glycine, 40 mM Tris and 10% MeOH for 15 minutes. A Fisher Scientific or BioRad semidry blotting apparatus was used for the electrotransfer of proteins to polyvinylidene fluoride (PVDF) membranes. Whatman 3 M filter paper, 2 x 6 layers, was soaked with transfer buffer. After wetting with methanol, the PVDF membrane was also soaked in transfer buffer. The filter paper, PVDF membrane and gel

were assembled and electrotransfer was carried out for 90 minutes at 60 mA constant current per gel. After transfer was complete, the PVDF membrane was allowed to air dry. Methanol was used to rehydrate the PVDF membrane. The membranes were washed twice for 5 minutes with TBS buffer (150 mM NaCl, 10 mM Tris, pH 7.6) then blocked with blocking buffer (5% nonfat dry milk, 0.1% Tween-20, 150 mM NaCl, 10 mM Tris, pH 7.6) for 1 hour, with shaking, at room temperature. The blocked membrane was washed three times for 10 minutes with TTBS (0.1% Tween-20, 150 mM NaCl, 10 mM Tris, pH 7.6).

Primary antibody directed against the FLAG epitope (Sigma) was used at 1/10,000 dilution. The antibody was prepared in blocking buffer and applied to the membrane. The PVDF membrane was incubated with the antibody mixture overnight at 4°C with shaking. Next, the PVDF membrane was washed using the following steps. The membrane was washed for 10 minutes with TTBS at room temperature with shaking. This procedure was repeated three times. A secondary antibody, directed toward the primary antibody, containing a phosphatase-conjugated IgG (Pierce) was prepared at a dilution of 1:10,000 in blocking buffer and applied to the membrane for 1 hour with shaking at room temperature. After the secondary incubation, the membrane was then washed using the above wash steps. The PVDF membranes were developed using NBT/BCIP (Pierce). After application, the membranes were visually monitored for development and stopped by rinsing the membranes several times with distilled water.

Digestion of Radiolabeled hDAT

In Situ Digest of Radiolabeled hDAT

For *in situ* proteolysis studies, radiolabeled hDAT membrane suspensions were treated with 5mg/ml trypsin (Worthington) at room temperature overnight with shaking. Membranes were centrifuged and the supernatant saved for gel electrophoresis analysis. The pellet was solubilized overnight and centrifuged again to obtain any bound radiolabeled DAT peptides. The supernatant was saved at 4°C for further use.

In-gel Digestion of Radiolabeled hDAT

The band of interest was cut from the gel and rehydrated with 0.1M NH_4CO_3 containing 1mg/ml concentration of the desired proteolytic enzyme. The gel pieces were incubated for 24 hrs at 37°C. Following the digest, excess digestion solution was removed from the gel pieces and saved. Elutions were performed over the span of about 3 days using 60% acetonitrile, 0.1%TFA in a warm sonicating bath. The final extraction was performed with 100% acetonitrile. All eluents were pooled together and dried in a speed vacuum. The dried extracts were brought up in solubilization buffer (if followed by SDS-PAGE) or 60% acetonitrile, 0.1%TFA (if followed by HPLC analysis).

Enzymatic Proteolysis with Trypsin

Trypsin is a degradative protease found in the digestive system that belongs to the serine protease family of enzymes. This class of proteases is distinguished by the presence and reactivity of a serine residue in the active site (Hedstrom, 2002). Trypsin is a globular protein of 24kDa, which is composed of 220 residues (Walsh and Neurath,

1964). The enzyme catalyzes the hydrolysis of peptide bonds on the C-terminal side of lysine and arginine residues, as well as autolysis of itself. Ca^{2+} has been shown to play a key role in autolysis by binding to the enzyme at the Ca^{2+} binding loop, which protects the protein against autolysis (Sipos and Merkel, 1970).

Substrates of trypsin that contain lysine residues are hydrolyzed to a lesser degree than those with arginine (Keil, 1992). Cleavage of lysine or arginine is hindered when either is adjacent to a proline residue and slowed when adjacent to an acidic residue (Smyth, 1967). Ozols (1990) used trypsin to investigate the amino acid sequence of flavin containing monooxygenase form 1 from rabbit liver microsomes. In this study, the hydrolysis of several lysine and arginine residues was hindered by the presence of adjacent acidic or hydrophobic residues.

The deep binding pocket of trypsin formed by Asp189, Gly216, and Gly226 creates a negatively charged binding site that specifically accommodates substrates containing arginine or lysine (Ibrahim and Pattabhi, 2004). Removal of the negative charge at position 189 reduces the catalytic rate by a factor of 10^5, which suggest that the negative electrostatic field is essential for substrate binding (Evnin et al., 1990). Substitution of Gly216 and Gly226 with alanine showed enhanced substrate specificity relative to the wild type enzyme (Craik et al., 1985). These mutations add a bulkier side chain to the binding pocket, which denies access to substrates with large side chains and thereby decreases the catalytic rate.

Enzymatic Proteolysis with Chymotrypsin

Chymotrypsin is a proteolytic enzyme synthesized by the pancreas. It is responsible for the hydrolysis of peptide bonds on the carboxyl side of aromatic residues, particularly tyrosine, phenylalanine, and tryptophan. In addition to aromatic residues, chymotrypsin also hydrolyzes the bonds of leucine, methionine, asparagine, and glutamine residues, but to a lesser degree (Baumann et al, 1970; Berezin and Martinek, 1970; Keil, 1992). Cleavage is favored when arginine or lysine is attached to the C-terminal side of the peptide bond hydrolyzed by chymotrypsin and hindered if proline is in this position (Keil, 1992). In a study performed by Knight and McEntee (1985) chymotrypsin was used to sequence *rec*A Protein from *E. coli.* They reported that chymotrypsin hydrolyzes tyrosine more rapidly than phenylanine.

The tertiary structure of chymotrypsin consist of two domains, each containing six beta barrels (Voet and Voet, 1995b; Hedstrom, 2002). The active site residues (His57, Asp102, and Ser195) are located between the two domains (Voet and Voet, 1995b; Hedstrom, 2002). Residues Ser189, Gly216, and Gly226, which are adjacent to the active site, creates a deep hydrophobic pocket that allows the bulky aromatic side chains in the substrate to extend into the interior of the pocket (Hedstrom, 2002).

As with most enzymes, the environment surrounding chymotrypsin controls the activity of the enzyme. Studies have shown that high concentrations of phosphate, zinc, and potassium chloride increase the hydrolytic activity of the enzyme (Blanco et al., 1992; Triantafyllou et al., 1997; Hedemann et al., 2006). On the other hand, organophosphorus compounds, diethyl ether, various alcohols, and aromatic hydrocarbons have been reported to inhibit chymotrypsin from hydrolyzing its substrates

(Kilby and Youatt, 1954; Miles et al., 1962; Miles 1963). These studies show that by varying the concentrations and adding substances to the environment surrounding chymotrypsin, the functionality of the enzyme can be altered. In the present work, all trypsin digest were performed in 100mM ammonium bicarbonate, which has little to no affect on the functionality of the enzyme.

Enzymatic Proteolysis with Thermolysin

Thermolysin is a thermostable metalloproteinase isolated from *Bacillus thermoproteolyticus* (Endo, 1962). It has 316 amino acid residues and specifically hydrolyzes peptide bonds on the amino side of bulky hydrophobic residues such as leucine, isoleucine, valine, and phenylalanine (Matsubara et al., 1965; Tatsumi et al., 2007). This cleavage is favored when an aromatic residue is attached to the N-terminal side of the hydrophobic amino acid, but hindered when this site is occupied by an acidic residue (Keil, 1992). Cleavage is also prevented when neighboring residues contain an α–amino or carboxyl group (Ambler and Meadway, 1968). Hydrolysis of peptide bonds involving tyrosine, alanine, methionine, histidine, asparagine, serine, threonine, glycine, lysine and acidic residues may also occur, but to a lesser degree (Heinrikson, 1977). Ambler and Meadway (1968) investigated the specificity of thermolysin using *Pseudomonas azurin*. They determined that the hydrolysis of tyrosine and alanine occurs occasionally, while cleavage of phenylalanine residues takes place rapidly. In another study, thermolysin was used to determine the complete primary structure of flammutoxin, a pore-forming cytolysin from *Flammulina velutipes*, by protein sequence analysis

(Tomita et al., 2004). Here, it was reported that the hydrolysis of phenylalanine, isoleucine, and valine was hindered by polar residues.

The activity of the enzyme depends on the presence of zinc ions, while the concentration of salt influences both the enzymatic activity and thermostability of thermolysin (Latt et al., 1969; Inouye et al., 1998). Removal of zinc inactivates the enzyme, whereas reincorporation of the metal restores activity. An increase in the salt concentration exponentially increases the activity and thermostability of thermolysin. In addition to salt, the structural stability of thermolysin also requires the binding of four calcium ions (Feder et al., 1971). Removal of the calcium atoms from the enzyme causes thermolysin to lose thermostability.

Along with zinc, calcium, and salt, the chemical nature of the solvent has also shown to play a significant role on the thermal stability and activity of thermolysin. Increasing the hydrophobicity of the solvent causes the thermostability of the enzyme to decrease (Pazhang et al., 2006). It has been suggested that this decrease inhibits or denatures thermolysin, as well as displace water near the active site, which may alter the native conformation of the enzyme. Thermolysin digest, performed in the present work, were carried out in an aqueous solution (100mM ammonium bicarbonate), which did not alter the functionality of the enzyme.

Chemical Cleavage with CNBr

Cyanogen Bromide (CNBr) is a highly selective chemical reagent used for the hydrolysis of peptide bonds on the C-termini of methionine residues. While the reaction

is usually performed in 70% formic acid or trifluoroacetic acid (TFA), decreasing the amount of acid enhances the bond cleavage between methionine and any amino acid residue (Kaiser and Metzka, 1999). In the present work, the reaction is performed in the dark with 70% TFA at room temperature for 24 hours. Formic acid and TFA are ideal solutions for the cleavage to occur because it gives an acidic environment as well as solubilizes most proteins (Steers et al., 1965). Studies performed using 70% TFA for hydrolysis of methionine suggested that TFA provides a poor solubility environment, in addition to causing degradation of the target peptides (Rodriguez et al., 2003). It has been shown that in basic conditions cyanogen bromide reacts not only with methionine but with basic side chains of various amino acids residues, making alkaline conditions unsuitable for hydrolysis (Schreiber and Witkop, 1964).

The reaction of methionine with cyanogen bromide is greatly influenced by the carboxyl group and sulfur atom (Gross, 1967). The nucleophilic attack by the sulfur atom on CNBr leads to the elimination of bromine, which causes a nucleophilic attack by the carbonyl oxygen to displace methyl thiocyanate. This then causes the sulfonium atom to form an unstable cyclic iminolactone in the acidic solvent. Iminolactone is later hydrolyzed by water, producing cleavage of the methionine peptide bond and generating a peptide that has a homoserine lactone at the C-terminal (Garrett and Grisham, 1999).

The usage of cyanogen bromide has shown to be advantageous for membrane proteins, where methionines are typically located in the hydrophobic transmembrane domains. Hydrolysis of methionines in this region reduces the size of the hydrophobic fragments, which eases the analysis and handling of the peptides (Kraft et al., 2001).

Conversion of Homoserine Lactone to Homoserine

Cyanogen Bromide cleaves the peptide bonds on the C-termini of methionine residues, forming a homoserine lactone and a new N-terminal peptide. To determine the optimal condition that converts homoserine lactone on methionine back to its original structure of homoserine, homoserine lactone (Aldrich) was incubated in pyridine (Pierce) with varying temperatures (37℃ and room temperature) and pH (9 and 10) for 24hrs. The opening of the lactone to form homoserine was analyzed with ESI-Mass Spectrometry.

Following the CNBr digest and the extraction of the radioactive peptides from the 16.5% or 18% gel, the homoserine lactone on the methionine was converted to homoserine. The conversion was performed by incubating the radioactive sample with 5:5:1; pyridine, 100mM ammonium bicarbonate, 2M NaOH @ pH 9 in 37℃ for 24hrs.

Separation and Digestion of Radiolabeled Peptides

HPLC and Monitoring of Radioactive Fractions

HPLC analysis of the radioligands and the peptide mixture extracted from the gel was performed on Hewlett Packard 1100 series HPLC. Separation occurred using a C_{18} column (4.6 mm ID x 150 mm, 5μm, Zorbax Rx) with H_2O (solvent A) and acetonitrile (solvent B) as the mobile phases, each solvent contained 0.1% TFA. The mobile phase gradient was 0%B for 3 min, 0-60%B in 90 min, 60-90%B in 20 min, 90-100%B in 3 min, and 100%B for 10 min. Fractions were collected at a flow rate of 1ml/min. UV detection at 220 nm is used to monitor column eluate. If further analysis was needed, the HPLC fractions were taken to dryness in a speed vacuum or collected directly in scintillation vials for radioactivity analysis. The dried fractions were resuspended in an

organic buffer (1:1, H_20: Isopropyl) and a fraction was used for ^{125}I counting in a Beckman LS 6500 Multipurpose Scintillation Counter.

Peptide Digestion of Radioactive Fractions

Radioactive fractions were subjected to subsequent enzymatic digestions. The radioactive fractions were evaporated to dryness and resuspended with the enzyme in an appropriate buffer according to the manufacturers' protocol. Secondary digestions were performed at 37ºC for 24 hours with thermolysin (Sigma-Aldrich), trypsin (Worthington), and chymotrypsin (Worthington).

Edman Degradation

Immobilization of Peptides and Manual Sequencing

An arylamine sequelon disc (obtained from Millipore) was placed on a mylar sheet on top of a heating block set at 55℃. The radioactive fraction collected from the HPLC was dried, redissolved in a solution of 50% H_20: 50% Isopropyl, and applied to the disc. Once the solution evaporated, the disc was removed from the heat block. Covalent linkage was accomplished by adding to the disc a solution of EDAC (1mg) in 100µl of 0.1M MES. After 1hr at room temperature, the disc was washed with methanol, acetonitrile, and a 25:25:1 solution of methanol: water: acetic acid. The disc was then dried in a speed vacuum and subjected to Edman degradation.

Manual sequencing (Edman degradation) of the immobilized radioactive peptide was carried out in a 2ml centrifuge tube. Washing and extraction of the disc were accomplished by vortexing the contents in the tube. Each cycle of degradation consists of

Chapter Three

Results

Introduction to Results

This chapter focuses on the studies performed to identify the photoaffinity labeling site of [^{125}I]MFZ 2-24 on the human dopamine transporter. An *in situ* trypsin proteolysis experiment was conducted to determine the proximity of the labeled residue to the transmembrane. Further characterization of the labeled region was carried out with both chemical and enzymatic digests, followed by HPLC analysis and Edman degradation. In addition to the techniques described above, several other methods were utilized for the determination of amino acid residue covalently bound to the radiolabel. The following section discusses the results obtained during each experiment.

Localization of Photoaffinity Labeled hDAT

The Affect Cocaine has on the Binding of hDAT Photoaffinity Labels

To test the effect cocaine has on the binding of hDAT photoaffinity labels, a protection experiment was performed with WIN 35,428 (cocaine analog). hDAT was labeled with [^{125}I]MFZ 2-24 and [^{125}I]DEEP separately. The labeled protein was then run on a 7.5% polyacrylamide gel and later exposed to autoradiography. Figure 3.1 shows the autoradiograph of [^{125}I]MFZ 2-24 labeled hDAT, and Figure 3.2 shows that of [^{125}I]DEEP labeled hDAT. Labeled hDAT migrates around 80kDa. This 80kDa band has been identified as hDAT using western blotting (Figure 3.3), where an anti-flag antibody

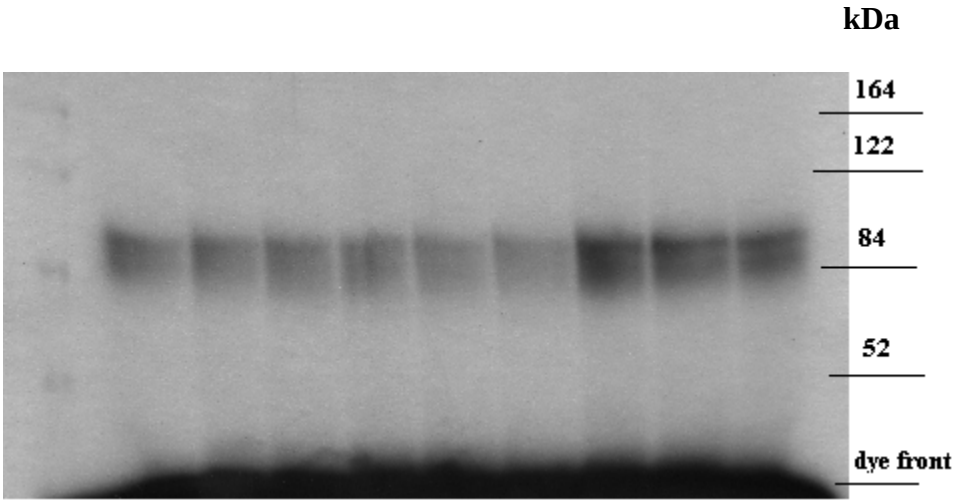

Figure 3.1 Autoradiograph of SDS-PAGE Separated [^{125}I]MFZ 2-24 Labeled hDAT. Radiolabeled hDAT was separated using a 7.5% polyacrylamide gel. Labeled hDAT migrates around 80kDa.

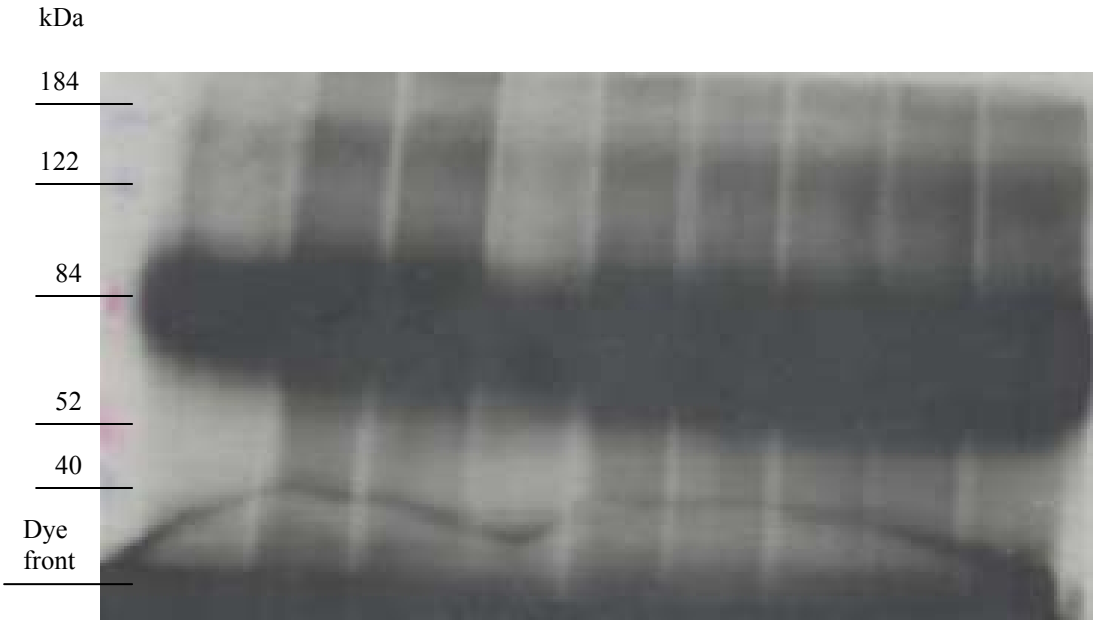

Figure 3.2 Autoradiograph of SDS-PAGE Separated [^{125}I]DEEP Labeled hDAT. Radiolabeled hDAT was separated using a 7.5% polyacrylamide gel. Labeled hDAT migrates around 80kDa.

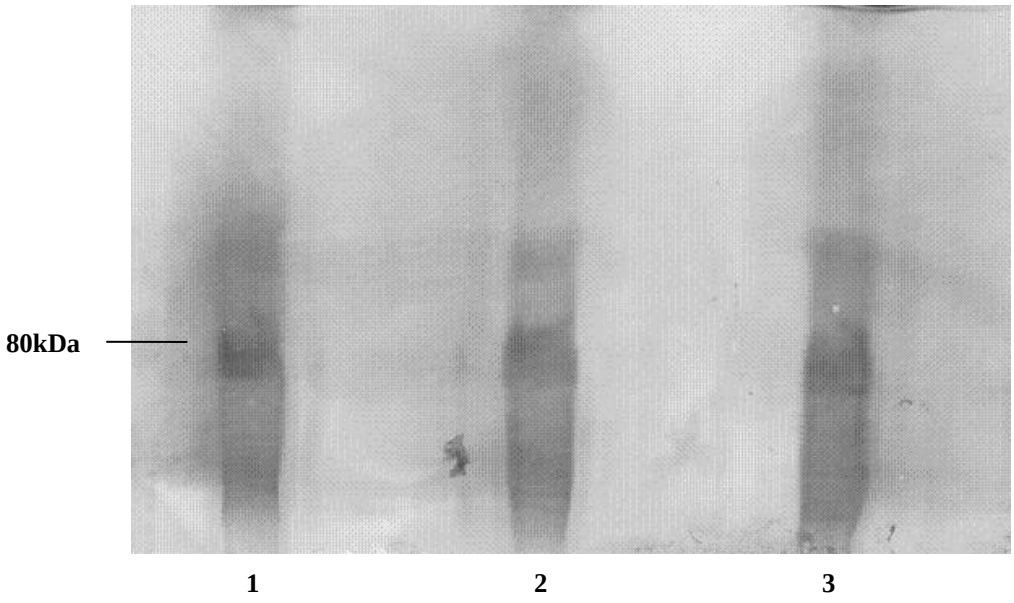

Figure 3.3 Western Blot Analysis of hDAT. Lanes 1 -3 represent hDAT, from HEK 293 cell membranes, that was solubilized and loaded on a 7.5% SDS-PAGE mini-gel. The solubilized protein samples from the mini-gel were then transferred onto a PVDF membrane and probed with an antibody directed to the FLAG epitope. The immunoreactive bands suggest that the 80kDa band is the dopamine transporter.

was directed toward the flag epitope on hDAT. For the protection experiments, membranes were first incubated with 1mM of WIN 35,428 prior to incubation of the radioligand. Control samples were incubated with the radioligand alone. Figure 3.4 shows the gel electrophoresis analysis of hDAT membranes labeled with [^{125}I]MFZ 2-24, [^{125}I]MFZ 3-37, and [^{125}I]DEEP in the presence and absence of WIN 35,428. In the presence of WIN 35,428 all three radioligand were unable to label hDAT.

Radioligands Label a Region Near or In the Transmembrane Domains of wt hDAT

To differentiate whether the labeled region was located near or in the intracellular loops, extracellular loops, C terminal, N terminal, or within transmembrane domains, [^{125}I]MFZ 2-24 and [^{125}I]RTI-82 labeled wild-type hDAT underwent *in situ* trypsin proteolysis. Figure 3.5 shows the autoradiograph of an *in situ* trypsin digest of [^{125}I]MFZ 2-24 and [^{125}I]RTI-82 labeled hDAT. Following the trypsin digest of labeled hDAT, the labeled peptides (from both [^{125}I]MFZ 2-24 and [^{125}I]RTI-82 labeled hDAT) were found to be attached to the transmembrane domains. This indicates that the labeled peptides were located in or near the transmembrane domains. Following autoradiography of one of the trials, the labeled region of the protein was excised from the gel and the radioactivity counted (Figure 3.6). The tryptic digested [^{125}I]MFZ 2-24 and [^{125}I]RTI-82 labeled hDAT fragments located in or near the transmembrane domains contained much more radioactivity than that contained in the supernatant.

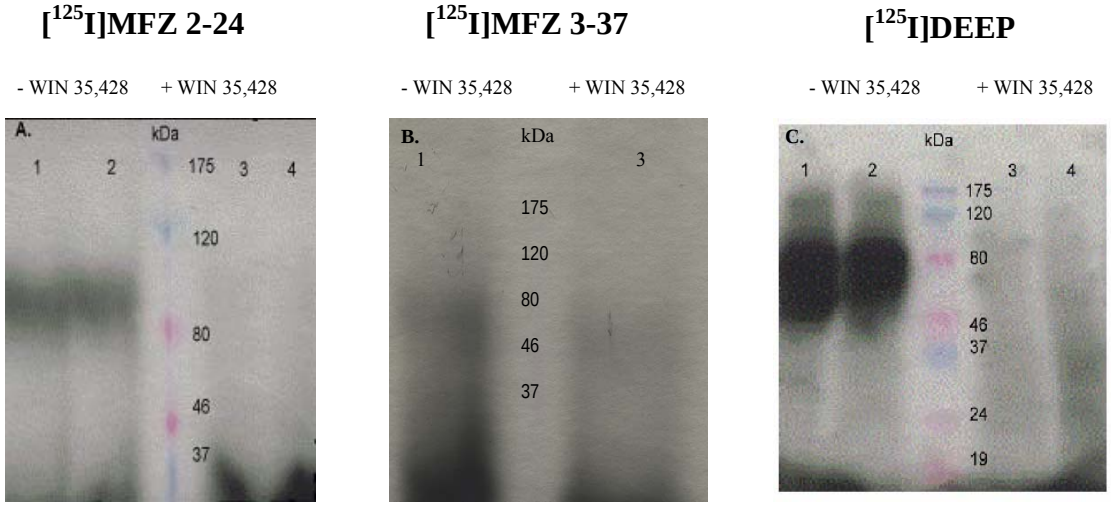

Figure 3.4 WIN 35,428 Protection Experiment. hDAT membranes labeled with A. [^{125}I]MFZ 2-24, B. [^{125}I]MFZ 3-37, and C. [^{125}I]DEEP with and without being preincubated in 1nM WIN 35,428. The 80 kDa band in lanes 1and 2 represent labeled hDAT while the lack of bands appearing in lanes 3 and 4 suggests that binding of WIN 35,428 blocks the radioligands from labeling the dopamine transporter. Radiolabeled hDAT was separated via SDS-PAGE using a 7.5% polyacrylamide gel.

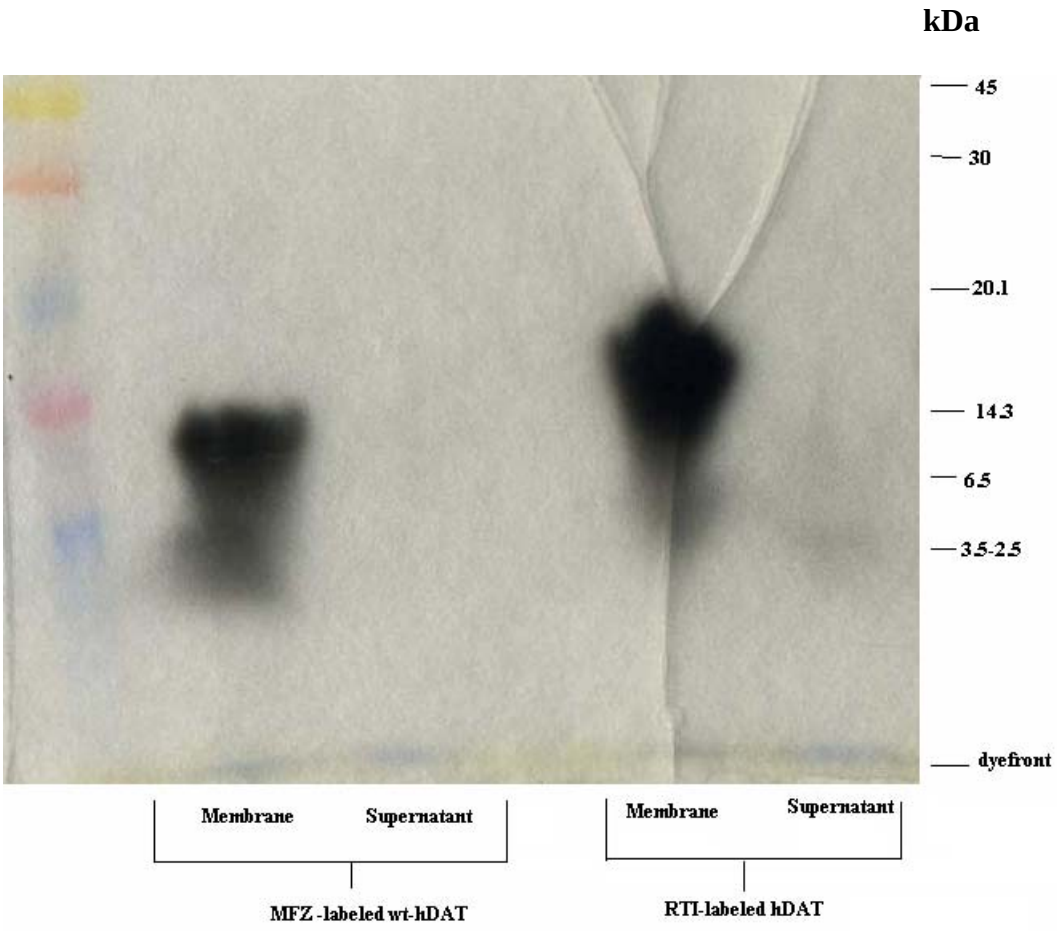

Figure 3.5 Autoradiograph of an *In Situ* Trypsin Proteolysis of [^{125}I]MFZ 2-24 and [^{125}I]RTI-82 Labeled hDAT (n=3). Following an *in situ* trypsin digest, radiolabeled peptides were separated via SDS-PAGE using an 18% Tris-HCl gel. The presence of the radioactive peptides in the membrane fraction suggests that both ligands were in, or in close proximity to, the transmembrane domains.

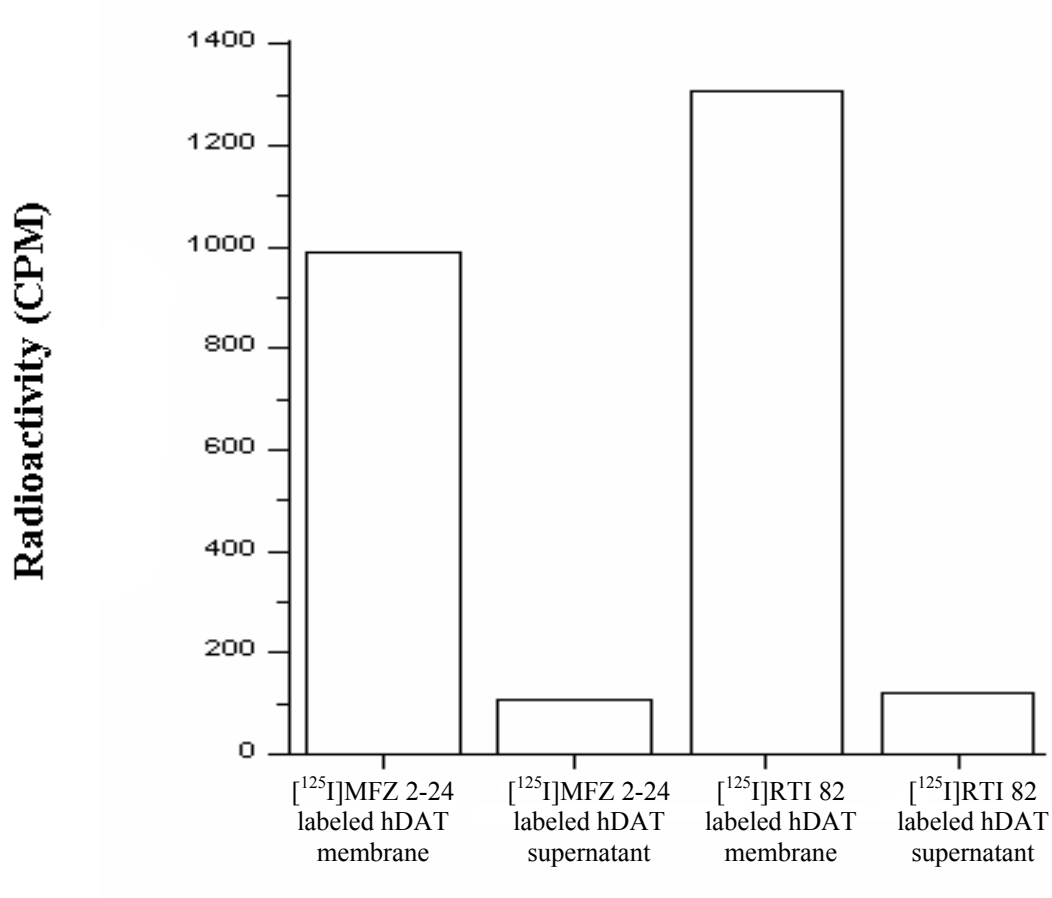

Figure 3.6 Radioactivity Analysis of an *In Situ* Trypsin Digest of [^{125}I]MFZ 2-24 and [^{125}I]RTI-82 Labeled Wild-Type hDAT (n=1). The labeled fragments were excised from an 18% Tris-HCl gel and the radioactivity counted. The regions located in or near the transmembrane domains of hDAT were labeled more than those located in the supernatant.

[^{125}I]RTI-82 Incorporated Near or In the Transmembrane Domains of x5C hDAT

To determine if the substitutions of alanine for C90, C135, C306, C342 and phenylalanine for C319 affect the ability of the radioligand to label a region near or in the transmembrane domains, mutant x5C hDAT (Figure 3.7) was labeled with [^{125}I]RTI-82 and then underwent an *in situ* trypsin proteolysis. Previous studies determined that TM6 and adjacent regions (residues 292-344) of hDAT is the fragment labeled by [^{125}I]RTI-82 (Vaughan et al., 2007). Since cysteine 319 and 342 are near the site of [^{125}I]RTI-82 photoincorporation, it is hypothesized that the absence of the cysteines will not affect the labeling of [^{125}I]RTI-82 to a region near or in the transmembrane domains. There is a possibility that the mutations will cause the radioligand to label a residue near or adjacent to its original labeling site. If this occurs, it is expected that the residue labeled will also be positioned in or near the transmembrane domains. For *in situ* proteolysis studies of mutant hDAT, a transporter construct, x5C, with five mutated cysteines (C90A, C135A, C306A, C319F, and C342A) was analyzed and compared to wild-type hDAT. Figure 3.8 shows the autoradiograph of an *in situ* trypsin digest of [^{125}I]RTI-82 labeled wild type and x5C hDAT. Following the trypsin digest of labeled hDAT, the labeled peptides (from both wild type and x5C hDAT) were attached to the transmembrane domains. This indicates that the labeled peptides were located in or near the transmembrane domains and the absence of the five cysteine residues did not did not prevent the photo-incorporation of the radioligand in or near the transmembrane domains. Following autoradiography, the labeled region was excised from the gel and the radioactivity counted (Figure 3.9). The tryptic digested [^{125}I]RTI-82 labeled wild type and x5C hDAT

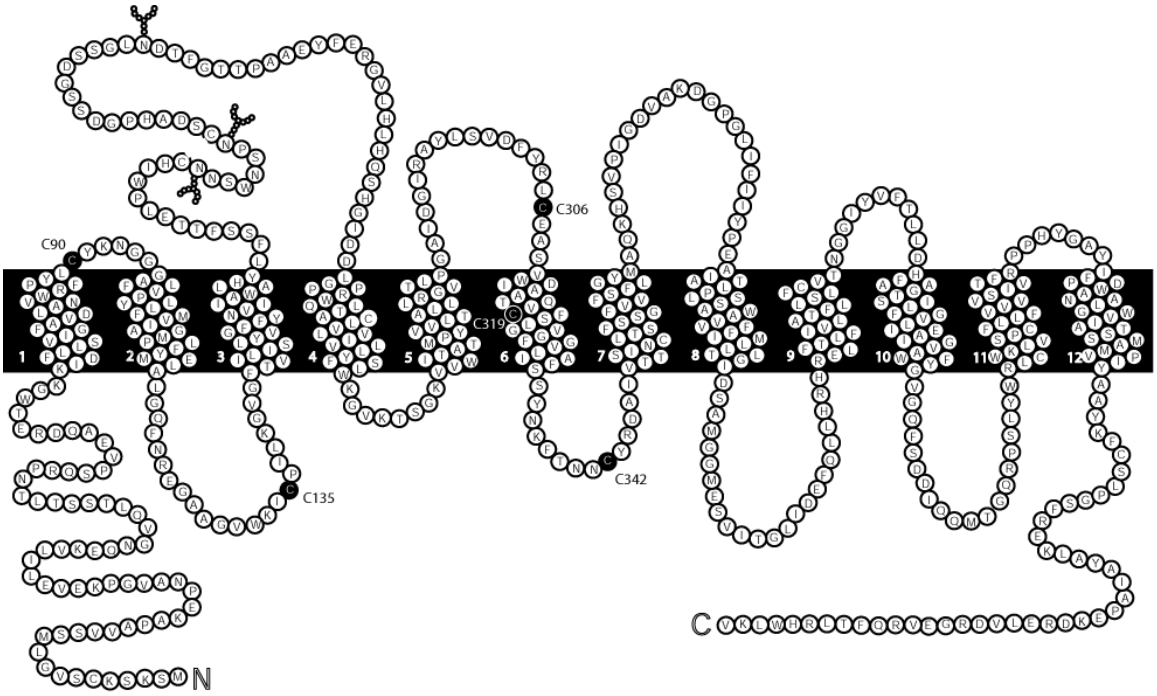

Figure 3.7 x5C Construct of hDAT. The black circles with white letters highlight the cysteine residues that have been mutated in the x5C transporter construct (C90A, C135A, C306A, 319F, C342A).

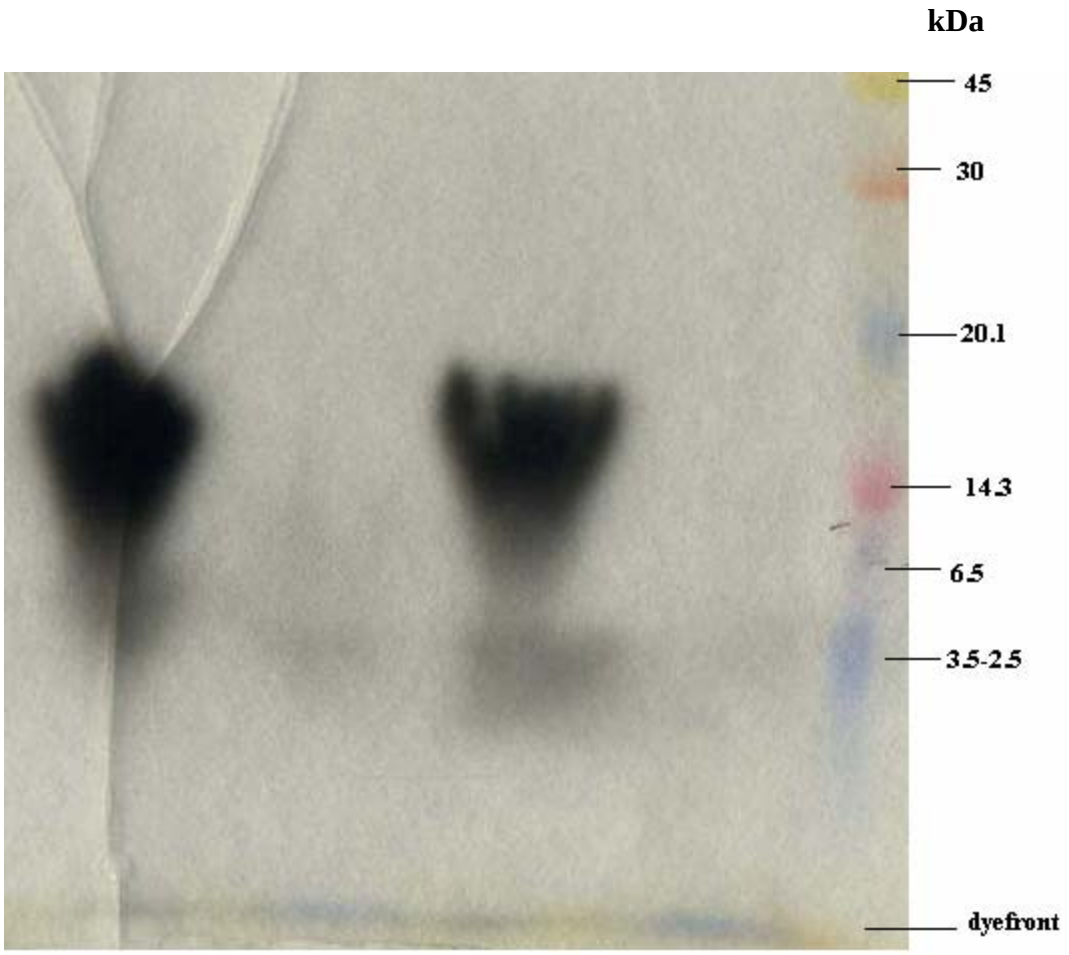

Figure 3.8 Autoradiograph of an *In Situ* Trypsin Proteolysis of [^{125}I]RTI-82 Labeled Wild-Type and x5C hDAT (n=3). Labeled peptides were localized in or near the membrane of both wild type and x5C hDAT. The absence of the 5 cysteines in the mutant did not affect the labeling of [^{125}I]RTI-82 to a region(s) near the transmembrane domain. Radiolabeled peptides were separated via SDS-PAGE using an 18% Tris-HCl gel.

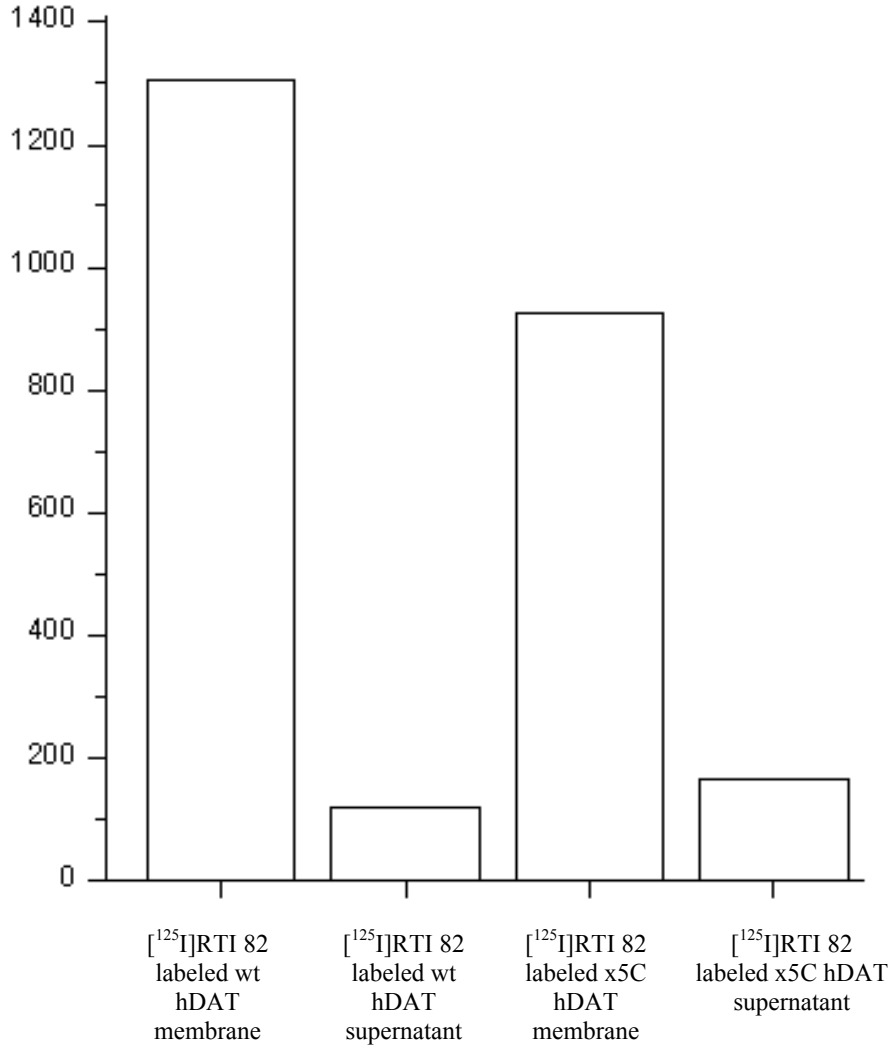

Figure 3.9 Radioactivity Analysis of an *In Situ* Trypsin Digest of [^{125}I]RTI-82 Labeled Wild-Type and x5C hDAT (n=1). The labeled fragments were excised from an 18% Tris-HCl gel and the radioactivity counted. The region located in or near the transmembrane domain of both wild type and x5C hDAT were labeled more than those contained in the supernatant. [^{125}I]RTI-82 also labeled a higher percentage of wild type hDAT compared to that of x5C hDAT.

fragments, located in or near the membrane, contained more radioactivity than the peptides contained in the supernatant. Figure 3.9 also shows that more of wild type hDAT was labeled by [^{125}I]RTI-82 than that of x5C hDAT.

CNBr Digest of [^{125}I]MFZ 2-24 Labeled hDAT

Gel Electrophoresis of [^{125}I]MFZ 2-24 Labeled hDAT CNBr Digestion

In an approach to cleave hDAT into smaller peptides for localizing the site of photoincorporation, hDAT was labeled with [^{125}I]MFZ 2-24 and digested with CNBr (Figure 3.10). The radioactive peptides produced from the digest migrated between 2-20kDa. The control sample, which was the undigested hDAT, did not migrate through the 16.5% polyacrylamide gel due to its large molecular weight. The gel only separates proteins and peptides between 45-2 kDa, which is why the 80kDa undigested transporter remained at the top of the gel.

CNBr Effect on the Structure of Methionine

During a CNBr digestion, the C-terminal of methionine is converted from a homoserine to a homoserine lactone (Gross, 1967; Garrett and Grisham, 1999). To determine the optimal condition that converts homoserine lactone in methionine back to its original structure of homoserine, homoserine lactone was incubated in varying temperatures (37°C and room temperature) and pH (9 and 10) for 24hrs (Table 3.1). The most favorable condition that converted homoserine lactone to homoserine occurred in a pH 9 solution at room temperature and 37°C. The opening of the lactone to form homoserine was analyzed with ESI-Mass Spectrometry.

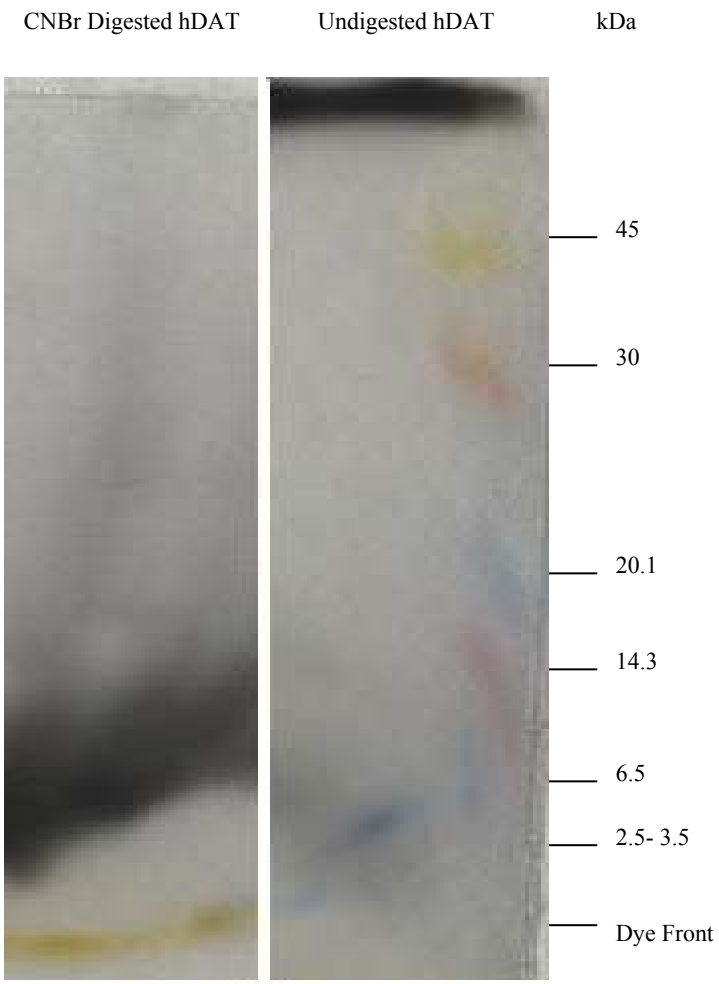

Figure 3.10 Autoradiograph of CNBr Digested [^{125}I]MFZ 2-24 Labeled hDAT (n=8). Labeled peptides were separated using a 16.5% polyacrylamide gel. Since the molecular weight of hDAT is 80kDA, undigested hDAT remained at the top of the gel due to its large size. CNBr digested peptides migrated between 2-20kDa.

pH	pH 10	pH 10	pH 9	pH 9
Temperature	**37°C**	**Room Temperature**	**37° C**	**Room Temperature**
Homoserine Lactone	1.7%	10%	0%	0%
Homoserine	100%	90%	100%	100%

Table 3.1 Summary of the Optimal Conditions for the Opening of Homoserine Lactone (n=2). Cleavage of methionine with CNBr converts the homoserine on the C-terminal of methionine to a homoserine lactone. To determine the optimal condition that converts homoserine lactone to homoserine, homoserine lactone was incubated in pyridine with varying temperatures and pH for 24hrs. The most favorable conditions that converted homoserine lactone to homoserine occurred in a pH 9 solution at room temperature and 37°C. The product of each conversion was confirmed by ESI-Mass Spectrometry.

CNBr Effect on hDAT Radioligands

To determine if the structures of [^{125}I]MFZ 2-24 and [^{125}I]AD 96-129 are stable during a CNBr digestion, the labels were incubated in a CNBr solution and assessed using High Performance Liquid Chromatography (HPLC). Nonirradiated [^{125}I]MFZ 2-24 was incubated in a 1mM CNBr solution with 70% TFA as the solvent (dotted line with filled circles) and 100% ethanol (solid line open squares) (Figure 3.11). [^{125}I]MFZ 2-24 produces two radioactive peaks with a retention time around 55 and 80 minutes. The chromatogram suggests that the major peak at 80 minutes is likely to be the intact label and the minor peak around 55 minutes is possibly a portion of the label that has degraded. Following the CNBr digest, the 55 minute peak migrated to 50 minutes. This suggests that the CNBr solution has an affect on the structural stability of nonirradiated [^{125}I]MFZ 2-24. A different effect was observed with irradiated [^{125}I]MFZ 2-24 (Figure 3.12) in the presence of 1mM CNBr in a solution of 70% TFA (open squares) and 100% ethanol (filled squares). The retention time of [^{125}I]MFZ 2-24 remained the same, suggesting that the structure of the radiolabel was altered by the UV light and the 1mM CNBr in 70%TFA solution.

The structural stability of [^{125}I]AD 96-129 was also analyzed following a CNBr digest. When incubated with both the CNBr solution and 70%TFA, the retention time of nonirradiated (Figure 3.13) and irradiated (Figure 3.14) [^{125}I]AD 96-129 varied. This suggests that the CNBr digest affects the stability of [^{125}I]AD 96-129, similarly to that of nonirradiated [^{125}I]MFZ 2-24. The radioactive trace of [^{125}I]AD 96-129 following irradiation also suggests that exposure to UV light affects the structural stability of the label.

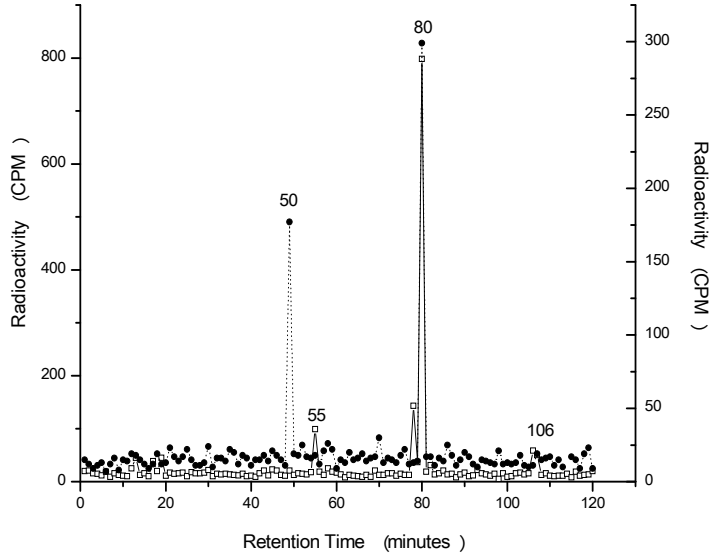

Figure 3.11 HPLC Examination of the Effect of CNBr and TFA on Nonirradiated [^{125}I]MFZ 2-24 (n=2). The radioligand was incubated in a 1mM CNBr solution with 70% TFA as the solvent (dotted line with filled circles) and 100% ethanol (solid line with open squares). Both samples were analyzed by HPLC, fractions collected, and the radioactivity counted. [^{125}I]MFZ 2-24 produces two radioactive peaks with a retention time around 55 and 80 minutes. The chromatogram suggests that the major peak at 80 minutes is likely to be the intact label and the minor peak around 55 minutes is possibly a portion of the label that has degraded. Following the CNBr digest, the 55 minute peak migrated to 50 minutes. This suggests that the CNBr solution has an affect on the structural stability of nonirradiated [^{125}I]MFZ 2-24. The radioligand was chromatographed using a C_{18} column and H_2O (solvent A) and acetonitrile (solvent B), each with 0.1% TFA. The mobile phase gradient was 0%B for 3 min, 0-60%B in 90 min, 60-90%B in 20 min, 90-100%B in 3 min, and 100%B for 10 min. These separation conditions were used for all chromatograms presented in this thesis.

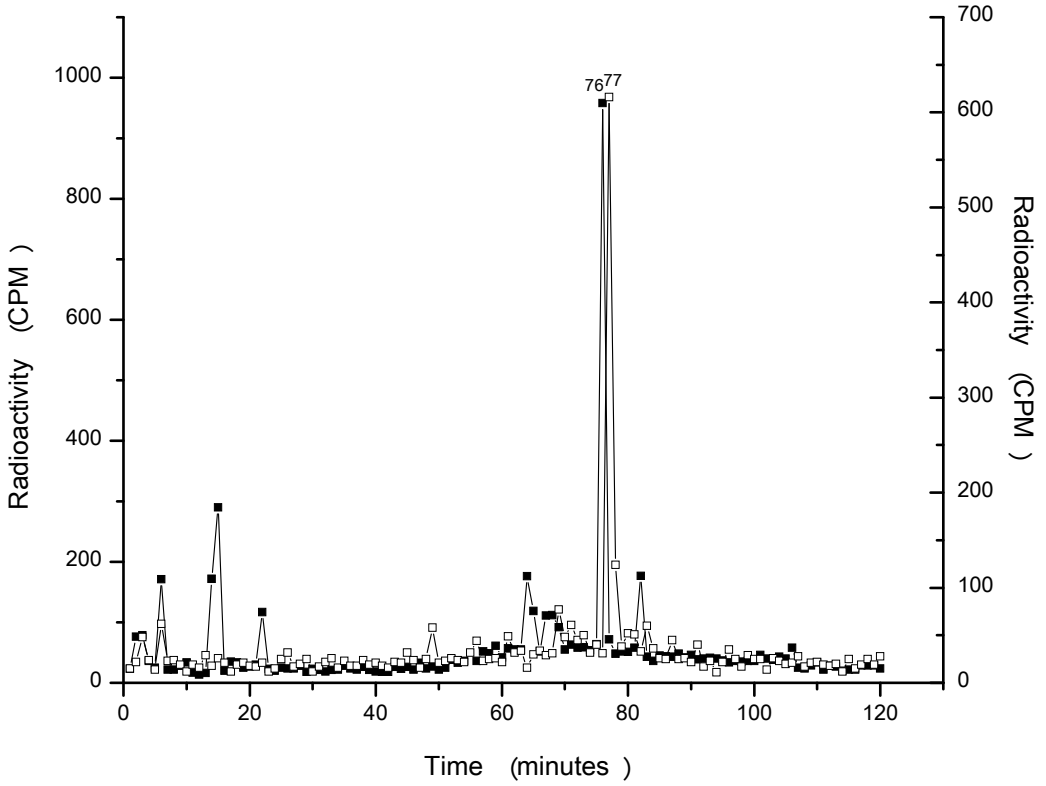

Figure 3.12 HPLC Examination of the Effect of CNBr and TFA on Irradiated [^{125}I]MFZ 2-24 (n=2). The radioligand were irradiated for 4 minutes and then incubated in a 1mM CNBr solution with 70% TFA as the solvent (open squares) and 100% ethanol (filled squares). Both samples were analyzed by HPLC and the radioactivity counted. The CNBr digest did not have an adverse effect on the radioactive peaks produced by irradiated [^{125}I]MFZ 2-24.

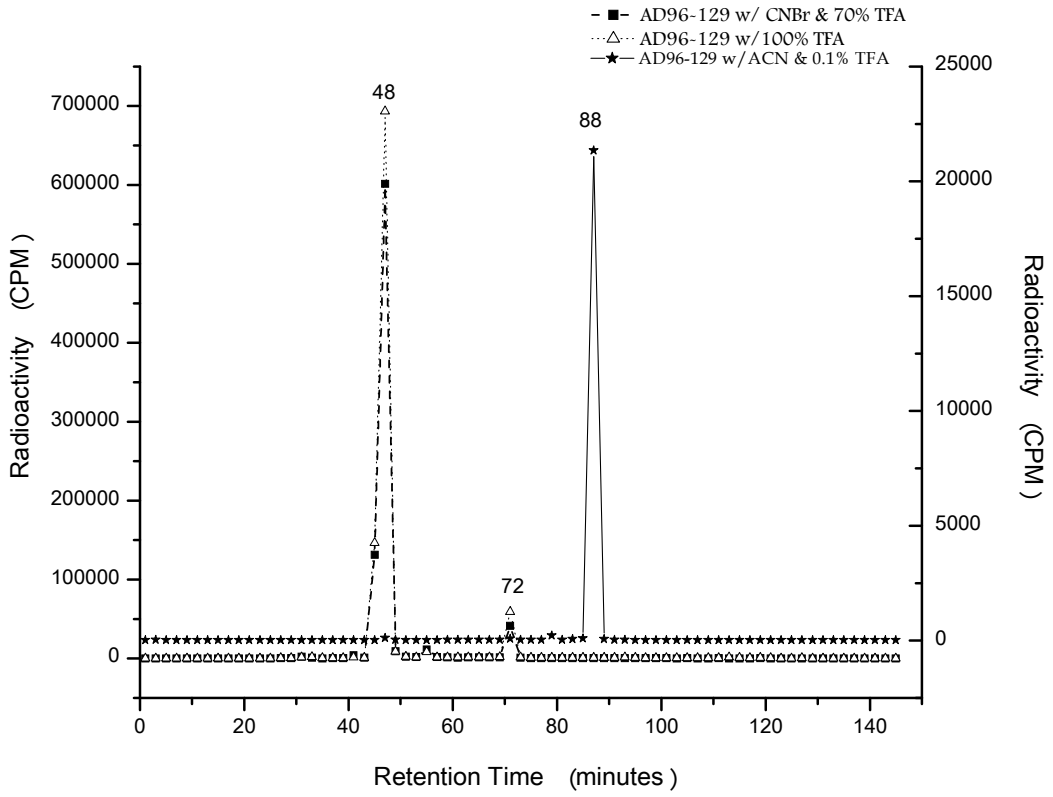

Figure 3.13 HPLC Examination of the Effect of CNBr and TFA on Nonirradiated [^{125}I]AD 96-129 (n=2). The radioligand was incubated in a 1mM CNBr solution with 70% TFA as the solvent (dotted line with square), 70% TFA alone (open triangle), and 100% ACN with 0.1% TFA (filled star). All three samples were analyzed by HPLC and the radioactivity counted. Both the CNBr solution and 70%TFA altered the retention time of nonirradiated [^{125}I]AD 96-129.

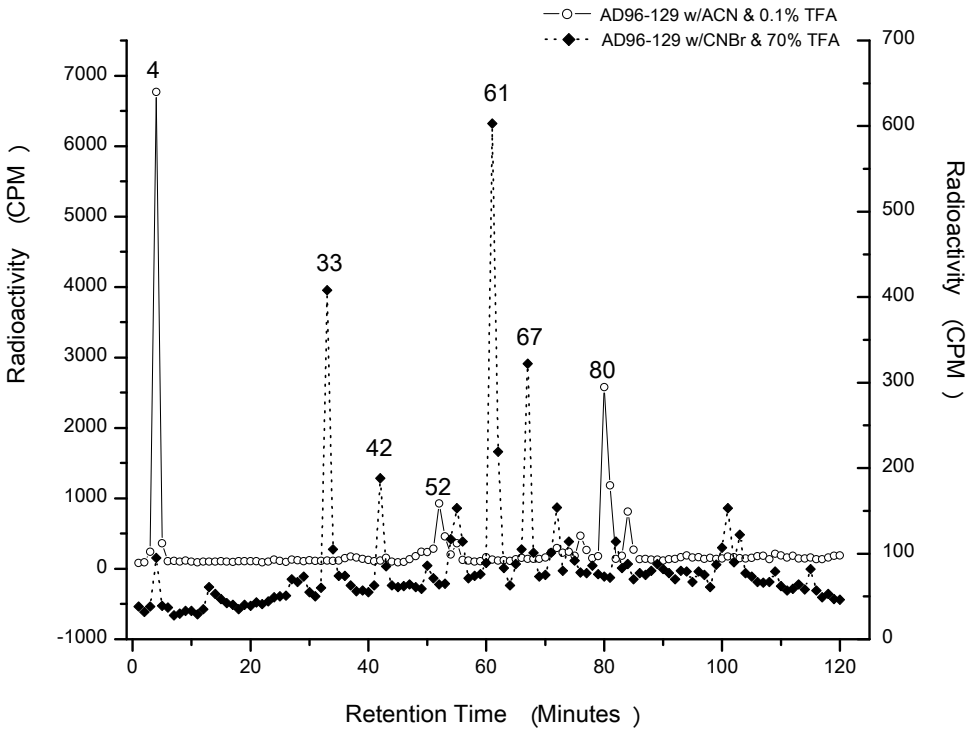

Figure 3.14 HPLC Examination of the Effect of CNBr and TFA on Irradiated [^{125}I]AD 96-129 (n=2). The radioligand was irradiated for 4 minutes and then incubated in 100% ACN with 0.1% TFA (open circle) and a 1mM CNBr solution with 70% TFA as the solvent (dotted line with diamond). Both samples were analyzed by HPLC and the radioactivity counted. Both the CNBr solution and irradiation affected the retention time of [^{125}I]AD 96-129.

CNBr Digest of [^{125}I]MFZ 2-24 Labeled hDAT

To obtain the hDAT peptides labeled by [^{125}I]MFZ 2-24, the protein was digested with CNBr and separated using HPLC (Figure 3.15). After the labeled peptides were run on a 16.5% polyacrylamide gel (Figure 3.10), they were excised from the gel and subjected to HPLC analysis. Two radioactive peaks were produced, a major peak at 79 minutes and a minor peak at 73 minutes. Previous experiments demonstrated that synthetic PLFYM labeled with MFZ 3-37 had a retention time of 79 minutes under the same chromatographic conditions (Wirtz, 2004). It is therefore possible that the 79 minute CNBr peak is PLFYM.

Chymotryptic Digest of [^{125}I]MFZ 2-24 Labeled CNBr Peptide

To determine if the labeled hDAT fragments produced from a CNBr digest contained a chymotrypsin cleavage site, the CNBr peptide was digested with chymotrypsin. Figure 3.16 represents the radioactivity profile of the CNBr peptide following a chymotrypsin digest. Once digested with chymotrypsin, the 79 minute CNBr peak (solid line) produced two radioactive peaks with shorter retention times of 67 and 60 minutes (dotted line). In a duplicate experiment (Wirtz, 2004) an additional minor peak at 47 minutes was observed (data not shown). The migration of the 79 minute peak to three peaks (67, 60, and 47 minutes) suggests that the original CNBr labeled peptide(s) contains a least one chymotrypsin cleavage site. The appearance of the peaks following the chymotrypsin digest also suggests that the digest may have been incomplete. This infers that the peptides produced from the chymotrypsin digest overlap, since the secondary peptides originated from a single radiolabeled CNBr peptide.

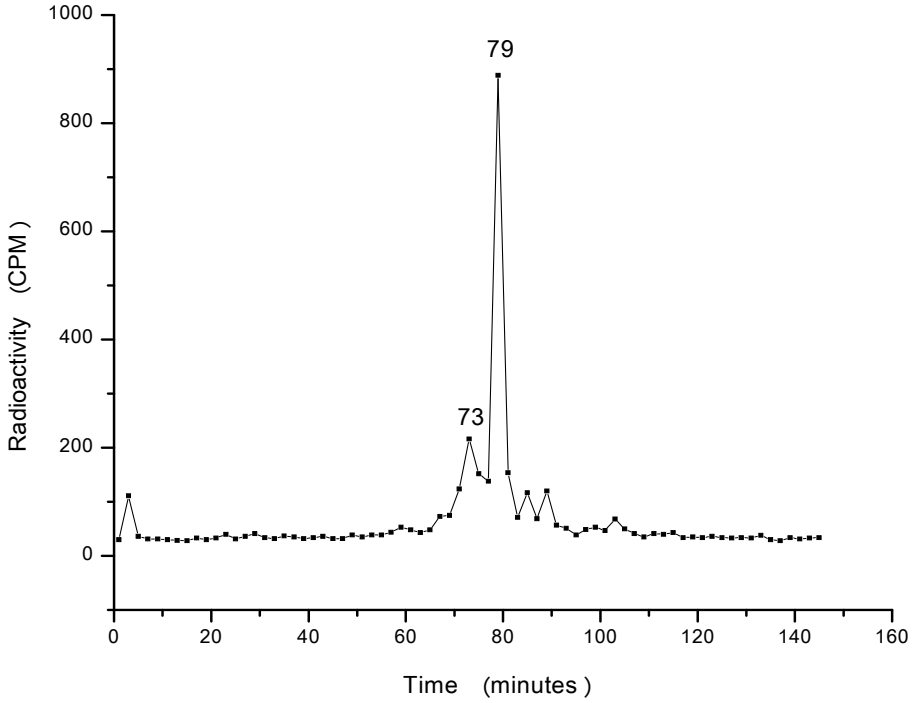

Figure 3.15 HPLC Analysis of CNBr Digested [^{125}I]MFZ 2-24 Labeled hDAT (n=8). Following SDS-PAGE, CNBr digested peptides were excised from the 16.5% polyacrylamide gel and separated with HPLC. A major peak was produced with the retention time of 79 minutes and a minor peak at 73 minutes.

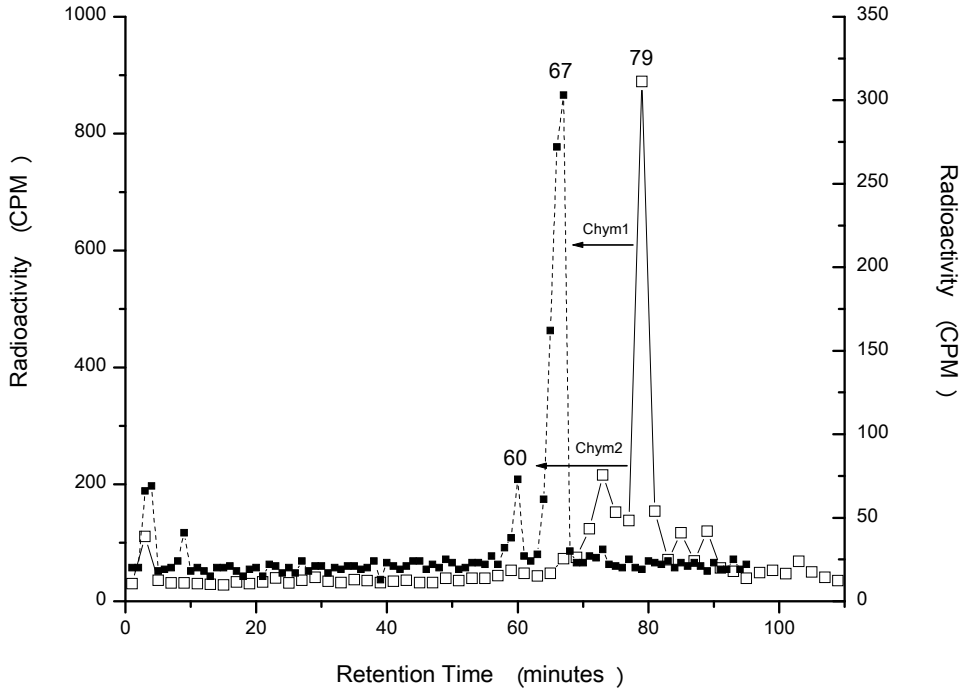

Figure 3.16 Chromatogram of [^{125}I]MFZ 2-24 Labeled CNBr Peptide Following a Chymotrypsin Digest (n=3). Subsequent chymotrypsin digestion (dotted line) of the 79 minute CNBr peak (solid line) produces radioactive peaks with shorter retention times of 67 and 60 minutes. The migration of the 79 peak to 67 and 60 suggest that the original CNBr labeled peptide(s) contains a chymotrypsin cleavage site.

Previous solid state photolabeling experiments (performed by Uliana Danilenko) suggested that YM labeled by MFZ 3-37 and that [^{125}I]MFZ 2-24 labeled [^{3}H]tyrosine has a retention time of 66.5 and 49.5 minutes, respectively. This suggests that the 67 and 47 minute peaks produced from a chymotryptic digest of [^{125}I]MFZ 2-24 labeled CNBr peptide are YM and Y, respectively.

Thermolysin Digest of [^{125}I]MFZ 2-24 Labeled CNBr Peptide

To determine if the labeled hDAT peptides produced from a CNBr digest contained a thermolysin cleavage site, the CNBr peptide was digested with thermolysin. Figure 3.17 shows a chromatogram of the radiolabeled CNBr peptide (solid line) digested with thermolysin (dotted line). Once digested with thermolysin, the 79 minute CNBr peak (solid line) produced three radioactive peaks with shorter retention times of 63, 69, and 76 minutes (dotted line). The disappearance of the 79 minute peak to three peaks at 63, 69, and 76 minutes suggests that the original CNBr labeled peptide(s) contains one or more thermolysin cleavage sites. The appearance of the peaks following the thermolysin digest also suggests that the thermolysin digest was incomplete. This infers that the peptides produced from the thermolysin digest overlap, since the secondary peptides originated from a single radiolabeled CNBr peptide.

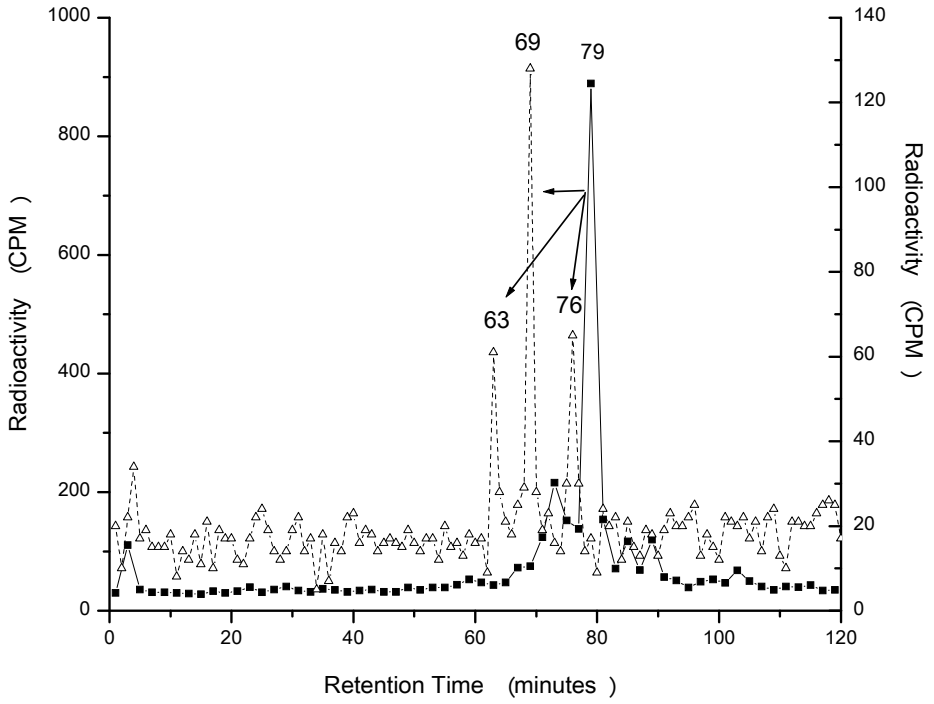

Figure 3.17 Chromatogram of [^{125}I]MFZ 2-24 Labeled CNBr Peptide Following a Thermolysin Digest (n=2). The 79 minute CNBr peak (solid line) was digested with thermolysin (dotted line), which produced three radioactive peaks with shorter retention times of 63, 69, and 76 minutes. The migration of the 79 peak suggests that the original CNBr labeled peptide(s) contains a thermolysin cleavage site(s).

Thermolysin Digest of [^{125}I]MFZ 2-24 Labeled hDAT

HPLC Analysis of [^{125}I]MFZ 2-24 Labeled hDAT Thermolysin Digest

To obtain the hDAT peptides labeled by [^{125}I]MFZ 2-24, the protein was digested with thermolysin and separated using HPLC (Figure 3.18). Four radioactive peaks were produced, two major peaks at 77 and 82 minutes and two minor peaks at 70 and 92 minutes.

Thermolysin Digest of HPLC Fractions From Initial Thermolysin Digest

To determine if the [^{125}I]MFZ 2-24 labeled hDAT fragments produced from an initial thermolysin were completely digested, the two major radioactive peaks at 77 and 82 minutes (solid line) were redigested by thermolysin and analyzed via HPLC (Figure 3.19). The 77 minute HPLC fraction migrated to 63 minutes and the 82 minute peak produced peaks at 63 and 73 minutes. The migration of both peaks (82 and 77) suggests that these labeled peptides contained thermolysin cleavage site(s) and were not completely digested with thermolysin initially.

Determination of [^{125}I]MFZ 2-24 Labeled Residue From a Thermolysin Digest

To identify the labeled amino acid residue, Edman degradation was applied to the peptides produced from the thermolysin digest of [^{125}I]MFZ 2-24 labeled hDAT. The N-terminal residue was cleaved one at a time and the radioactivity counted. Figure 3.20 shows the radioactive profile from each Edman degradation cycle. The second amino acid in the peptide is the site of [^{125}I]MFZ 2-24 incorporation.

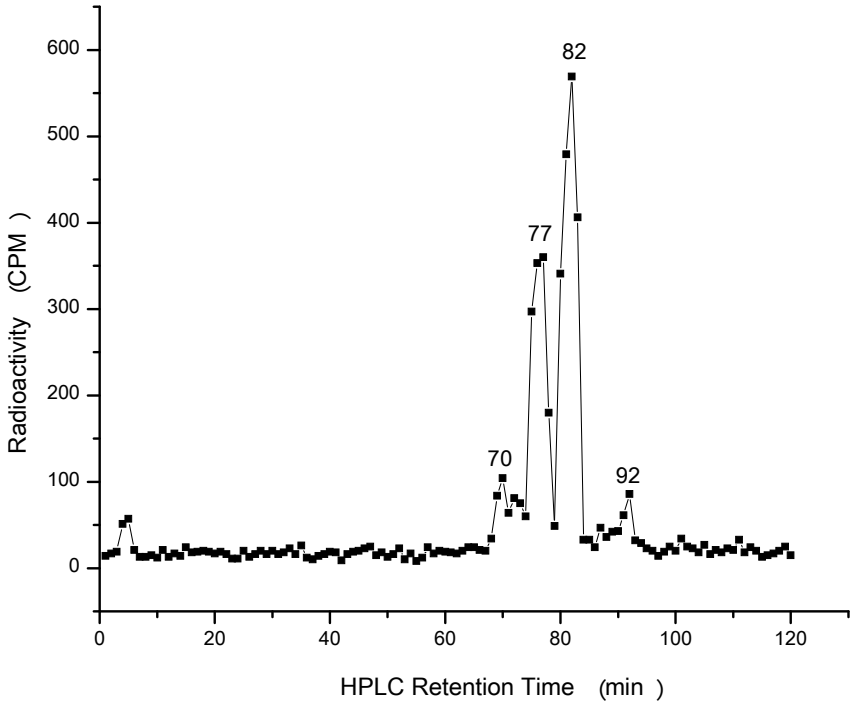

Figure 3.18 HPLC Analysis of Thermolysin Digested [^{125}I]MFZ 2-24 Labeled hDAT (n=8). Following SDS-PAGE, hDAT was excised from the 7.5% polyacrylamide gel and digested with thermolysin. The radioactive peptides produced from the digest were separated with High Performance Liquid Chromatography. The digest produced two major peaks at 77 and 82 minutes, as well as two minor peaks at 70 and 92 minutes.

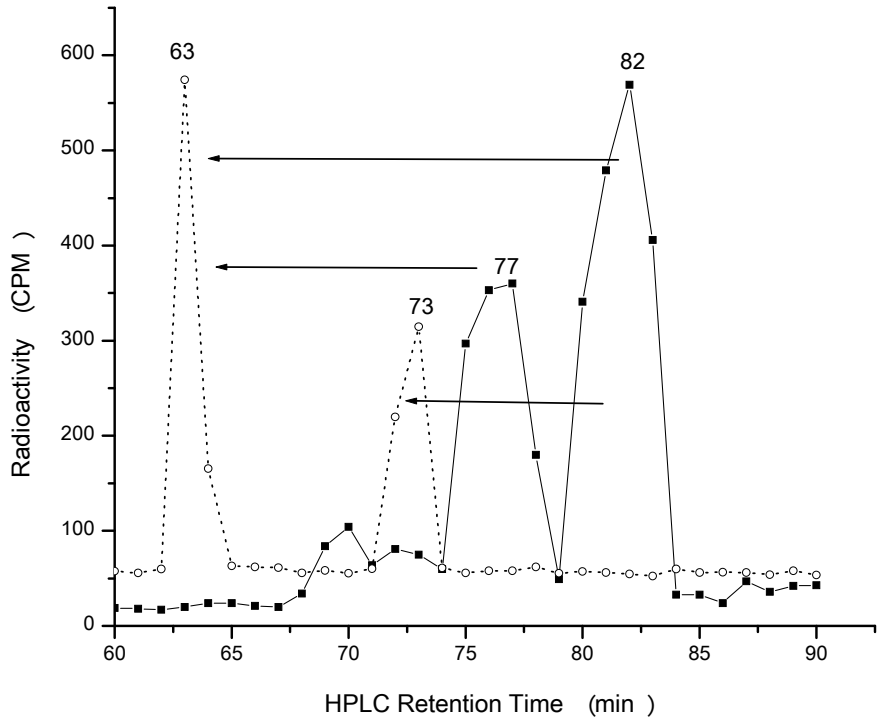

Figure 3.19 Thermolysin Digest of HPLC Fractions From Initial Thermolysin Digest (n=5). Both the 82 and 77 minute radioactive peaks (solid line) produced from the initial thermolysin digest of [^{125}I]MFZ 2-24 labeled hDAT were re-digest with thermolysin (dotted line) and separated with HPLC. The 77 minute peak migrated to 63 minutes, while the 82 minute peak produced peaks at 63 and 73 minutes. The migration of both peaks (82 and 77) suggests that the original thermolysin labeled peptide(s) was not completely digested.

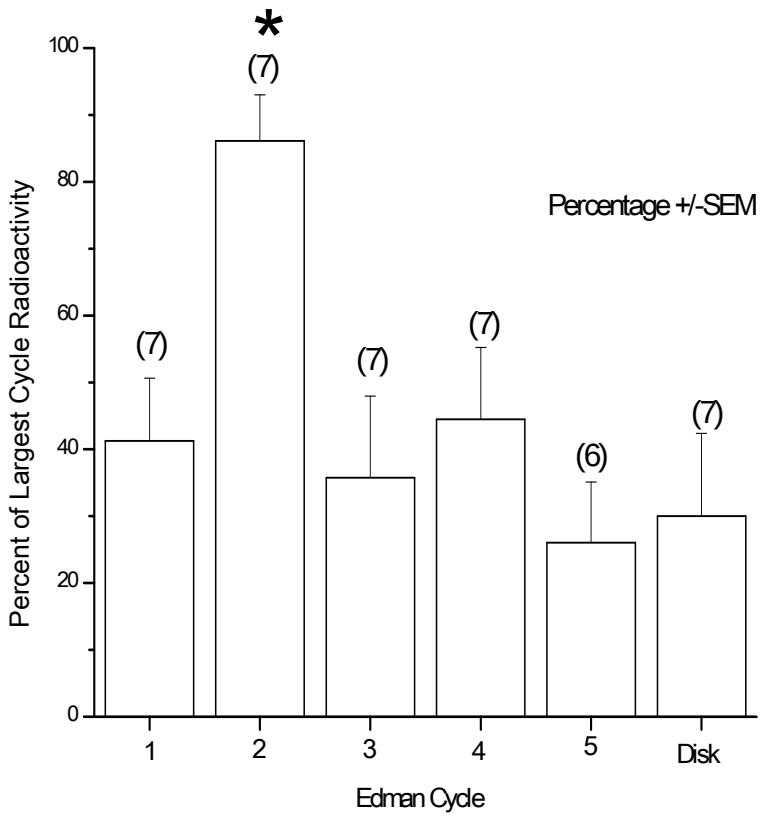

Figure 3.20 Determination of [^{125}I]MFZ 2-24 Labeled Residue From a Thermolysin Digest. For each Edman degradation run, the data is expressed as percent of the cycle with the highest radioactivity in that run. Most of the runs have been done for five cycles plus the disk. The radioactivity remaining on the disk was counted to account for any labeled sites beyond the cycles in a given run. The data indicates that the second amino acid in the peptide is the site of labeling. One way ANOVA using SPSS version 13.0 showed a significant difference at the 0.01 level between all the cycles. Following ANOVA, Least Significant Difference (t test) indicated that cycle 2 is significantly different at the 0.01 level from cycles 1,3,4,5 and the disk.

Chapter Four

Discussion

Introduction to the Discussion

The following sections will delineate the data presented in an effort to localize the region of hDAT photolabeled by [^{125}I]MFZ 2-24. Various enzymatic and chemical digests, followed by HPLC separation and Edman degradation, were used to narrow the site of [^{125}I]MFZ 2-24 photoincorporation. These studies suggest that [^{125}I]MFZ 2-24 is photoincorporated within transmembrane domain 2 of the human dopamine transporter. Also included in this chapter is a discussion of the mechanism by which CNBr cleavages occur, as well as an analysis of the inhibitor binding site of several neurotransmitter transporters.

Analysis of the Labeled Region of hDAT

The Effect of WIN 35,428 on the Binding of hDAT Ligands

When [^{125}I]MFZ 2-24, [^{125}I]MFZ 3-37, and [^{125}I]DEEP were each incubated separately in the presence of WIN 35,428 (cocaine analog), they were unable to label hDAT. Similarities within the pharmacophores (tropane ring) of cocaine, WIN 35,428, [^{125}I]MFZ 2-24, and [^{125}I]MFZ 3-37 (Figure 4.1) suggest that all 4 ligands may bind to the same domain. In contrast, the bulkiness of the diphenyl ether moiety present in [^{125}I]DEEP may hinder its ability to bind to the same domain as the other 4 ligands, thus forcing [^{125}I]DEEP to bind to a nearby domain. The ability of WIN 35,428 to inhibit the binding of all the radioligands suggests that the radioligands may bind to the same region as cocaine. It is also possible that the binding of WIN 35,428 can change the conformation of hDAT, which thereby inhibits the binding of the radioligands.

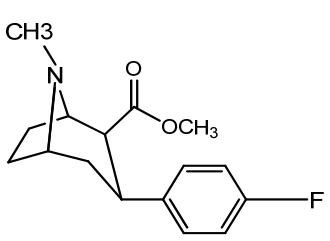

WIN 35,428

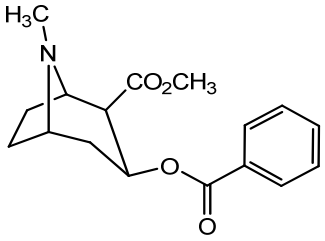

Cocaine

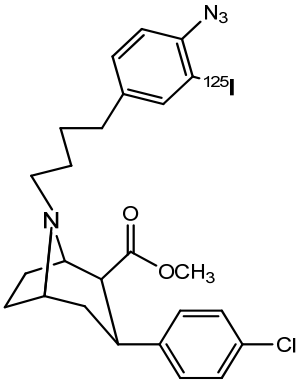

[^{125}I] MFZ 2-24

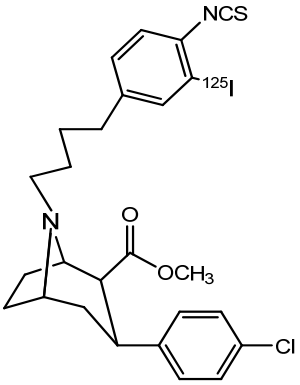

[^{125}I] MFZ 3-37

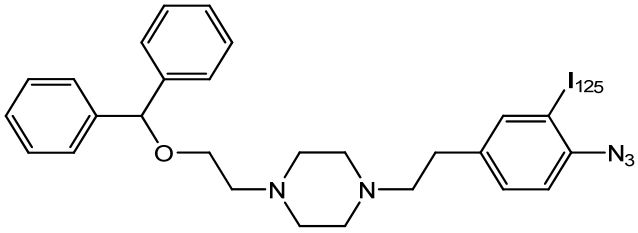

[^{125}I] DEEP

Figure 4.1 Inhibitors of DAT Used in Protection Experiment. WIN 35,428, [^{125}I]MFZ 2-24, and [^{125}I]MFZ 3-37 are cocaine analogs that contain a tropane ring. [^{125}I]DEEP has a diphenyl ether moiety present in its structure.

[^{125}I]MFZ 2-24 Labels Near or In the Transmembrane Domains of wt hDAT

Following the *in situ* trypsin digest of [^{125}I]MFZ 2-24 labeled hDAT, most of the radioactivity was located in or near the transmembrane domains as opposed to the supernatant, indicating that the labeled peptides were located in or near the transmembrane domains. Trypsin is responsible for the hydrolysis of peptide bonds on the C-terminal end of lysine and arginine residues. Lysine residues are catalyzed to a lesser degree than arginine residues (Keil, 1992). Cleavage of both lysine and arginine residues are slowed when adjacent to an acidic residue and hindered when either is adjacent to a proline residue (Smyth, 1967).

An enzymatic digestion of membrane bound hDAT only allows those amino acids that are accessible to the enzyme to be recognized and cleaved. Hydrolysis of an enzyme's substrate occurs upon specific binding of the substrate to the binding cavity on the enzyme. Amino acids buried in the membrane are inaccessible to enzymes, which prevents enzymatic hydrolysis of those residues. Hence, only the residues located near the surface of the transmembrane domain and in the intra and extracellular loops undergo hydrolysis.

The primary structure of hDAT contains approximately 39 lysine and arginine residues that may be hydrolyzed during an *in situ* trypsin digest of hDAT (Figure 4.2). Of the 39 residues, 13 lysine and arginine residues may be inaccessible to the enzyme, which thereby prevents their hydrolysis (Figure 4.3). Following the digest, the membrane bound fraction contained most of the radioactivity, suggesting that [^{125}I]MFZ 2-24 labels a region near or within the transmembrane domains. Figure 4.3 depicts the peptides that are possibly labeled by [^{125}I]MFZ 2-24.

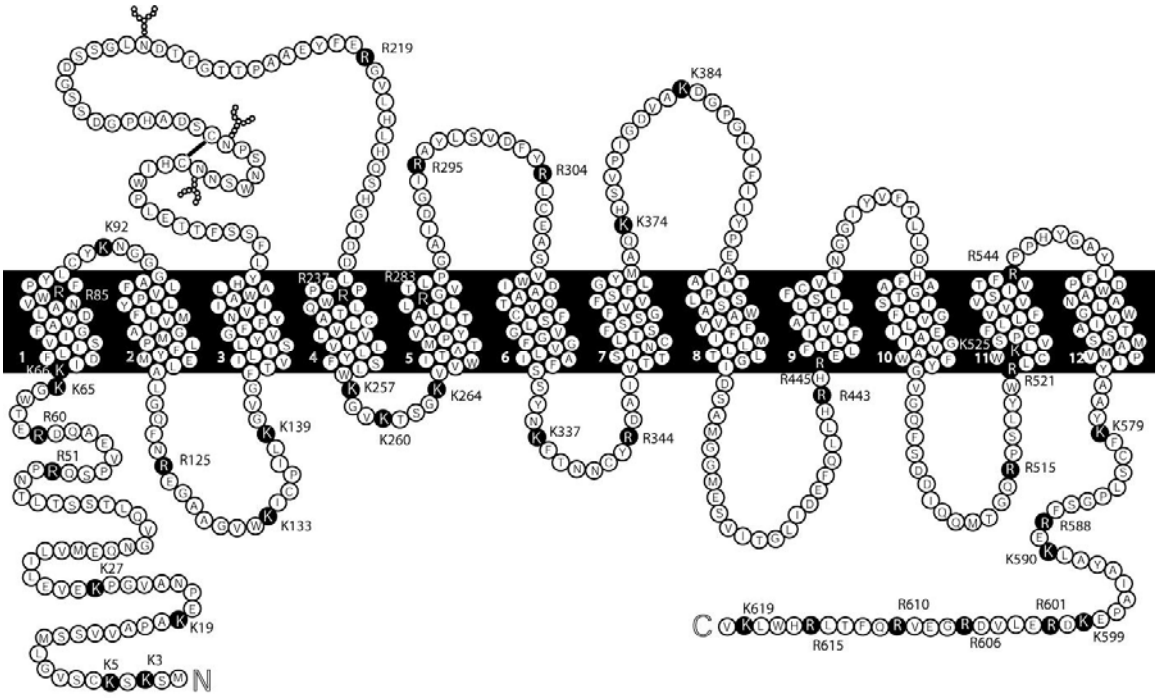

Figure 4.2 Possible Trypsin Cleavage Sites of hDAT. Arginine and lysine residues are indicated as black circles with white letters. The primary structure of hDAT contains 39 lysine and arginine residues that may be hydrolyzed during an *in situ* trypsin digest of hDAT (adapted from Giros and Caron, 1993).

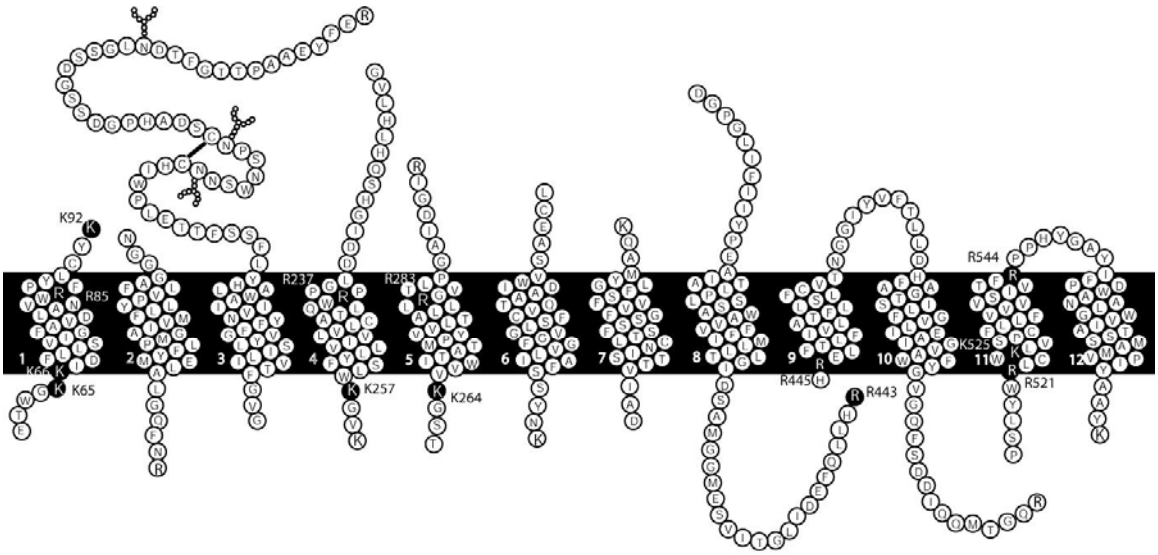

Figure 4.3 Possible Membrane Bound Peptides Produced from an *In Situ* Trypsin Digest of hDAT. Arginine and lysine residues that may not be accessible to trypsin are indicated as black circles with white letters. Thirteen lysine and arginine residues may not be hydrolyzed during an *in situ* trypsin digest of hDAT.

Immunoprecipitation studies have identified a region within TM1-2, specifically residues 68-80, as being the region of [^{125}I]MFZ 2-24 incorporation (Parnas et al., 2003; Parnas et al., 2008). This eliminates TM3-12 as possible labeling sites. Within TM1-2 there are 13 possible trypsin cut sites (Figure 4.4). Residues K3, K5, K19, K27, R51, R60, R125, K133, and K139 seem to be accessible to trypsin during an *in situ* digest; therefore these are likely to be hydrolyzed. The hydrolysis of these amino acids would cause the peptides formed during the digest to become displaced from the membranes and be found in the solution, which was shown to contain limited to no radioactivity. These results suggest that within TM1-2 amino acids 1-60 and 126-139 do not contain the radiolabeled residue. By combining the immunoprecipitation studies mentioned above with that from the *in situ* trypsin digest, the region between E61-R125 likely contains the radiolabeled residue (Figure 4.5).

Figures 4.2, 4.3, and 4.4 are predicted trypsin cleavage sites of hDAT taken from a hydropathy plot (Giros and Caron, 1993). Depending on the accuracy of the hydropathy plot, residues K65, K66, R85, and K92 may or may not be accessible to the enzyme (Figure 4.4). If either K65 or K66 are hydrolyzed by trypsin, the labeled region would extend from K66/I67 to R125 instead of E61 to R125 as shown in Figure 4.4. On the other hand R85 is predicted to be located inside the membrane, causing it to be inaccessible to the enzyme and hydrolysis. According to the hydropathy plot, K92 is positioned in the middle of extracellular loop 1 and seems to be accessible to hydrolysis by trypsin. In an attempt to determine if cleavage at K92 occurs during an *in situ* trypsin digest, the labeled peptides produced from an *in situ* trypsin digest were solubilized from

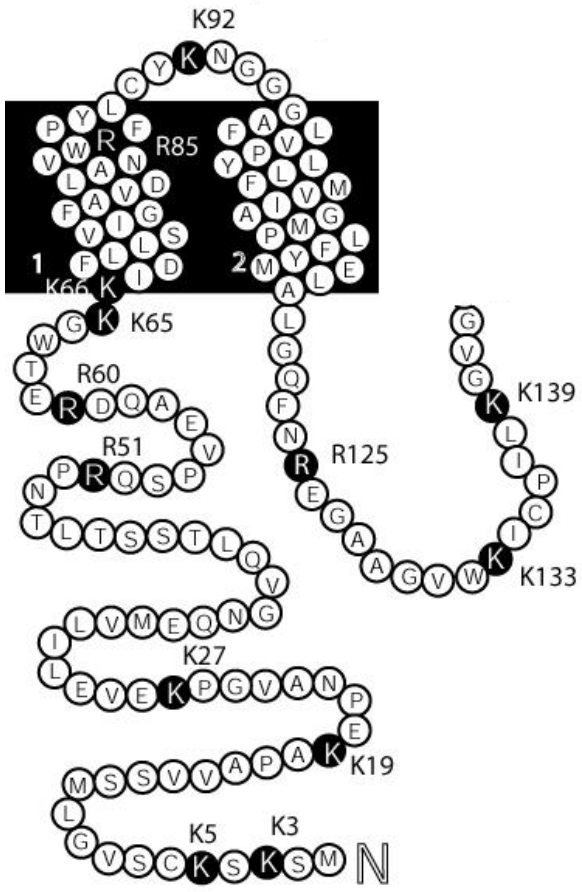

Figure 4.4 *In Situ* Trypsin Digest of TM1 and TM2 of hDAT. Within TM1-2 there are 13 trypsin cleavage sites. Arginine and lysine residues are indicated as black circles with white letters. Residues K3, K5, K19, K27, R51, R60, R125, K133, and K139 seem to be accessible to the enzyme, therefore are likely to be hydrolyzed by trypsin. Amino acid residues K65, K66, and K92 are estimated to be close to the membrane, which may render the residues inaccessible to the enzyme. Thus, the hydrolysis of K65, K66, and K92 by trypsin is possibly inhibited. R85 is pictured as being inside of the membrane, which prevents the enzymatic hydrolysis of the residue (adapted from Giros and Caron, 1993).

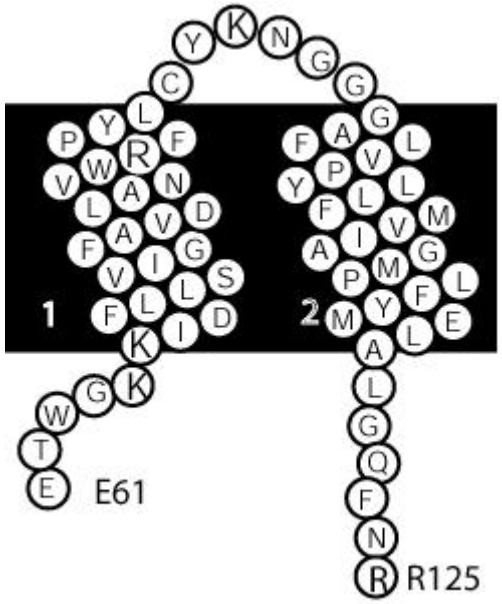

Figure 4.5 Possible Region Photolabeled by [^{125}I]MFZ 2-24. The region between E61-R125 likely contains the radiolabeled residue (adapted from Giros and Caron, 1993).

the membrane and redigested with trypsin (data not shown). The size of the [^{125}I]MFZ 2-24 labeled peptide did not change following the secondary trypsin digest, suggesting that cleavage at K92 occurs during an *in situ* trypsin digest of hDAT. With the hydrolysis of K92, the peptide photolabeled by [^{125}I]MFZ 2-24 extends from E61/K66/I67 to K92 (TM1) or N93 to R125 (TM2) (Figure 4.6).

Using the recently crystallized structure of the leucine transporter (LeuT) (Yamashita et al., 2005) as a model for hDAT, insight is given into the positioning of amino acid residues near TM1 and TM2 of hDAT. Figure 4.7 shows TM1 and TM2 of LeuT. Residue T10 (K65 in hDAT) is located at the surface of the intracellular side of TM1 of LeuT. The C terminal of T10, which is in the region hydrolyzed by trypsin in hDAT, is buried in the membrane. This suggests that K65 of hDAT is not accessible to be hydrolyzed by trypsin. It is likely that K66 is inaccessible as well since it is embedded further into the membrane than K65. Therefore, E61 would be the N terminal residue of the labeled peptide. Residue R30 (R85 in hDAT) is a highly conserved residue located in the middle of TM1. The positioning of this residue is similar to that predicted by the hydropathy plot of hDAT, in which R85 is inaccessible to trypsin due to its hydrophobic environment and structural nature in the membrane. The C terminal of E37 (K92 in hDAT), which is located at the surface of the extracellular side of TM1 in LeuT, seems accessible to hydrolysis. This is consistent with the data from the secondary digest of the labeled peptide produced from an *in situ* trypsin digest, suggesting that cleavage at K92 occurs during an *in situ* trypsin digest of hDAT. In addition to E37, the C terminal of G70 in LeuT (R125 in hDAT), positioned on the intracellular surface of TM2, seems accessible to enzymatic hydrolysis as well. It is also possible that G70 is inaccessible to

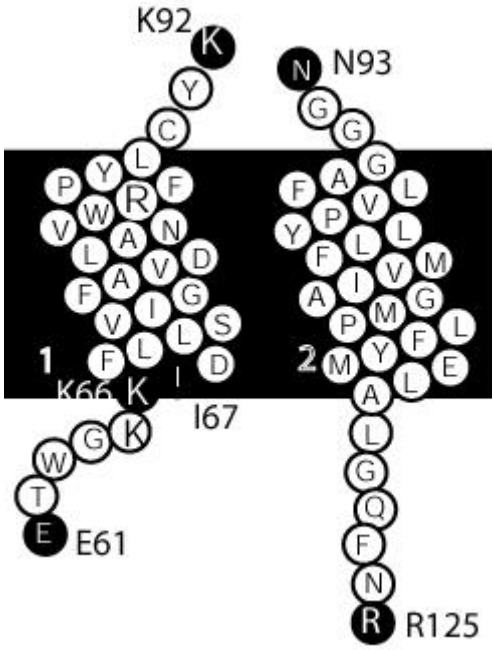

Figure 4.6 Possible Peptides Within TM1 and TM2 Photolabeled by [^{125}I]MFZ 2-24. N and C terminal residues of the labeled peptide are indicated as black circles with white letters. The region between E61/K66/I67- K92 (TM1) or N93-R125 (TM2) likely contains the radiolabeled residue (adapted from Giros and Caron, 1993).

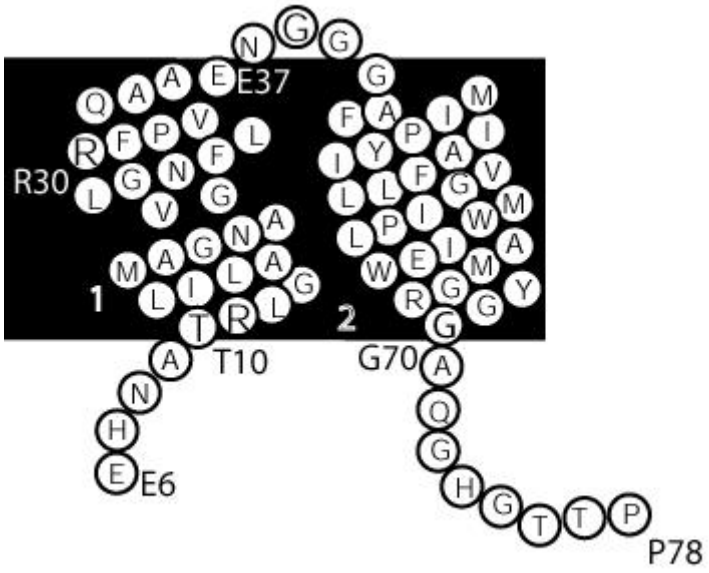

Figure 4.7 TM1 and TM2 of LeuT. E6, T10, R30, E37, G70 and P78 correspond to E61, K65, R85, K92, R125, and K133 in hDAT, respectively (adapted from Yamashita et al., 2005).

enzymatic hydrolysis, which would render P78 (K133 in hDAT) as the C terminal residue of the labeled peptide. Using LeuT as a template for the structure of hDAT, it is suggested that the region of [^{125}I]MFZ 2-24 incorporation is located near TM1 (E61-K92) or TM2 (N93-R125/K133). When taking this into consideration with the immunoprecipitation and mutational studies previously determined by Parnas et al. (2008), it can be inferred that [^{125}I]MFZ 2-24 is located near TM1 (E61-K92).

[^{125}I]RTI-82 Labels Near or In the Transmembrane Domains of wt & x5C hDAT

Following an i*n situ* trypsin digest of [^{125}I]RTI-82 labeled wild type hDAT, the region located in or near the transmembrane domains of hDAT was heavily labeled more than those contained in the supernatant. This suggests that the site of [^{125}I]RTI-82 incorporation is near or in the membrane. Figure 4.3 shows the peptides possibly labeled by [^{125}I]RTI-82. Previous studies determined that TM6 and adjacent regions (residues 292-344 in hDAT and 290-336 in rDAT) are the fragments labeled by [^{125}I]RTI-82 (Vaughan et al., 2007). Using the leucine transporter as a template for the structure of hDAT, there are 4 trypsin cleavage sites within residues 292-344 (Figure 4.8). Amino acid R295 is located in extracellular loop 3, which is positioned in an α-helix. Depending on the orientation of R295 in the helix, trypsin may not be able to hydrolyze the residue. R304 and K337 seem to be accessible to the enzyme, therefore are likely to be hydrolyzed by trypsin. R344 is located inside of TM7, which can prevent enzymatic hydrolysis of the residue. Based on the diagram of hDAT, modeled after LeuT, it is suggested that the region of [^{125}I]RTI-82 incorporation is located within 3 possible peptides (D292-R295, A296-R304, or L305-K337). This is consistent with previous

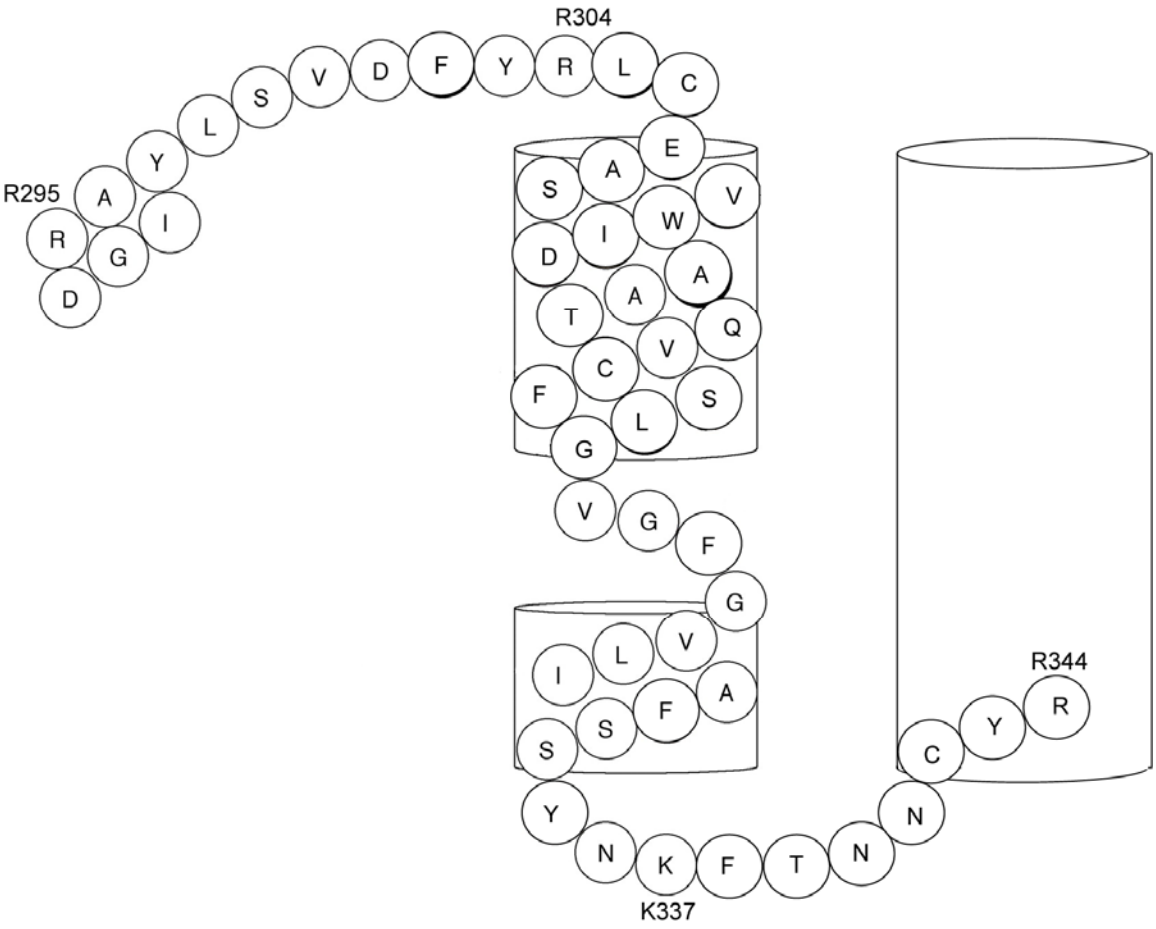

Figure 4.8 *In Situ* Trypsin Digest of [^{125}I]RTI-82 Labeled Fragment. Schematic diagram of residues D292-R344 of hDAT, modeled after LeuT. Within TM6 and adjacent regions there are 4 trypsin cleavage sites. Arginine and lysine residues are labeled. Residues R304 and K337 seem to be accessible to the enzyme, therefore are likely to be hydrolyzed by trypsin. Amino acid residue R295 is located in extracellular loop 3 in an α-helix. Due to the positioning of R295 in the helix, trypsin may not be able to hydrolyze the residue. R344 is illustrated as being inside of TM7, which can hinder the enzymatic hydrolysis of the residue (adapted from Vaughan et al., 2007).

rDAT studies performed by Vaughan et al. (2007), which suggested photoincorporation of the radioligand within M290-K336 (I292-K337 in hDAT).

Similarly to wt hDAT, the *in situ* trypsin digest of [^{125}I]RTI-82 labeled mutant hDAT also showed that the labeled residue is positioned near or in the transmembrane domains. The mutant transporter construct, x5C, contains five mutated cysteines (C90A, C135A, C306A, C319F, and C342A) (Figure 3.7). Since [^{125}I]RTI-82 has been shown to label within residues D292-R344 (Vaughan et al., 2007), only 3 cysteines (306,319,342) in the mutant construct are capable of affecting the labeling of [^{125}I]RTI-82 (Figure 4.9). Cysteine 306 and 319 have been shown to not substantially affect cocaine binding when mutated (Ferrer and Javitch, 1998; Vaughan et al., 2007), therefore the substitution of these residues to an alanine and phenylalanine, respectively, should not influence the labeling of [^{125}I]RTI-82. C342 is a highly conserved residue in neurotransmitter transporters (DAT, NET, SERT, GlyT1) and has been reported to be involved in ligand binding and transporter function (Ferrer and Javitch, 1998; Park et al., 2002; Ravna et al. 2003b; Yamashita et al., 2005). Although C342 is essential in the function of hDAT, it has been determined that C342 is not labeled by [^{125}I]RTI-82 (Vaughan et al., 2007). The presence of radioactivity (from wt and mutant hDAT) near or in the membrane suggests that [^{125}I]RTI-82 labels the same region in both constructs. It can also be assumed that the absence of the five cysteine residues will not affect the labeling of [^{125}I]RTI-82 to a region near or in the transmembrane domains. There is a possibility that the mutations will cause the radioligand to label a residue near or adjacent to its original labeling site. If this occurs, it is expected that the residue labeled should also be positioned in or near the transmembrane domains.

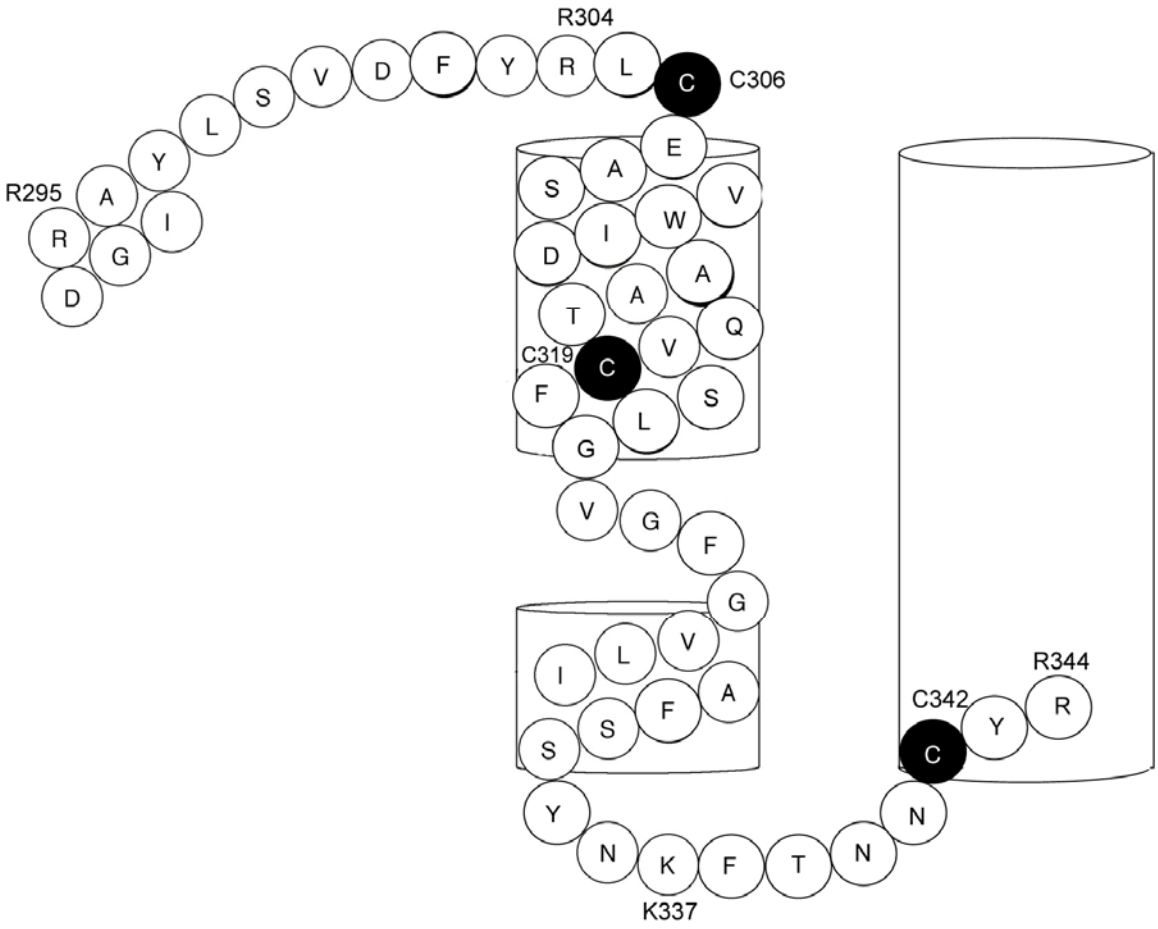

Figure 4.9 *In Situ* Trypsin Digest of [^{125}I]RTI-82 Labeled Mutant hDAT. Schematic diagram of residues D292-R344 of hDAT, modeled after LeuT. The mutant transporter construct, x5C, contains three mutated cysteines (C306A, C319F, and C342A) within TM6 and adjacent regions. Cysteine residues are indicated as black circles with white letters. Arginine and lysine residues are labeled (adapted from Vaughan et al., 2007).

The *in situ* digest also shows that more of wild type hDAT is labeled by [^{125}I]RTI-82 than that of mutant hDAT. According to studies performed by Ferrer and Javitch (1998), the x5C construct expresses about 30-50% less hDAT than wild type. Therefore, [^{125}I]RTI-82 is capable of labeling more wt hDAT than mutant hDAT.

Analysis of Radiolabeled CNBr peptide

Mechanism by Which CNBr Cleaves Methionine

Cyanogen bromide (CNBr) hydrolyzes peptide bonds at the C-terminus of methionine residues. Cleavage of this bond is hindered when a serine or threonine residue is adjacent to methionine on the C-terminal side. A high concentration of acid in the presence of Met-Ser or Met-Thr causes CNBr to react with methionine without peptide bond cleavage (Kaiser and Metzka, 1999). Within hDAT Met-Thr is not present, but Met-Ser occurs in the N terminal and intracellular loop 5. Since [^{125}I]MFZ 2-24 is thought to label a region within TM1-2 (Parnas et al., 2003; Parnas et al., 2008), a CNBr digest of hDAT will not hinder localization of the site photolabeled by [^{125}I]MFZ 2-24. The reaction is usually performed in an acidic environment, which inhibits the side chain oxidation of methionine (Kaiser and Metzka, 1999; Steers et al., 1965). In basic conditions CNBr reacts not only with methionine but also with basic side chains of various amino acids residues, making alkaline conditions unsuitable for hydrolysis (Schreiber and Witkop, 1964).

The reaction between CNBr and methionine is initiated by a nucleophilic attack of CNBr on the sulfur atom in the side chain of methionine (Figure 4.10). This attack displaces bromine, forming a cyanosulfonium bromide intermediate. The methyl thiocyanate is then displaced by the carbonyl oxygen, producing an iminolactone bromide. The iminolactone is later hydrolyzed by water, which cleaves the methionine peptide bond and generates a peptide that has a homoserine lactone at the C-terminal (Gross, 1967; Garrett and Grisham, 1999).

CNBr Digestion of hDAT

The primary sequence of hDAT contains 14 methionine residues (Figure 4.11). Hydrolysis of hDAT with CNBr produces a single residue (M1) and 14 peptides with varying lengths (Table 4.1). Half of the peptides have retention times less than 52 minutes while the other half elutes after 90 minutes. The HPLC retention times of the peptides were calculated using the gradient from the experimental HPLC analysis of radiolabeled hDAT (Sakamoto *et al.*, 1988; GPMAW 6.11, Lighthouse Data). The retention times shown are based on the peptides alone, without the radiolabel attached.

Cleavage of [^{125}I]MFZ 2-24 labeled hDAT with CNBr yields a radiolabeled peptide with a retention time of 79 minutes. In the control experiments where irradiated [^{125}I]MFZ 2-24 was incubated with both ethanol and CNBr solution separately, the retention of the radioligand remained the same. This suggests that the CNBr digest does not have an adverse effect on the irradiated structure of [^{125}I]MFZ 2-24 and that the 79 minute peak produced from the digest contains the intact radioligand. When attached to a

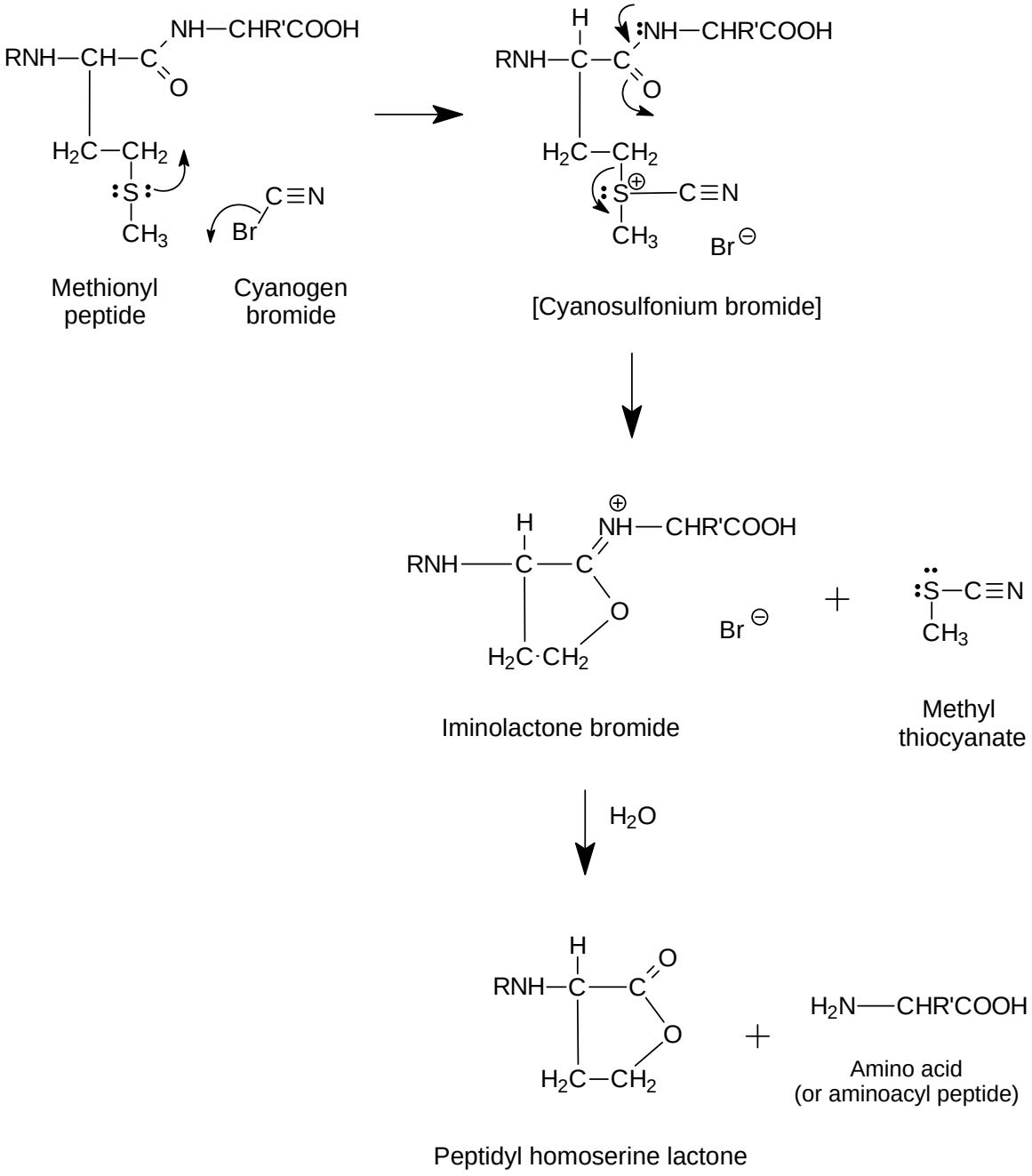

Figure 4.10 CNBr Cleavage Reaction (from Gross, 1967).

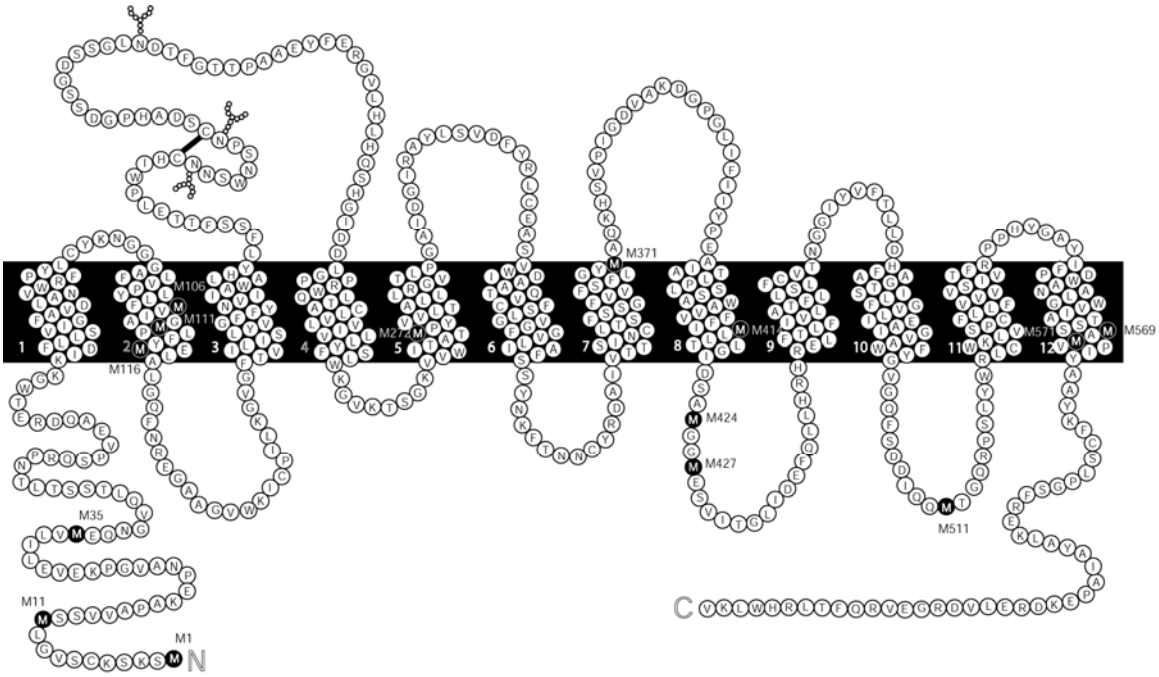

Figure 4.11 CNBr Digest of hDAT. Methionine residues are indicated as black circles with white letters. There are 14 methionine residues in hDAT (adapted from Giros and Caron, 1993).

Calculated Unlabeled HPLC RT (min)	Sequence	From-To	# of Amino Acids	Location
7.5	M	1-1	1	N-terminus
37.4	SKSKCSVGLM	2-11	10	N-terminus
27.3	VIAGM	107-111	5	TM 2
46.2	PLFYM	112-116	5	TM 2
49.3	LLTLGIDSAM	415-424	10	TM 8 - IL 4
11.7	GGM	425-427	3	IL 4
8.7	AM	570-571	2	TM 12
51.3	SSV…LVM	12-35	24	N-terminus
112.9	EQN…LFM	36-106	71	N-terminus- TM2
174.5	ELA…ATM	117-272	156	IL 1 – TM 5
142.2	PYV…GYM	273-371	99	TM 5 – TM 7
95.8	AQK…FIM	372-414	43	EL 4 – TM 8
141.6	ESV…QQM	428-511	84	IL 4 – IL 5
119.9	TGQ…SSM	512-569	58	IL 5 – TM 12
94.8	VPI…LKV	572-620	49	TM 12 - C-terminus

Table 4.1 Retention Times of hDAT Peptides Produced From a CNBr Digest. Above the dashed line are all peptides eluting in less than 52 min. Below the line are peptides with retention times greater than 90 min. These retention times do not take into consideration the effect [^{125}I]MFZ 2-24 would have on the elution rate of the peptides. It is hypothesized that the presence of the hydrophobic label will increase the retention time of any peptide. See Figure 1.3 for complete sequences of peptides below the dashed line (from Wirtz, 2004).

small peptide, the hydrophobicity of [^{125}I]MFZ 2-24 causes it to extend the retention time of that particular peptide. Since the 79 minute CNBr peptide is attached to the radiolabel, it can be assumed that the retention time of the peptide alone is less than 79 minutes. Table 4.1 suggests that following a CNBr digest of hDAT, only 7 peptides elute from the HPLC in less than 79 minutes. Immunoprecipitation studies determined that a region within TM1-2 is the site of [^{125}I]MFZ 2-24 incorporation (Parnas et al., 2003; Parnas et al., 2008), eliminating the N terminal and TM3-12 as possible labeling sites. Thus, M, SKSKCSVGLM, LLTLGIDSAM, SSV…LVM, GGM, and AM are not labeled by [^{125}I]MFZ 2-24. On the other hand, both VIAGM and PLFYM are located within TM1-2 and have retention times of less than 79 minutes. Previous labeling experiments with MFZ 3-37, an isothiocyanate version of MFZ 2-24, determined that labeled PLFYM and VIAGM have retention times of 79 and 58.8 minutes, respectively (Wirtz, 2004). Therefore, it is suggested that the 79 minute CNBr peak is PLFYM, located in transmembrane domain 2 (Figure 4.12). In contrast, a recent digest of hDAT with CNBr suggests that a 12kDA peptide which extends from M1/S2/M11/S12 – M106 is produced from a CNBr digest of [^{125}I]MFZ 2-24 labeled hDAT (Parnas et al., 2008). In addition, mutational experiments performed in the same study determined that residues 68-80 are the site of [^{125}I]MFZ 2-24 incorporation. In these experiments, hDAT was electroeluted, dried down, and reconstituted with an acidic CNBr solution. The drying down of hDAT, which is a hydrophobic protein, causes the protein to aggregate, become unmanageable, and difficult to solubilize. Aggregation of hDAT can hinder hydrolysis of the protein, by making cleavage sites inaccessible to chemical and/or enzymatic proteolysis. This may

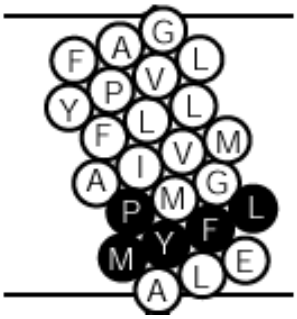

Figure 4.12 Schematic Diagram of Transmembrane Domain 2 of hDAT. PLFYM is likely the [^{125}I]MFZ 2-24 labeled peptide produced from a CNBr digest of hDAT. The PLFYM peptide is shown as black circles with white letters (adapted from Giros and Caron, 1993).

explain why a 12kDa peptide was seen instead of a smaller fragment with a retention time of 79 minutes. Ten of the eleven digestions performed by Parnas et al. (2008) seem to be incomplete due to the massive amount of undigested hDAT located at the upper region of the gels. In the mutational study where hDAT was completely digested, either a different digestion protocol was used to obtain a fully digested peptide or the sample lacked hDAT. The inconsistency in these CNBr digestions suggests that the results obtained by Parnas et al. (2008) may be invalid. By properly solubilizing, completely digesting, and not drying down hDAT, the 12kDa peptide, seen by Parnas and colleagues (2008) following a CNBr digest of the protein, may decrease to a smaller fragment with a retention time of 79 minutes.

Chymotryptic Digest of CNBr Peptide

Chymotrypsin is a proteolytic enzyme found in the digestive system that cleaves peptide bonds on the carboxyl side of tyrosine, phenylalanine, and tryptophan, and to a lesser extent, leucine, methionine, asparagine, and glutamine (Baumann et al, 1970; Berezin and Martinek, 1970; Keil, 1992). Following the chymotrypsin digest of the 79 minute CNBr peptide (PLFYM), the radioactivity shifted to three peaks with retention times of 67, 60, and 47 minutes. The migration of the 79 minute peak, following the chymotrypsin digest, further confirms that VIAGM is not labeled by [^{125}I]MFZ 2-24. Since VIAGM lacks any chymotrypsin cleavage sites, the 79 minute radioactive peak would not have shifted to shorter eluting peaks. The appearance of the new peaks following the chymotrypsin digest suggests that the digest may have been incomplete. Missed cleavages may also arise from the enzyme's inability to hydrolyze substrates near

the labeled residue. Previous photolabeling studies using 8-azidoadenosine 5'-triphosphate (N_3-ATP) and tritiated phenyl azide have shown that chymotrypsin is capable of hydrolyzing labeled tyrosine (Knight and McEntee., 1985; de Ravel et al., 2001). Since the molecular weight of N_3-ATP is 615g/mol and that of [^{125}I]MFZ 2-24 is 578 g/mol, it is unlikely that the presence of the radioligand interferes with the enzyme's ability to recognize and hydrolyze its substrate. Therefore, the 47 minute peak is possibly a completely chymotrypsin digested peptide that was nested in the CNBr peptide, PLFYM.

A complete chymotrypsin digest of PLFYM should produce PLF, Y, and M. Taking into consideration the possibility of an incomplete digest the 67, 60, and 47 minute peaks are potentially PLFY, M, PLF, and/or YM. Previous solid state photolabeling experiments have shown that MFZ 3-37 labeled YM and [^{125}I]MFZ 2-24 labeled [^{3}H]tyrosine have retention times of 66.5 and 49.5 minutes, respectively (performed by Uliana Danilenko). This suggests that the 67 and 47 minute peaks produced from a chymotryptic digest of [^{125}I]MFZ 2-24 labeled CNBr peptide are YM and Y, respectively. The identification of the 60 minute peak has yet to be determined; additional experiments are needed to confirm its identity. Using the results from the previous solid state photolabeling, Y115 is likely the hDAT residue labeled by [^{125}I]MFZ 2-24. In contrast, residues D68-L80 in TM1 have been suggested by Parnas et al. (2008) as the region labeled by [^{125}I]MFZ 2-24. Taking these residues (D68-L80) into consideration, along with the 3 radioactive peaks (47, 60, 67) produced from a chymotrypsin digest of the CNBr peptide, the predicted retention time of GKKIDF (G64-F69) and AVDLANVW (A77-W84) correlates with the 60 minute peak produced from

the chymotrypsin and CNBr digest. Therefore, if [^{125}I]MFZ 2-24 is incorporated within residues D68-L80, the labeled peptide is likely GKKIDF (G64-F69) or AVDLANVW (A77-W84).

Thermolysin Digest of CNBr Peptide

Thermolysin hydrolyzes peptide bonds on the amino side of bulky hydrophobic residues such as leucine, isoleucine, valine, and phenylalanine (Matsubara et al., 1965; Tatsumi et al., 2007). This cleavage is favored when an aromatic residue is attached to the N-terminal side of the hydrophobic amino acid, but hindered when this site is occupied by an acidic residue (Keil, 1992). Hydrolysis of peptide bonds involving tyrosine, alanine, methionine, histidine, asparagine, serine, threonine, glycine, lysine and acidic residues may also occur, but to a lesser degree (Heinrikson, 1977).

Digestion of the 79 minute CNBr peptide with thermolysin, produced three radioactive peaks with shorter retention times of 63, 69, and 76 minutes. The appearance of the three peaks following the digest suggests that the digestion was incomplete. Hypothetically a complete thermolysin digest of PLFYM should produce P, L, and FYM. Taking into consideration the possibility of an incomplete digest the 76, 69, and 63 minute peaks are potentially undigested PLFYM, LFYM, and FYM, respectively. A missed cleavage between P-L would suggest that the dipeptide PL is also a potential peptide labeled by [^{125}I]MFZ 2-24. The 63 minute hDAT peptide is higher than the predicted 45 minute retention time of radiolabeled PL. Thus, PL can be excluded as being a possible radiolabeled peptide. Due to thermolysin's lack of specificity, minor or secondary cleavages of the N terminal bond of tyrosine, alanine, methionine, histidine,

asparagine, serine, threonine, glycine, lysine and acidic residues may also occur. It is possible that minor cleavages are capable of occurring between F-Y and Y-M, which will produce a labeled residue with a retention time less than 50 minutes. Since the hDAT labeled peptides had retention times greater than 60, it its unlikely that any minor cleavages occurred. Therefore, FYM (residues 114-116) is likely the peptide labeled by [^{125}I]MFZ 2-24. According to Parnas et al. (2008) residues D68-L80 in TM1 are the sites of [^{125}I]MFZ 2-24 incorporation. By comparing the retention time of the 3 radioactive peaks (63, 69, 76) to that of the predicted retention times of the possible peptides produced from a thermolysin digest of residues D68-L80, F76-A77 is likely the dipeptide labeled by [^{125}I]MFZ 2-24 using the results obtained from Parnas and coworkers (2008).

Analysis of Thermolysin Digested hDAT

Thermolysin Digest of Labeled hDAT

Thermolysin catalyzes the hydrolysis of the peptide bond on the N-terminal side of leucine, isoleucine, valine, and phenylalanine (Matsubara et al., 1965; Tatsumi et al., 2007). Hydrolysis of hDAT with thermolysin produces over 200 peptides. Since Parnas et al. (2003) determined that [^{125}I]MFZ 2-24 labels within TM1-2, then TM3-12, as well as the N and C terminals, can be eliminated as possible labeling sites. A thermolysin digest of TM1-2 of hDAT contains 45 cleavage sites (Figure 4.13). By combining the results from Parnas et al. (2003) and the *in situ* trypsin digest, a thermolysin digest of the region

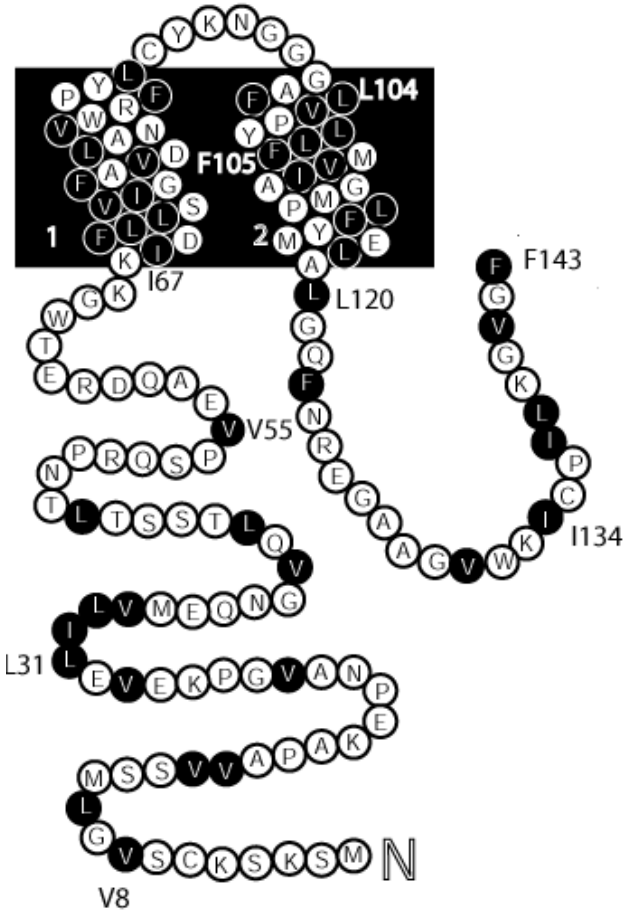

Figure 4.13 Thermolysin Digest of TM1 and TM2 of hDAT. Within TM1-2 there are 45 thermolysin cleavage sites. Leucine, isoleucine, valine, and phenylalanine residues are indicated as black circles with white letters (adapted from Giros and Caron, 1993).

between E61-R125 contains 25 cleavage sites (Figure 4.14). Cleavage of [^{125}I]MFZ 2-24 labeled hDAT with thermolysin produces two radioactive peaks with retention times of 77 and 82 minutes. A subsequent thermolysin digest of the 77 minute peak produced a peak with a shorter retention time of 63 minutes. A secondary thermolysin digest of the 82 minute peak shifted the radioactivity to two peaks with retention times of 63 and 73 minutes. The migration of the peaks following the thermolysin digestion suggests that the digest may have been incomplete. The 63 minute radiolabeled peptide was then attached to an arylamine sequelon disc and Edman degradation was applied. The second amino acid in the peptide was labeled by [^{125}I]MFZ 2-24.

Peptides are attached to the arylamine sequelon disc via carbodiimide activation with the carboxyl groups, which are present on the C-terminal, glutamic acid, and aspartic acid residues. The stability of the bond between the peptide and the disc allows the peptide to stay attached to the disc during the degradation process. Therefore, peptides with E or D as the second residue, along with dipeptides, can only release one amino acid. This excludes peptides with E or D as the second residue and dipeptides as possible labeled peptides because the second amino acid was detached from the 63 minute radiolabeled peptide.

The results from the previously mentioned trypsin *in situ* digest of [^{125}I]MFZ 2-24 labeled hDAT suggests that the region between residues 61-125 is the site of [^{125}I]MFZ 2-24 incorporation (Figure 4.5). The Edman degradation results along with the *in situ* data identified 21 possible residues that are capable of being labeled by [^{125}I]MFZ 2-24 (Table 4.2). Of the 21 amino acids, 8 are located in TM1 and 13 are positioned in TM2.

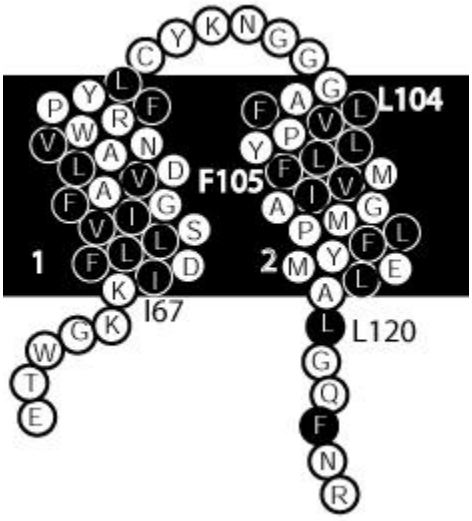

Figure 4.14 Thermolysin Digest of Region Labeled by [^{125}I]MFZ 2-24. Within E61 and R125 of hDAT there are 25 thermolysin cleavage sites. Leucine, isoleucine, valine, and phenylalanine residues are indicated as black circles with white letters (adapted from Giros and Caron, 1993).

TM1 Residues	TM2 Residues
L70 L71 S72 I74 A77 W84 P87 C90	L99 V100 P101 L104 F105 M106 I108 A109 F114 Y115 A119 G121 N124

Table 4.2 Possible Amino Acid Residues in hDAT Labeled by [^{125}I]MFZ 2-24 Within E61 –R125. There are 8 residues in transmembrane domain 1 and 13 in transmembrane domain 2 that are potential targets for the photoincorporation of [^{125}I]MFZ 2-24.

Within amino acids 68-80, which is the proposed site of [^{125}I]MFZ 2-24 incorporation (Parnas et al., 2008),there are 5 possible residues (L70, L71, S72, I74, A77) that are targets of [^{125}I]MFZ 2-24. Previous amino acid reactivity studies performed by Schwartz (1989) suggest that only 6 (C90 >W84> Y115> F105≈ F114 > G121) of the 21 residues are likely to react with phenyl nitrene (Table 1.1). Cysteine is the most reactive amino acid and glycine is the least reactive. Mutational studies of cysteine 90 to alanine in DAT demonstrated that cocaine potentiates CFT (cocaine analog) binding to the transporter (Ferrer and Javitch, 1998). This suggests that the binding of cocaine causes a conformational change that alters the accessibility of C90 (Ferrer and Javitch, 1998), which possibly increases the reactivity rate of the residue. In an attempt to determine if [^{125}I]MFZ 2-24 photolabels C90, Uliana Danilenko labeled mutant (X90C) hDAT with [^{125}I]MFZ 2-24 following the reaction of C90 with a MTS reagent. The mutant transporter construct, X90C, contains one cysteine residue (C90), which will react readily with a MTS reagent. The reaction of C90 with the MTS reagent did not prevent photoincorporation of the radioligand. This suggests that the labeling of [^{125}I]MFZ 2-24 is not specific to position 90 and the reacted C90 may have caused the radioligand to label a residue near or adjacent to its original labeling site. It can also be inferred from this study that C90 is not the site of [^{125}I]MFZ 2-24 photoincorporation. The crystal structure of LeuT suggests that A35, the residue aligned with C90 in DAT, is positioned near the substrate and inhibitor binding site (Yamashita et al., 2005; Zhou et al. 2007). Therefore, substitutions of A35 are capable of altering the binding of both substrates and inhibitors of LeuT. These findings suggest that C90 is possibly a target for [^{125}I]MFZ 2-24, due to its close proximity to the inhibitor binding site.

In addition to C90, phenylalanines 105 and 114 are also highly reactive residues that have been shown to be a key element in the binding and transport properties of DAT (Wu and Gu, 2003; Sen et al., 2005). Both F105 and F114 are conserved residues in mammalian DAT and monoamine transporters, respectively, that are located in TM2 (Wu and Gu, 2003; Beuming et al., 2006). Substitution of phenylalanine 114 for cysteine reduced transport by more than 10-fold (Sen et al., 2005). Similarly, mutations of F105 to alanine, leucine, isoleucine, serine, threonine, asparagine or glutamine resulted in transporters with low transport activity (Wu and Gu, 2003). However, switching F105 to a methionine or cysteine lowers cocaine sensitivity (Wu and Gu, 2003). Replacing F105 with aromatic residues such as tyrosine and tryptophan allowed the transporters to retain more than 75% transport activity and high cocaine sensitivity (Wu and Gu, 2003). These results suggest that phenylalanine at position 105 is involved in substrate transport as well as cocaine binding. Further characterization of F105 and other surrounding residues led to a functional triple mutant (L104V, F105C, and A109V), which was dramatically less sensitive to cocaine inhibition when compared to wild type DAT (Chen et al., 2005). This suggests that residues 104, 105, and 109 are near or in the cocaine binding site, which renders them capable of being photolabeled by [^{125}I]MFZ 2-24.

Despite the low reactivity rate of proline with phenyl nitrene, mutational studies have shown that this residue is vital to the structure and function of DAT (Lin et al., 2000). Proline 87 and 101 in the dopamine transporter are highly conserved residues among Na^+/Cl^--dependent transporters (Povlock and Amara, 1997; Lin et al., 2000; Yamashita et al., 2005). Proline residues can play important roles in the structure of transporter proteins as well as contribute to substrate and ion translocation. Substitution

of P87A altered expression patterns of DAT to less than one-third of wild-type DAT (Lin et al., 2000). This suggests that P87 is directly involved in the trafficking of DAT to the plasma membrane. Lin and co-workers (2000) also investigated the role of proline 101 in dopamine uptake, cocaine recognition, and expression. They determined that by substituting proline 101 for alanine, the expression patterns of wild-type DAT and the mutant are indistinguishable. In contrast, the P101A mutant displayed a fivefold increase in the affinity for dopamine compared to wild-type. The mutation also caused a significant decrease in the affinity of DAT for cocaine. These studies suggest that proline at position 101 is critical for recognition and binding of cocaine, which makes P101 a potential target for [^{125}I]MFZ 2-24 photoincorporation.

Recently, Sen and colleagues (2005) performed mutational studies on 25 residues in TM2, which included some of the least reactive residues in hDAT that may be labeled by [^{125}I]MFZ 2-24. They demonstrated that by substituting residues in TM2 with cysteine, one at a time, disrupts binding and transport properties of DAT. The G121C mutant produced an inactive DAT that was expressed sufficiently on the plasma membrane. Most of the other mutations (L99, V100, L104, M106, I108, A109, Y115, A119) led to the reduction of transport. Surface expression was only affected by the substitution of L99 for cysteine. The affinity of DAT for cocaine increased when L99, V100, L104, and M106 was mutated. However, by switching I108, A109, and Y115 to cysteine, the affinity of DAT for cocaine decreased. Their results highlighted the influence these residues in TM2 have on cocaine binding, which suggests the possibility of them being photolabeled by [^{125}I]MFZ 2-24.

Transmembrane Domains 1 & 2 of Neurotransmitter Transporters

The experimental data presented in this thesis suggests that [^{125}I]MFZ 2-24 is photoincorporated within transmembrane domain 1 and/or 2, which may also correspond to the binding site of cocaine. Using the recently crystallized structure of the leucine transporter (LeuT) as a model for hDAT, insight is gained into the positioning of amino acid residues near TM1 and TM2 of hDAT. Yamashita and co-workers (2005) crystallized the bacterial leucine transporter (LeuT), in which they identified TM1 and TM6 as being in direct contact with the substrate (leucine) and sodium ion binding site. Recently, the crystal structure of LeuT in the presence of an inhibitor (desipramine) was determined (Zhou et al., 2007). The authors overlayed both structures and noticed that the overall structure of LeuT with desipramine bound was similar to that of LeuT bound with leucine. Kinetic studies performed by Zhou and colleagues (2007) showed that the binding of desipramine only affects the transport of leucine, leaving the affinity of LeuT for leucine unaltered. They suggested that the binding of the inhibitor causes a conformational change that allows the substrate to bind, but allosterically inhibits transport of the substrate. This indirect inhibition of transport implies that the binding sites of the substrate and inhibitor are nonoverlapping, although F253 is a residue shared by both molecules. The binding site of desipramine and leucine is separated by the extracellular gate of the transporter, which is formed by R30, Y108, and F253 (Zou et al., 2007). The desipramine binding pocket is formed by interactions of the inhibitor with R30, Q34, F253, F319, F320, L400, and D401 of LeuT (Figure 1.9). The intermolecular contacts made by R30 and Q34, which are both located in TM1, suggest the critical role of TM1 in the binding of LeuT inhibitors. Using LeuT as a model for hDAT, one can

infer that TM1 of hDAT may also contribute to inhibitor binding and possibly be a target for [^{125}I]MFZ 2-24 photoincorporation.

Along with DAT, the serotonin transporter (SERT) is also a Na^+/Cl^- dependent monoamine transporter that lacks a crystal structure. In lieu of a structure, mutational studies have been performed on SERT to determine the functional contribution of TM1 (Henry et al., 2003; Henry et al., 2006b) and TM2 (Sato et al., 2004; Korkhov et al., 2006), which may give some insight into the roles of both domains in DAT. To probe the contribution of TM1 in SERT, 21 residues in TM1 were mutated to cysteine one at a time and analyzed (Henry et al., 2003). Most of the residues in TM1 demonstrated a decrease in substrate binding and transport when mutated to cysteine. The binding of inhibitors to the mutants was slightly decreased by the mutations. The authors suggest that the conformation of residues in TM1 (specifically Y107 and I108) are allosterically altered by the binding of cocaine, which causes inhibition of transport. Mutational studies performed by Korkhov and colleagues (2006) demonstrated a role for a TM2 residue (E136) in substrate and inhibitor binding, as well as substrate transport. Substitution of E136 for glutamine and alanine eliminated transport and decreased inhibitor binding. The E136D mutant showed a decrease in transport, while the inhibitor binding affinity was comparable to that of wild-type SERT, suggesting that the similar structure of glutamic acid and aspartic acid minimally alters inhibitor binding. Korkhov and coworkers concluded that E136 regulates the binding and transport of serotonin by stabilizing the structural conformation of SERT during the transport cycles. If DAT is structurally similar to SERT, these findings suggest that TM2 in DAT may be directly involved in the binding of inhibitors, while TM1 has an indirect contribution to inhibitor binding.

The norepinephrine transporter (NET) is also a Na^+/Cl^- dependent monoamine transporter, similar to that of DAT and SERT. Previous mutation studies on TM2 of NET suggest a range of roles that TM2 plays in determining the expression and function of the transporter (Sucic et al., 2002; Paczkowski and Bryan-Lluka, 2004; Sucic et al., 2005). Analysis of a TM2 conserved residue (E113 in NET) among monoamine and Na^+/Cl^- dependent transporters determined that the size, not the charge or polarity, of the residue at position 113 is essential for the function and expression of NET (Sucic et al., 2002). Mutation of E113 with glutamine displayed minor functional consequences in the binding of the substrate and inhibitor. In contrast, the substitution of E113 with alanine or aspartate caused a reduction in surface expression and functionality of NET. By combining these results with that of SERT, it is hypothesized that TM2 in DAT is directly involved in the binding of inhibitors (Wu and Gu, 2003), which likely suggests that [^{125}I]MFZ 2-24 labels a residue(s) in TM2.

Substitution of residues in TM1 and TM2 of DAT suggests an involvement of both domains in inhibitor binding. Mutational analysis of Asp79 in TM1 of DAT has shown that aspartate at this position is important for cocaine binding (Kitayama et al., 1992). In this study, replacing aspartate with alanine, glycine, and glutamate reduced the affinity for the tritium-labeled cocaine analog, CFT. A mutation of aspartate to asparagine at position 68 also decreased the binding affinity of CFT, suggesting that aspartate at this location has an influence on cocaine binding as well (Chen et al., 2001). It has been suggested that the tropane nitrogen in cocaine interacts with acidic DAT amino acids (Uhl and Lin, 2003). In 2005, Sen and co-workers performed a study on TM2 of DAT, where 21 residues in TM2 were mutated to cysteine one at a time and

analyzed. They reported results suggesting that TM2 was not water accessible due to its lack of reaction with MTS derivatives and the inability to alter uptake in the presence of MTS derivatives. TM2 was further analyzed in the same study by crosslinking several residues in TM2 with mercuric chloride in the presence of an inhibitor. Crosslinking of these residues was inhibited by the presence of the cocaine analog MFZ 2-12. From these findings, the authors suspect that TM2 indirectly contributes to the cocaine binding site (Sen et al., 2005). The studies above suggest an involvement of both TM1 and TM2 in cocaine binding to DAT. It has yet to be determined whether these interactions occur directly or indirectly. By correlating the structure of DAT to that of LeuT, it can be inferred that TM1 is directly involved in the binding site of cocaine. In contrast, by analyzing the molecular structure of DAT to mutational studies performed on SERT and NET, it is shown that TM2 demonstrates a direct interaction with the binding of cocaine. Without a crystal structure, the modeling of DAT using structural and mutational analysis of other transporters only predicts the residues contributing to the cocaine binding cavity in DAT. It is possible that cocaine interacts with both domains (TM1 and TM2) directly or indirectly depending on its structural orientation.

The evidence presented above supports the proposal that either TM1 and/or TM2 are labeled by [^{125}I]MFZ 2-24. The thermolysin digest and Edman degradation data reported in this dissertation suggest that residues (Table 4.2) in both TM1 and TM2 are capable of being covalently linked with [^{125}I]MFZ 2-24. More specifically, the previously mentioned CNBr experiments performed on hDAT suggest that PLFYM, particularly Y115, in TM2 is labeled by [^{125}I]MFZ 2-24. In order to definitely conclude that Y115 is photolabeled by [^{125}I]MFZ 2-24, further analysis involving Edman degradation and/or

mass spectrometry must be applied to PLFYM. The current caveat to using Edman degradation arises from the discontinued manufacture of the arylamine sequelon disc, which is needed to separate the target peptide from the amino acid removed during each cycle. Along with Edman degradation, there are also limitations with using mass spectrometry as an approach to identify the residue photolabeled by [^{125}I]MFZ 2-24. The inability to obtain an adequate quantity of hDAT hinders one from obtaining data needed to identify the labeled residue via this analysis technique. The signals of the hydrophobic transmembrane peptides produced from hDAT are suppressed by that of hydrophilic peptides, which are more readily ionized and thus easily detected with MALDI than are the hydrophobic transmembrane peptides. Another issue that renders the use of mass spectrometry difficult when analyzing MFZ 2-24 labeled hDAT is the low labeling efficiency of MFZ 2-24. Previous studies have shown that phenyl azides have a low level of photoincorporation (about 1%) (Watt et al., 1989; Niedel et al., 1980). Obtaining a sufficient amount of labeled hDAT will lead to the identification of the labeled residue(s) using mass spectrometry.

Further application of MFZ 2-24, along with other irreversible photoaffinity labels, will lead to the discovery of the specific amino acid residues that form the inhibitor binding site of hDAT. Peptide mapping studies of DAT, using data obtained from the labels, suggest that one inhibitor binding pocket exists and each label binds in a distinct manner according to its molecular structure (Vaughan et al., 2001). Mutations to this binding pocket may provide evidence as to whether cocaine interacts with the same binding domain as other dopamine uptake inhibitors. These studies will

extend our knowledge in understanding the structural basis of the cocaine binding site on hDAT and the individual role of each amino acid.

References

Abramson J., Smirnova I., Kasho V., Verner G., Kaback H.R., and Iwata S. (2003) Structure and Mechanism of the Lactose Permease of Escherichia Coli. *Science*, **301**, 610-615.

Agoston G., Wu J.H., Izenwasser S., George C., Katz J., Kline R.H., and Newman A.H. (1997) Novel N-Substituted 3α-[Bis(4'-fluorophenyl)methoxy]tropane Analogs: Selective Ligands for the Dopamine Transporter. *J. Med. Chem.*, **40**, 4329-4339.

Ambler R.P. and Meadway R.J. (1968) The Use of Thermolysin in Amino Acid Sequence Determination. *J. Biochem.*, **108**, 893-895.

Anderson P.H. (1989) The Dopamine Inhibitor GBR 12909: Selectivity and Molecular Mechanism of Action. *Eur. J. Pharmacol.*, **166**, 493-504.

Baumann W.K., Bizzozero S.A., and Dutler, H. (1970) Specificity of Alpha-Chymotrypsin. Dipeptide substrates. *FEBS Lett.,* **8**, 257-260.

Berezin I.V. and Martinek K. (1970) Specificity of Alpha-Chymotryspin. *FEBS Lett.*, **8**, 261-262.

Bergman J., Madras B.K., Johnson S.E., and Spealman R.D. (1989) Effects of Cocaine and Related Drugs in Nonhuman Primates: III. Self-administration by Squirrel Monkeys. *J. Pharmacol. Exp. Ther*., **251**, 150-55.

Beuming T., Shi L., Javitch J.A., and Weinstein H. (2006) A Comprehensive Structure-Based Alignment of Prokaryotic and Eukaryotic Neurotransmitter/Na Symporters (NSS) Aids in the Use of the LeuT Structure to Probe NSS Structure and Function. *Mol. Pharm.*, **70**, 1630-1642.

Blakely R.D. and DeFelice L.J. (2007) All Aglow abut Presynaptic Receptor Regulation of Neurotransmitter Transporters. *Mol. Pharmacol.*, **71**, 1206-1208.

Blakely R.D., De Felice L.J., and Hartzell H.C. (1994) Molecular Physiology of Norepinephrine and Serotonin Transporters. *J. Exp. Biol.*, **196**, 263-281.

Blanco R.M., Halling P.J., Bastida A., Cuesta C., and Guisan J.M. (1992) Effect of Immiscible Organic Solvents on Activity/Stability of Native Chymotrypsin and Immobilized-Stabilized Derivatives. *Biotech. Bioeng.*, **39**, 75-84.

Bogdanov M., Zhang W., Xie J., and Dowham W. (2005) Transmembrane Protein Topology Mapping by the Substituted Cysteine Accessibility Method (SCAM^{TM}): Application to a Lipid-Specific Membrane Protein Topogenesis. *Methods*, **36**, 148-171.

Carneiro A.M., Ingram S.L., Beaulieu J.M., Sweeney A., Amara S.G., Thomas S.M., Caron M.G., and Torres G.E. (2002) The multiple LIM Domain-Containing Adaptor

Protein Hic-5 Synaptically Colocalizes and Interacts with the Dopamine Transporter. *J. Neurosci*., **22**, 7045-7054.

Carroll F.I, Gao Y., Rahman M.A., Abraham P., Parham K., Lewin A.H, Boja J.W., and Kuhar M.J. (1991a) Synthesis, Ligand Binding, QSAR, and CoMFA Study of 3β-(*p*-Substituted phenyl)tropane-2β-carboxylic Acid Methyl Esters. *J. Med. Chem*., **34**, 2719-2725.

Carroll F.I., Lewin A.H., Abraham P., Parham K., Boja J.W., and Kuhar M.J. (1991b) Synthesis and Ligand Binding of Cocaine Isomers at the Cocaine Receptor. *J. Med. Chem.*, **34**, 883-886.

Carroll F., Lewin A.H., Boja J., and Kuhar M.J. (1992) Cocaine Receptor: Biochemical Characterization and Structure-Activity Relationships of Cocaine Analogues at the Dopamine Transporter. *J. Med. Chem.*, **35**, 969-981.

Carroll F., Howell L., and Kuhar M.J. (1999) Pharmacotherapies for Treatment of Cocaine Abuse: Preclinical Aspects. *J. Med. Chem.*, **42**, 2721-2736.

Carvelli L., McDonald P.W., Blakely R.D., and DeFelice L.J. (2004) Dopamine Transporters Depolarize Neurons by a Channel Mechanism. *PNAS*, **101**, 16046-16051.

Carvelli L., Moron J.A., Kahlig K.M., Ferrer J.V., Sen N., Lechleiter J.D., Leeb-Lundberg L.M.F., Merrill G., Lafer E.M., Ballou L.M., Shippenberg T.S., Javitch J.A., Lin R.Z., and Galli A. (2002) PI 3-kinase Regulation of Dopamine Uptake. *J. Neurochem.*, **81**, 859-869.

Chait L.D., Uhlenhuth E.H., and Johanson C.E. (1987) Reinforcing and Subjective Effects of Several Anorectics in Normal Human Volunteers. *J. Pharmacol. Exp. Ther.*, **242**, 777-783.

Chen N. and Reith M.E. (2000) Structure and Function of the Dopamine Transporter. *Eur. J. Pharm.*, **405**, 329-339.

Chen N., Vaughan R.A., and Reith M.E.A. (2001) The Role of Conserved Tryptophan and Acidic Residues in the Human Dopamine Transporter as Characterized by Site-Directed Mutagenesis. *J Neurochem.*, **77**, 1116-1127.

Chen R., Han D.D., and Gu H.H. (2005) A Triple Mutant in the Second Transmembrane Domain of Mouse Dopamine Transporter Markedly Decreases Sensitivity to Cocaine and Methylphenidate. *J. Neurochem.*, **94**, 352-359.

Clarke R.L., Daum S., Gambino A., Aceto M., Pearl J., Levitt M., Cumiskey W., and Bogado E. (1973) Compounds Affecting the Central Nervous System. 4.3β-Phenyltropane-2-carboxylic Esters and Analogs. *J. Med. Chem.*, **16**, 1260-1267.

Cook E.H., Stein M.A., Krasowski M.D., Cox N.J., Olkon D.M., Kieffer J.E., and Leventhal B.L. (1995) Association of Attention-Deficit Disorder and the Dopamine Transporter Gene. *Am. J. Hum. Genet.,* **56**, 993–998.

Coyle J.T. and Snyder S.H. (1969) Antiparkinsonian Drugs: Inhibition of Dopamine Uptake in the Corpus Striatum as a Possible Mechanism of Action. *Science,* **166**, 899-901.

Craik C.S., Largman C., Fletcher T., Roczniak S., Barr P.J., Fletterick R.J., and Rutter W.J. (1985) Redesigning Trypsin: Alteration of Substrate Specificity. *Science*, **228**, 291-297.

de Ravel M.R., Blachere T., Delolme F., Dessalces G., Coulon S., Baty D., Grenot C., Mappus E., and Cuilleron C.Y. (2001) Specific Photoaffinity-Labeling of Tyr-50 on the Heavy Chain and of Tyr-32 on the Light Chain in the Steriod Combining Site of a Mouse Monoclonal Anti-Estradiol Antibody Using C3-, C6-, and C7- Linked 5-Azido-2-Nitrobenzoylamidoestradiol Photoreagents. *Biochemistry*, **40**, 14907-14920.

Deseke E., Nakatani Y., and Ourisson G. (1998) Intrinsic Reactivities of Amino Acids Towards Photoalkylation with Benzophenone – A Study Preliminary to Photolabeling of the Transmembrane Protein Glycophorin A. *Eur. J. Org. Chem.*, **2**, 243-251.

Dorman G. and Prestwhich G.D. (1994) Benzophenone Photophores in Biochemistry. *Biochem*., **33**, 5661-5673.

Dorman G. and Prestwich G.D. (2000) Using Photolabile Ligands in Drug Discovery and Development. *TIBTECH*, **18**, 64-77.

Dusek D.E. and Girdano D.A. (1988) Stimulants: Cocaine, Amphetamines, and Caffeine, in *Drug Education: Content and Methods*. 4th edition. Newbery Award Records Inc., New York, N.Y., 166-183.

Dutta A.K., Zhang S., Kolhatkar R., and Reith M.E.A. (2003) Dopamine Transporter as a Target for Drug Development of Cocaine Dependence Medications. *Eur. J. Pharm*., **479**, 93-106.

Endo S. (1962) Studies on Protease Produced by Thermophilic Bacteria. *J. Ferment. Technol.*, **40**, 346-353.

Evnin L.B. and Craik C.S. (1990) Substrate Specificity of Trypsin Investigated by Using a Genetic Selection. *PNAS*, **87**, 6659-6663.

Fang K., Hashimoto M., Jockusch S., Turro N.J., and Nakanishi K. (1998) A Bifunctional Photoaffinity Probe for Ligand/Receptor Interaction Studies. *J. Am. Chem. Soc*., **120**, 8543-8544.

Feder J., Garrett L.R., and Wildi B.S. (1971) Studies on the Role of Calcium in Thermolysin. *Biochem.,* **10**, 4552-4556.

Ferrer J.V. and Javitch J.A. (1998) Cocaine Alters the Accessibility of Endogenous Cysteines in Putative Extracellular and Intracellular Loops of the Human Dopamine Transporter. *Proc. Natl. Acad. Sci.*, **95**, 9238- 9243.

Garrett R. and Grisham C. (1999) Proteins: Their Biological Functions and Primary Structure *in Biochemistry*, **2nd ed**., Saunders College Publishing Co., Philadelphia, Pennsylvania, 107-150.

Giros B. and Caron M. (1993) Molecular Characterization of the Dopamine Transporter. *Trends Pharmacol. Sci*., **14,** 43-49.

Giros B., Jaber M., Jones S.R., Wightman R.M., and Caron M.G. (1996) Hyperlocomotion and Indifference to Cocaine and Amphetamine in Mice Lacking the Dopamine Transporter. *Nature*, **379**, 606-612.

Gomez G.E., Cauerhff A., Craig P.O., Goldbaum F.A., and Delfino J.M. (2006) Exploring Protein Interfaces with a General Photochemical Reagent. *Prot. Sci*., **15**, 744-752.

Gross E. (1967) The Cyanogen Bromide Reaction *in Methods in Enzymology*, **11**, Ed. by C.H.W. Hirs, Academic Press, Inc., New York, 238-255.

Hedemann M.S., Jensen B.B, and Poulsen H.D. (2006) Influence of Dietary Zinc and Copper on Digestive Enzyme Activity and Intestinal Morphology in Weaned Pigs. *J. Anim. Sci.*, **84**, 3310-3320.

Hedstrom L. (2002) Serine Protease Mechanism and Specificity. *Chem. Rev*., **102**, 4501-4523.

Heinrikson R.L. (1977) Applications of Thermolysin in Protein Structural Analysis in *Methods Enzymol*., **47**, C.H.W. Hirs and S.N. Timasheff (ed.), Academic Press, Inc., New York, 175-189.

Henry L.K., Adkins E.M., Han Q., and Blakely R.D. (2003) Serotonin and Cocaine-Sensitive Inactivation of Human Serotonin Transporters by Methanethiosulfonates Targeted to Transmembrane Domain I. *J. Biol. Chem*., **278**, 37052-37063.

Henry L.K., DeFelice L.J., and Blakely R.D. (2006a) Getting the Message Across: A Recent Transporter Structure Shows the Way. *Neuron*, **49**, 791-796.

Henry L.K., Field J.R., Adkins E.M., Parnas M.L., Vaughan R.A., Zou M.F., Newman A.H., and Blakely R.D. (2006b) Tyr-95 and Ile-172 in Transmembrane Segments 1 and 3

of Human Serotonin Transporter Interact to Establish High Affinity Recognition of Antidepressants. *J. Biol. Chem.*, **281**, 2012-2023.

Hubbard J.W., Srinivas N.R., Quinn D., and Midha K.K. (1989) Enantioselective Aspects of the Disposition of dl-threo-Methylphenidate After the Administration of a Sustained-Release Formulation to Children with Attention Deficit-Hyperactivity Disorder. *J. Pharm Sci.*, **11**, 944-7.

Hyttel J. (1982) Citalopram-Pharmacological Profile of a Specific Serotonin Uptake Inhibitor with Antidepressant Activity. *Prog. Neuropsychopharm. Biol. Psych.*, **6**, 277-295.

Ibrahim B.S. and Pattabhi V. (2004) Crystal Structure of Trypsin-Turkey Egg White Inhibitor Complex. *Biochem. Biophys. Res. Commun.*, **313**, 8-16.

Inouye K., Kuzuya K., and Tonomura B. (1998) Sodium Chloride Enhances Markedly the Thermal Stability of Thermolysin as well as its Catalytic Activity. *Biochim. Biophys. Acta.*, **1388**, 209-214.

Janowsky A., Schweri M.M., Berger P., Long R., Skolnick P., and Paul S.M. (1985)The Effects of Surgical and Chemical Lesions on Striatal [^{3}H]threo-(±)-Methylphenidate Binding: Correlation with [^{3}H] Dopamine Uptake. *Eur. J. Pharm.*, **108**, 187-191.

Javitch J.A. (1998) Probing Structure of Neurotransmitter Transporters by Substituted-Cysteine Accessibility Method. *Methods Enzymol*., **296**, 331-346.

Jiang Y., Lee A., Chen J., Cadene M., Chait B.T., and MacKinnon R. (2002) Crystal Structure and Mechanism of a Calcium-Gated Potassium Channel. *Nature*, **417**, 515-522.

Kahlig K.M., Binda F., Khoshbouei H., Blakely R.D., McMahon D.G., Javitch J.A., and Galli A. (2005) Amphetamine Induces Dopamine Efflux Through a Dopamine Transporter Channel. *PNAS*, **102**, 3495-3500.

Kaiser R. and Metzka L. (1999) Enhancement of Cyanogen Bromide Cleavage Yields for Methionyl-Serine and Methionyl-Threonine Peptide Bonds. *Anal. Biochem*., **266**, 1-8.

Kampen J.M.V., McGeer E.G., and Stoessl A.J. (2000) Dopamine Transporter Function Assessed by Antisense Knockdown in the Rat: Protection From Dopamine Neurotoxicity. *Synapse*, **37**, 171-178.

Kaneda M., Masuda S., Tomohiro T., and Hatanaka Y. (2007) A Simple and Efficient Photoaffinity Method for Proteomics of GTP-Binding Proteins. *ChemBioChem*., **8**, 595-598.

Keil B. (1992) Specificity of Proteolysis. Springer-Verlag, New York.

Khoshbouei H., Sen N., Guptaroy B., Johnson L., Lund D., Gnegy M.E., Galli A., and Javitch J.A. (2005) Biogenic Amine Neurotransmitter Transporters: Just When You Thought You Knew Them. *Physiology*, **20**, 225-231.

Kilby B.A. and Youatt G. (1954) The Inhibition of Trypsin and Chymotrypsin by Certain Organic Phosphorus Esters. *J. Biochem.,* **57**, 303- 309.

Kim D.I., Schweri M.M., and Deutsch H. (2003) Synthesis and Pharmacology of Site Specific Cocaine Abuse Treatment Agents: 8-Substituted Isotropane (3-Azabicyclo[3.2.1.]octane) Dopamine Uptake Inhibitors. *J. Med. Chem.*, **46**, 1456-1464.

Kitayama S., Shimada S., Xu H., Markham L., Donovan D.M., and Uhl G.R. (1992) Dopamine Transporter Sited-Directed Mutations Differentially Alter Substrate Transport and Cocaine Binding. *Proc. Natl. Acad. Sci.,* **89**, 7782-7785.

Kline R.H., Izenwasser S., Katz J., Joseph D., Bowen W., and Newman A.H. (1997) 3'-Chloro-3α-(diphenylmethoxy)tropane But Not 4'-Chloro-3α-(diphenylmethoxy)tropane Produces a Cocaine-like Behavioral Profile. *J. Med. Chem.*, **40**, 851-857.

Knight K.L. and McEntee K. (1985) Tyrosine 264 in the recA Protein From Escherichia coli is the Site of Modification by the Photoaffinity Label 8-azidoadenosine 5'-triphosphate. *J. Bio. Chem.,* **260**, 10185-10191.

Koob G.F. (2000) Neurobiology of Addiction: Toward the Development of New Therapies. *Ann. N.Y. Acad. Sci.*, **909**, 170-185.

Koob G.F. and Bloom F.E. (1988) Cellular and Molecular Mechanisms of Drug Dependence. *Science,* **242**, 715-723.

Korkhov V.M., Holy M., Freissmuth M., and Sitte H.H. (2006) The Conserved Glutamate (Glu^{136}) in Transmembrane Domain 2 of the Serotonin Transporter Is Required for the Conformational Switch in the Transport Cycle. *J. Biol. Chem*., **281,** 13439-13448.

Kotzyba-Hibert F., Kapfer I., and Goeldner M. (1995) Recent Trends in Photoaffinity Labeling. *Angew. Chem. Int. Ed. Engl*., **34**, 1296-1312.

Kraft P., Mills J., and Dartz E. (2001) Mass Spectrometric Analysis of Cyanogen Bromide Fragments of Integral Membrane Proteins at the Picomole Level: Application to Rhodopsin. *Anal. Biochem*., **292**, 76-86.

Kreek M.J. (2001) Drug Addictions, Molecular and Cellular Endpoints. *Ann. N.Y. Acad. Sci.*, **937**, 27-49.

Kuhar M.J., Ritz M.C., and Boja J.W. (1991) The Dopamine Hypothesis of the Reinforcing Properties of Cocaine. *Trends Neurosci.*, **14**, 299-302.

Latt S.A., Holmquist B., and Vallee B.L. (1969) Thermolysin: a Zinc Metalloenzyme. *Biochem. Biophys. Res. Commun.*, **37**, 333-339.

Lee F.J., Liu F., Pristupa Z.B., and Niznik H.B. (2001) Direct Binding and Functional Coupling of Alpha-Synuclein to the Dopamine Transporters Accelerate Dopamine-Induced Apoptosis. *FASEB J.*, **15**, 916-926.

Lee S., Chang M., Lee K., Park B.S., Lee Y., Chin H.R., and Lee Y. (2000) Importance of Valine at Position 152 for the substrate Transport and 2β-Carbomethoxy-3β-(4-fluorophenyl)tropane Binding of Dopamine Transporter. *Mol. Pharm.*, **57**, 883-889.

Li G.D., Chiara D.C., Sawyer G.W., Husain S., Olsen R.W., and Cohen J.B. (2006) Identification of a $GABA_A$ Receptor Anesthetic Binding Site at Subunit Interfaces by Photolabeling with an Etomidate Analog. *J. Neurosci.*, **26**, 11599-11605.

Li Y.Z., Kirby J.P., George M.W., Poliakoff M., and Schuster G.B. (1988) 1,2-Didehydroazepines From the Photolysis of Substituted Aryl Azides: Analysis of Their Chemical and Physical Properties by Time-Resolved Spectroscopic Methods. *J. Am. Chem. Soc.*, **110**, 8092-8098.

Lin Z., Itokawa M., and Uhl G.R. (2000) Dopamine Transporter Proline Mutations Influence Dopamine Uptake, Cocaine Analog Recognition, and Expression. *FASEB*., **14**, 715-728.

Lin Z., Zhang P., Zhu X., Melgari J., Huff R., Spieldoch R.L., and Uhl G.R. (2003) Phosphatidylinositol 3-Kinase, Protein Kinase C, and MEK1/2 Kinase Regulation of Dopamine Transporter (DAT) Require N-terminal DAT Phosphoacceptor Sites. *J. Bio. Chem.*, **278**, 20162-20170.

Locher K.P., Bass R.B., and Rees D.C. (2003) Structural Biology: Breaching the Barrier. *Science Perspectives*, **301**, 603-604.

Loland C.J., Norgaard-Nielsen K., and Gether U. (2003) Probing Dopamine Transporter Structure and Function by Zn^{2+}-Site Engineering. *Euro. J. Pharm.*, **479**, 187-197.

Madhusoodanan K.S. and Colman R.F. (2001) Adenosine 5'-0-[S-(4-succinimidyl-benzophenone)thiophosphate]: a New Photoaffinity Label of the Allosteric ADP Site of Bovine Liver Glutamate Dehydrogenase. *Biochem.*, **13**, 1577-1586.

Matecka D., Lewis D., Rothman R.B., Dersch CM., Wojnicki F., Glowa J., DeVries C., Pert A., and Rice K. (1997) Heteroaromatic Analogs of 1-[2-(Diphenylmethoxy)ethyl]- and 1-[2-[Bis(4flurophenyl methoxy]ethyl]-4-(3-phenylpropyl)piperazines (GBR 12935

and GBR 12909) as High Affinity Dopamine Reuptake Inhibitors. *J. Med. Chem.*, **40**, 705-716.

Matsubara H., Singer A., Sasaki R., and Jukes T. H. (1965) Observations on the Specificity of a Thermostable Bacterial Protease "Thermolysin". *Biochem. Biophys. Res. Commun.*, **21**, 242-247.

Meiergerd S. and Schenk J. (1994) Kinetic Evaluation of the Commonality Between the Site(s) of Action of Cocaine and Some Other Structurally Similar and Dissimilar Inhibitors of the Striatal Transporter for Dopamine. *J. Neurochem.*, **63**, 1683-1692.

Middleton S.A., Johnson D.L., Jin R., McMahon F.J., Collins A., Tullai J., Gruninger R.H., Jolliffe L.K., and Mulcahy L.S. (1996) Identification of a Critical Ligand Binding Determinant of the Human Erythropoietin Receptor. *J. Bio. Chem.*, **272**, 4985-4992.

Miles J.L., Morey E., Crain F., Gross S., San Julian J., and Canady W.J. (1962) Inhibition of α-Chymotrypsin by Diethyl Ether and Certain Alcohols: a New Type of Competitive Inhibition . *J. Bio Chem.*, **237**, 1319-1322.

Miles J.L., Robinson D.A., and Canady W.J. (1963) Thermodynamics of the Solution Process: Some Applications to Enzyme Catalysis, and Inhibition of α-Chymotrypsin by Aromatic Hydrocarbons. *J. Biol. Chem.*, **238**, 2932-2937.

Miller G.W., Staley J.K., Heilman C.J., Perez J.T., Mash D.C., Rye D.B., and Levey A.I. (1997) Immunochemical Analysis of Dopamine Transporter Protein in Parkinson's Disease. *Ann. Neurol.*, **41**, 530-539.

Mishchenko E.L., Kozhanova L.A., Denisov A.Y., Gritsan N.P., Markushin Y.Y., Serebriakova M.V., and Godovikova T.S. (2000) Study of the Chemical Structures of the Photo-Cross-Linking Products Between Tyr and the 5-azido-2-nitrobenzoyl residue. *J. Photochem. Photobiol. B: Biol.*, **54**, 16-25.

Morón J.A., Zakharova I., Ferrer J.V., Merrill G.A., Hope B., Lafer E.M., Lin Z.C., Wang J.B., Javitch J.A., Galli A., and Shippenberg T.S. (2003) Mitogen-Activated Protein Kinase Regulates Dopamine Transporter Surface Expression and Dopamine Transport Capacity. *J. Neurosci.*, **23**, 8480-8488.

Newman A.H., Allen A., Izenwasser S., and Katz J. (1994) Novel 3α-(Diphenylmethoxy)tropane Analogs: Potent Dopamine Uptake Inhibitors Without Cocaine-like Behavioral Profiles. *J. Med. Chem.*, **37**, 2258-2261.

Newman A.H., Kline R.H., Allen A.C., Izenwasser S., George C., and Katz J. (1995) Novel 4'-Substituted and 4',4''-Disubstituted 3α-(Diphenylmethoxy)tropane Analogs as Potent and Selective Dopamine Uptake Inhibitors. *J. Med. Chem.,* **38**, 3933-3940.

Newman A.H. and Kulkarni S. (2002) Probes for the Dopamine Transporter: New Leads Toward a Cocaine-Abuse Therapeutic-A Focus on Analogues of Benztropine and Rimcazole. *Med. Res. Rev.*, **22**, 429-464.

Niedel J., Davis J., and Cuatrecasas P. (1980) Covalent Affinity Labeling of the Formyl Peptide Chemotactic Receptor. *J. Biol. Chem.*, **255**, 1980.

Norregaard L., Frederiksen D., Nielsen E.O., and Gether U. (1998) Delination of an Endogenous Zinc-Binding Site in the Human Dopamine Transporter. *EMBO J.*, **17**, 4266-4273.

Norregaard L., Loland C.J., and Gether U. (2003) Evidence for Distinct Sodium-, Dopamine-, and Cocaine-Dependent Conformational Changes in Transmembrane Segments 7 and 8 of the Dopamine Transporter. *J. Bio. Chem.*, **278**, 30587-30596.

Ozols J. (1990) Covalent Structure of Liver Microsomal Flavin-Containing Monooxygenase Form 1. *J. Biol. Chem.*, **265**, 10289-10299.

Paczkowski F.A. and Byan-Lluka L.J. (2004) Role of Proline Residues in the Expression and Function of the Human Noradrenaline Transporters. *J. Neurochem.*, **88**, 203-211.

Pan D., Gatley S.J., Dewey S.L., Chen R., Alexoff D.A., Ding Y.S., and Fowler J.S. (1994) Binding of Bromine-Substituted Analogs of Methylphenidate to Monoamine Transporters. *Eur. J. Pharm.*, **264**, 177-182.

Park S.U., Ferrer J.V., Javitch J.A., and Kuhn D.M. (2002) Peroxynitrite Inactivates the Human Dopamine Transporter by Modification of Cysteine 342: Potential Mechanism of Neurotoxicity in Dopamine Neurons. *J. Neurosci*., **22**, 4399-4405.

Parnas M.L., Gaffaney J.D., Newman A.H., Zou M.F., Lever J.R., and Vaughan R.A. (2003) Irreversible Cocaine Analogs Map to Multiple Sites on the Dopamine Transporter. *Soc. Neurosci. Abs*., **253.18.**

Parnas M.L., Gaffaney J.D., Zou M.F., Lever J.R., Newman A.H., and Vaughan R.A. (2008) Labeling of Dopamine Transporter Transmembrane Domain 1 with the Tropane Ligan N-[4-(4-Azido-3-[^{125}I]iodophenyl)butyl]-2β-carbomethoxy-3 β -(4-chlorophenyl)tropane Implicates Proximity of Cocaine and Substrate Actives. *Mol. Pharmacol.,* **73**, 1141-1150.

Pazhang M., Khajeh K., Ranjbar B., and Hosseinkhani S. (2006) Effects of water-Miscible Solvents and Polyhydroxy Compounds on the Structure and Enzymatic Activity of Thermolysin. *J. Biotech.,* **127,** 45-53.

Perodin J., Deraet M., Auger-Messier M., Boucard A.A., Rihakova L., Beaulieu M.E., Lavigne P., Parent J.L., Guillemette G., Leduc R., and Escher E. (2002) Residues 293-294 Are Ligand Contact Points of the Human Angiotensin Type 1 Receptor. *Biochem*., **41**, 14348-14356.

Povlock S.L. and Amara S.G. (1997) The Structure and Function of Norepinephrine, Dopamine, and Serotonin Transporters, in *Neurotransmitter Transporters: Structure, Function, and Regulation.* Humana Press, Totowa, N.J., 1–28.

Qian Y., Melikian H.E., Rye D.B., Levey A.I., and Blakely D. (1995) Identification and Characterization of Antidepressant-Sensitive Serotonin Transporter Proteins Using Site-Specific Antibodies. *J. Neurosci*., **15**, 1261-1274.

Ravna A.W., Sylte I., and Dahl S.G. (2003a) Molecular Mechanism of Citalopram and Cocaine Interactions with Neurotransmitter Transporters. *J. Pharm. Exp. Ther*., **307**, 34-41.

Ravna A.W., Sylte I., and Dahl S.G. (2003b) Molecular Model of the Neural Dopamine Transporter. *J. Comp. Aid. Mol. Des*., **17**, 367-382.

Reith M.E.A. (1997) Mechanisms of Biogenic Amine Neurotransmitter Transporters, in *Neurotransmitter Transporters: Structure, Function, and Regulation*. Humana Press, Totowa, New Jersey, 43-100.

Ritz M., Lamb R., Goldberg S., and Kuhar M.J. (1987) Cocaine Receptors on Dopamine Transporter Are Related to Self-Administration of Cocaine. *Science,* **237**, 1219-1223.

Robinette D., Neamati N., Tomer K.B., and Borchers C.H. (2006) Photoaffinity Labeling Combined with Mass Spectrometric Approaches as a Tool for Structural Proteomics. *Ex. Rev. Prot.*, **3**, 399-408.

Rodriguez J.C., Wong L., and Jennings P.A. (2003) The Solvent in CNBr cleavage Reactions Determines the Fragmentation Efficiency of Ketosteroid Isomerase Fusion Proteins Used in the Production of Recombinant Peptides. *Prot. Exp. Purif.*, **28**, 224-231.

Rothman R., Mele A., Reid A., Akunne H., Greig N., Thurkauf A., Rice K. and Pert A. (1989) Tight Binding Dopamine Reuptake Inhibitors as Cocaine Antagonists. A Strategy for Drug Development. *FEBS Lett.*, **257**, 341-344.

Sakamoto Y., Kawakami N., and Sasagawa T. (1988) Prediction of Peptide Retention Times. *J. Chromatogr.,* **442**, 69-79.

Sato Y., Zhang Y.W., Androutsellis-Theotokis A., and Rudnick G. (2004) Analysis of Transmembrane Domain 2 of Rat Serotonin Transporter by Cysteine Scanning Mutagenesis. *J. Biol. Chem.*, **279**, 22926-22933.

Scholze P., Norregaard L., Singer E.A., Freissmuth M., Gether U., and Sitte H.H. (2002) The Role of Zinc Ions in Reverse Transport Mediated by Monoamine Transporters. *J. Bio. Chem.*, **277**, 21505-21513.

Schreiber J. and Witkop B. (1964) The Reaction of Cyanogen Bromide with Mono- and Diamino Acids. *J. Am. Chem. Soc*., **86**, 2441-45.

Schwartz M. A. (1989) Studying the Cytoskeleton By Label Transter Crosslinking: Uses and Limitations. *Photochem. Probes Biochem*., **189**, 157-168.

Sen N., Shi L., Beuming T., Weinstein H., and Javitch J.A. (2005) A Pincer-Like Configuration of TM2 in the Human Dopamine Transporter is Responsible for Indirect Effects on Cocaine Binding. *Neuropharm*., **49**, 780-790.

Sipos T. and Merkel J. (1970) An Effect of Calcium Ions on the Activity, Heat Stability, and Structure of Trypsin. *Biochem.,* **9**, 2766-2775.

Smyth D.G. (1967) in *Methods Enzymol*., **11**, C.H.W. Hirs (ed), Academic Press, Inc., New York, 214-236.

Steers E., Craven G.R., Anfinsen C.B., and Bethune J.L. (1965) Evidence for Nonidentical Chains In the Beta-Galactosidase of *Escherichia Coli K12*. *J. Biol. Chem*., **240**, 2478-84.

Strasburg G.M., Hogan M., Birmachu W., Thomas D.D. and Louis C.F. (1988) Site-Specific Derivatives of Wheat Germ Calmodulin. Interactions With Troponin and Sarcoplasmic Reticulum. *J. Biol. Chem*., **263**, 542-548.

Sucic S. and Byan-Lluka L.J. (2005) Roles of Transmembrane Domain 2 and the First Intracellular Loop in Human Noradrenaline Transporter Function: Pharmacological and SCAM Analysis. *J. Neurochem*., **94**, 1620-1630.

Sucic S., Paczkowski F.A., Runkel F., Bonisch H., and Bryan-Lluka L.J. (2002) Functional Significance of a Highly Conserved Glutamate Residue of the Human Noradrenaline Transporter. *J. Neurochem*., **81**, 344-354.

Surratt C.K., Ukairo O.T., and Ramanujapuram S. (2005) Recognition of Psychostimulants, Antidepressants, and Other Inhibitors of Synaptic Neurotransmitter Uptake by the Plasma Membrane Monoamine Transporters. *AAPS J*., **7**, E739-E751.

Tatsumi C., Hashida Y., Yasukawa K., and Inouye K. (2007) Effects of Site-Directed Mutagenesis of the Surface Residues Gln128 and Gln225 of Thermolysin on its Catalytic Activity. *J. Biochem*., **141**, 835-842.

Tomita T., Mizumachi Y., Chong K., Ogawa K., Konishi N., Sugawara-Tomita N., Dohmae N., Hashimoto Y., and Takio K. (2004) Protein Sequence Analysis, Cloning, and Expression of Flammutoxin, a Pore-Forming Cytolysin from *Flammulina velutipes*. *J. Biol. Chem*., **279**, 54161-54172.

Tomohiro T., Hashimoto M., and Hatanaka Y. (2005) Cross-Linking Chemistry and Biology Development of Multifunctional Photoaffinity Probes. *The Chemical Record*, **5**, 385-395.

Torres G.E. (2006) The Dopamine Transporter Proteome. *J. Neurochem*., Apr; 97 Supplement 1:3-10.

Torres G.E., Carneiro A., Seamans K., Fiorentini C., Sweeney A., Yao W.D., and Caron M.G. (2003a) Oligomerization and Trafficking of the Human Dopamine Transporter. *J. Bio. Chem.,* **278**, 2731-2739.

Torres G. E., Gainetdinov R.R., and Caron M.G. (2003b) Plasma Membrane Monoamine Transporters: Structure, Regulation, and Function. *Nature Review; Neuro.,* **4**, 13-25.

Torres J., Stevens T.J., and Samso M. (2003c) Membrane Proteins: the 'Wild West' of Structural Biology. *Trends Biochem. Sci*., **28**, 137-144.

Triantafyllou A.O., Wehtje E., Adlercreutz P., and Mattiasson B. (1997) How do Additives Affect Enzyme Activity and Stability in Nonaqueous Media? *Biotech. Bioeng*., **54**, 67-76.

Uhl G.R., Hall F.S., and Sora I. (2002) Cocaine, Reward, Movement, and Monoamine Transporters. *Mol. Psychiatry*, **7**, 21-26.

Uhl G.R. and Lin Z. (2003) The Top 20 Dopamine Transporters Mutants: Structure-Function Relationships and Cocaine Actions. *Eur. J. Pharm.,* **479**, 71-82.

Vaughan R.A. (1995) Photoaffinity-Labeled Ligand Binding Domains on Dopamine Transporters Identified by Peptide Mapping. *Mol. Pharm*., **47**, 956-964.

Vaughan R.A., Agoston G.E., Lever J.R., and Newman A.H. (1999) Differential Binding of Tropane-Based Photoaffinity Ligands on the Dopamine Transporter. *J. Neurosci.*, **19**, 630-636.

Vaughan R.A., Gaffaney J.D., Lever J.R., Reith M., and Dutta A. (2001) Dual Incorporation of Photoaffinity Ligands on Dopamine Transporters Implicates Proximity of Labeled Domains. *Mol. Pharmacol.*, **59**, 1157-1164.

Vaughan R.A. and Kuhar M.J. (1996) Dopamine Transporter Ligand Binding Domains. *J. Biol. Chem.*, **271**, 21672-21680.

Vaughan R.A., Sakrikar D.S., Parnas M.L., Adkins S., Foster J.D., Duval R.A., Lever J.R., Kulkarni S.S., and Hauck-Newman A. (2007) Localization of Cocaine Analog [^{125}I]RTI-82 Irreversible Binding to Transmembrane Domain Six of the Dopamine Transporter. *J. Biol. Chem*., **282**, 8915-25.

Vik S.B. and Ishmukhametov R.R. (2005) Structure and Function of a Subunit of the ATP Synthase of Escherichia Coli. *J Bioenerg. Biomembr*., **37**, 445-449.

Voet D. and Voet J.G. (1995a) Three-Dimensional Structures Of Proteins, in *Biochemistry*. 2nd Edition, John Wiley & Sons, Inc., New York, N.Y., 162-173.

Voet D. and Voet J.G. (1995b) Enzymatic Catalysis, in *Biochemistry*. 2nd Edition, John Wiley & Sons, Inc., New York, N.Y., 371- 408.

Voet D. and Voet J.G. (1995c) Transport through Membranes, in *Biochemistry*. 2nd edition. John Wiley & Sons, Inc., New York, N.Y., 513-536.

Volkow N.D.J., Fowler J.S., Fischman M.W., Foltin R.W., Abumrad N.N., Gately S.J., Logan J., Wong C., Gifford A., Ding Y.S., Hitzemann R., and Pappas N. (1999) Methylphenidate and Cocaine Have Similar In Vivo Potency to Block Dopamine Transporters in the Human Brain. *Life Sci.,* **65**, 7-12.

Volkow N.D.J., Wang G.J., Fischman M.W., Foltin R.W., Fowler J.S., Abumrad N.N., Vitkun S., Logan J., Gatley S.J., Pappas N., Hitzemann R., and Shea C.E. (1997) Relationship Between Subjective Effects of Cocaine and Dopamine Transporter Occupancy. *Nature*, **386**, 827-830.

Walsh K. and Neurath H. (1964) Trypsinogen and Chymotrypsinogen as Homologous Proteins. *Proc. Natl. Acad. Sci. U S A,* **52**, 884 - 889.

Ward D.G., Brewer S.M., Cornes M.P., and Trayer I.P. (2003) A Cross-Linking Study of the N-Terminal Extension of Human Cardiac Troponin I. *Biochem*., **42**, 10324-10332.

Watt D.S., Kawada K., Leyva E., and Platz M.S. (1989) Exploratory Photochemistry of Iodinated Aromatic Azides. *Tetrahedron Lett*., **30**, 899-902.

Weiss F., Hurd Y.L., Ungerstedt U., Markou A., Plotsky P.M., and Koob G.F. (1992) Neurochemical Correlates of Cocaine and Ethanol Self-Administration. *Ann. N.Y. Acad. Sci*., **654**, 220-241.

Wersinger C. and Sidhu A. (2003) Attenuation of Dopamine Transporter Activity by α-Synuclein. *Neurosci. Lett*., **340**, 189-192.

White B.H. and Cohen J.B. (1992) Agonist-Induced Changes in the Structure of the Acetylcholine Receptor M2 Regions Revealed by Photoincorporation of an Uncharged Nicotinic Noncompetitive Antagonist. *J. Biol. Chem*., **267**, 15770-15783.

White B.H., Howard S., Cohen S.G., and Cohen J.B. (1991) The Hydrophobic photoreagent 3-(trifluoromethyl)-3-*m*-([^{125}I]iodophenyl)diazirine is a Novel

Noncompetitive Antagonist of the Nicotinic Acetylcholine Receptor. *J. Biol. Chem.,* **266**, 21595-21607.

Wirtz S. (2004) Identification of an MFZ 2-24 Affinity Labeling Site on the Human Dopamine Transporter, Ph.D. Dissertation, Emory University.

Wu X. and Gu H.H. (2003) Cocaine Affinity Decreased by Mutations of Aromatic Residue Phenylalanine 105 in the Transmembrane Domain 2 of Dopamine Transporter. *Mol. Pharm.,* **63**, 653-658.

Yamashita A., Singh S.K., Kawate T., Jin Y., and Gouaux E. (2005) Crystal Structure of a Bacterial Homologue of Na^+/Cl^--Dependent Neurotransmitter Transporters. *Nature*, **437**, 215-222.

Yu S.M., McQuade D.T., Quinn M.A., Hackenberger C.P.R., Krebs M.P., Polans A.S., and Gellman S. H. (2000) An Improved Tripod Amphiphile for Membrane Protein Solubilization. *Prot Sci.,* **9**, 2518-2527.

Zou M.Z., Kopajtic T., Katz J.L., Wirtz S., Justice J.B., and Newman A.H. (2001) Novel Tropane-Based Irreversible Ligands for the Dopamine Transporter. *J. Med. Chem*., **44,** 4453-4461.

Zhou Z., Zhen J., Karpowich N.K., Goetz R.M., Law C.J., Reith M.E.A., and Wang D. (2007) LeuT-Desipramine Structure Reveals How Antidepressants Block Neurotransmitter Reuptake. *Science*, **317**, 1390-1393.